International Journal of Photoenergy

Laser Photobiomodulation in Health and Disease

Lead Guest Editor: Rodrigo Alvaro Lopes-Martins
Guest Editors: Jan M. Bjordal and Ernesto Cesar Pinto Leal-Junior

Laser Photobiomodulation in Health and Disease

International Journal of Photoenergy

Laser Photobiomodulation in Health and Disease

Lead Guest Editor: Rodrigo Alvaro Lopes-Martins
Guest Editors: Jan M. Bjordal and Ernesto Cesar Pinto Leal-Junior

Copyright © 2021 Hindawi Limited. All rights reserved.

This is a special issue published in “International Journal of Photoenergy.” All articles are open access articles distributed under the Creative Commons Attribution License, which permits unrestricted use, distribution, and reproduction in any medium, provided the original work is properly cited.

Chief Editor

Giulia Grancini, Italy

Academic Editors

Mohamed S.A. Abdel-Mottaleb, Egypt
Angelo Albini, Italy
Mohammad Alghoul, Malaysia
Alberto Álvarez-Gallegos, Mexico
Vincenzo Augugliaro, Italy
Detlef W. Bahnemann, Germany
Simona Binetti, Italy
Fabio Bisegna, Italy
Thomas M. Brown, Italy
Joaquim Carneiro, Portugal
Yatendra S. Chaudhary, India
Kok-Keong Chong, Malaysia
Věra Cimrová, Czech Republic
Laura Clarizia, Italy
Gianluca Coccia, Italy
Daniel Tudor Cotfas, Romania
P. Davide Cozzoli, Italy
Dionysios D. Dionysiou, USA
Elisa Isabel Garcia-Lopez, Italy
Wing-Kei Ho, Hong Kong
Siamak Hoseinzadeh, Italy
Jürgen Hüpkes, Germany
Fayaz Hussain, Brunei Darussalam
Mohamed Gamal Hussien, Egypt
Adel A. Ismail, Kuwait
Chun-Sheng Jiang, USA
Zaiyong Jiang, China
Yuanzuo Li, China
Manuel Ignacio Maldonado, Spain
Santolo Meo, Italy
Claudio Minero, Italy
Regina De Fátima Peralta Muniz Moreira, Brazil
Maria da Graça P. Neves, Portugal
Tsuyoshi Ochiai, Japan
Kei Ohkubo, Japan
Umapada Pal, Mexico
Dillip K. Panda, USA
Carlo Renno, Italy
Francesco Riganti-Fulginei, Italy
Leonardo Sandrolini, Italy
Jinn Kong Sheu, Taiwan
Kishore Sridharan, India
Elias Stathatos, Greece
Jegadesan Subbiah, Australia
Chaofan Sun, China
K. R. Justin Thomas, India
Koray Ulgen, Turkey
Ahmad Umar, Saudi Arabia
Qiliang Wang, China
Xuxu Wang, China
Huiqing Wen, China
Weijie Yang, China
Jiangbo Yu, USA

Contents

Hindawi
International Journal of Photoenergy
Volume 2021, Article ID 3947895, 10 pages
https://doi.org/10.1155/2021/3947895

Research Article

Experimental Study of the Effect of Photobiomodulation Therapy on the Regulation of the Healing Process of Chronic Wounds

Sergey B. Pavlov[1,2], **Nataliia M. Babenko**[1,2], **Marina V. Kumetchko**[1], **Olga B. Litvinova**[1,2] and **Rostyslav N. Mikhaylusov**[3]

[1]*Central Research Laboratory, Kharkiv Medical Academy of Postgraduate Education, Kharkiv 61176, Ukraine*
[2]*Department of Human Anatomy and Physiology, H.S. Skovoroda Kharkiv National Pedagogical University, Kharkiv 61168, Ukraine*
[3]*Department of Endoscopy and Surgery, Kharkiv Medical Academy of Postgraduate Education, Kharkiv 61176, Ukraine*

Correspondence should be addressed to Nataliia M. Babenko; natali_babenko@ukr.net

Received 23 April 2021; Revised 28 May 2021; Accepted 29 July 2021; Published 7 September 2021

Academic Editor: Rodrigo Alvaro Lopes-Martins

Copyright © 2021 Sergey B. Pavlov et al. This is an open access article distributed under the Creative Commons Attribution License, which permits unrestricted use, distribution, and reproduction in any medium, provided the original work is properly cited.

Currently, wound treatment is an urgent task of medicine around the world. In the process of wound healing, various types of cells are involved under the control and regulation of cytokines and growth factors. Disruption of the synchronization process between the various types of cells and intercellular mediators involved in the restoration of tissue damage can lead to impaired healing and the development of chronic wounds. Photobiomodulation (PBM) therapy promotes platelet activation and aggregation, reduces inflammation and oxidative stress, and accelerates cell migration and proliferation. PBM also induces the production of the extracellular matrix and the release of key growth factors, thereby improving tissue regeneration and accelerating wound healing. The aim of our work was to study the effect of photobiomodulation therapy on the regulation of reparative processes in chronic wounds monitored by biomarkers and platelet aggregation activity. 54 Wistar rats were divided into three groups. Intact animals were not manipulated. In animals of the control and experimental groups, a chronic wound was simulated by reproducing the conditions of local hypoxia and microcirculation disorders. The wounds of the experimental group received PBM therapy. The device Lika-therapist M (Ukraine) was used in a continuous mode at a wavelength of 660 nm, an output power of 10 mW, and an energy density of 1 J/cm^2. The wounds of the animals in the control group were treated with sham. The animals were euthanized on days 3, 7, 14, and 28 after the surgery (6 animals, each from the control and experimental groups). Measurements of the levels of interleukin-6 (IL-6), interleukin-10 (IL-10), tumor necrosis factor alpha (TNF-α), the basic fibroblast growth factor (bFGF), and reactive oxygen species (ROS) were carried out by ELISA. Results revealed the multidirectional effect of PBM therapy on the expression of the studied biomarkers. The results of the histological examination indicated a positive effect of PBM therapy with the applied parameters on the repair processes of chronic wounds. We concluded that the use of PBM therapy made it possible to regulate disturbances in reparative processes by modulating ROS, cytokines, and platelet aggregation activity.

1. Introduction

The theoretical foundations of the possibility of creating a laser were laid by Albert Einstein, who first touched upon the possibility of stimulated radiation in a 1917 article. And in 1960, the revolutionary discovery of the laser by Theodore Maiman changed the world. Maiman presented his invention to the scientific community in an article in the journal *Nature*, which contained just under 300 words. Soon, a first application of low-intensity laser therapy for wound healing was demonstrated by the Hungarian doctor Endre Mester and his colleagues [1].

Today, photobiomodulation (PBM) therapy has found applications not only in the treatment of chronic wounds but also in the treatment of many diseases, including neurological and musculoskeletal [2]. Also, this noninvasive

method is used to reduce pain [3]. Despite widespread studies of various aspects of the action of PBM therapy, the exact mechanisms of laser-tissue interaction are not fully understood. It also requires a deeper understanding of the parameters that determine the therapeutic results and effectiveness of this method of treatment.

Currently, the treatment of wounds, called the "silent epidemic" [4], continues to be an urgent task of medicine around the world. Wound healing is a multifaceted process driven by sequential but overlapping phases including hemostasis, inflammation, proliferation, and remodeling [5]. Acute wounds usually heal in a consistent and timely manner. Chronic wounds remain blocked in one of these stages (oftentimes the inflammatory phase). This process involves various types of cells under the control and regulation of cytokines and growth factors. Reactive oxygen species (ROS) are also important regulators of wound healing phases [6]. Disruption of the synchronization of dynamic interactions among these various types of cells and intercellular mediators can lead to impaired healing and the development of chronic wounds. PBM therapy promotes platelet activation and aggregation, reduces inflammation and oxidative stress, and accelerates cell migration and proliferation. It also induces the production of the extracellular matrix and the release of key growth factors, thereby improving tissue regeneration and accelerating wound healing [7, 8].

In the literature, there are numerous works that demonstrate positive effects of PBM therapy on individual phases of the healing process, mainly on the inflammation stage. Overall, it is of interest to study the regulation of the repair process of chronic wounds by intercellular mediators at all stages of healing when using PBM therapy. Animal models remain the best available alternative for studying the complex cellular and molecular interactions that occur during the wound healing process [9].

The aim of our work was to study the effect of photobiomodulation therapy on the regulation of reparative processes in chronic wounds using biomarkers (for example, interleukin-6 (IL-6), interleukin-10 (IL-10), tumor necrosis factor alpha (TNF-α), the basic fibroblast growth factor (bFGF), and reactive oxygen species (ROS)) and platelet aggregation activity.

2. Materials and Methods

The work included 54 Wistar rats weighing 250 ± 25 g at the age of 8-9 months. The study was approved by the Committee on Ethical Animal Care and Use of the Kharkiv Medical Academy of Postgraduate Education, Ukraine (Protocol No. 5 dated November 12, 2019). All animal handling procedures were performed in accordance with the rules and guidelines set by this Committee.

2.1. Study Design. All rats were randomly divided into three groups (see Figure 1). Intact (Int) animals were not manipulated. Wounds were induced in animals of the control (Con) and experimental (Exp) groups.

The literature mainly contains models of acute wounds or wounds in animals with systemic diseases, such as diabetes. We have chosen a model of a chronic wound that reproduces the conditions of local hypoxia and impaired microcirculation [10].

Each animal was anesthetized (zoletil 10 mg/kg body weight) and depilated. In the proximal part of the back, the skin was excised with surgical scissors to the superficial fascia in the form of a circle with a diameter of about 20 mm. After that, a perpendicular loop-shaped fascial skin suture was applied along the edges of the wound. On the surface of the bottom of the formed wound, the superficial fascia was dissected by mutually perpendicular transverse and longitudinal cuts, which formed cells measuring 5 × 5 mm, which were then sutured with U-shaped sutures (see Figure 2).

The wounds of the experimental group received PBM therapy. The wounds of the animals in the control group were treated with sham.

For PBM therapy, the laser device Lika-therapist M (Ukraine) was used once a day for 5 days, starting from 24 hours after the formation of the wound. The parameters of low-intensity laser radiation are shown in Table 1. The beam of the laser tip was held perpendicular to the surface of the irradiated tissue. The distance between the extension handle and the wound was selected so as to illuminate the entire area of the wound. Taking into account the divergence of the diode laser beam (0.5 rad ±20%) and the aperture diameter of the laser device extension handle (0.2 cm) (recommended by Lika-therapist M), the distance between the extension handle and the wound was 3.53 cm.

The animals were taken out of the experiment on days 3, 7, 14, and 28 after surgery (6 animals, each from the control and experimental groups). Animals were euthanized by inhalation of chloroform in a confined space.

Blood samples were taken by open cardiac puncture. Measurements of the levels of the studied indicators in the blood serum of animals were carried out by the method of enzyme-linked immunosorbent assay (ELISA). The method is based on a sandwich version of ELISA using mono- and polyclonal antibodies. ROS and bFGF concentrations were determined using ELISA kits (Elabscience Biotechnology Inc., USA) ROS (Catalog No: E-EL-H5436) and bFGF (Catalog No: E-EL-H0483) according to the manufacturers' instructions. The levels of IL-6, IL-10, and TNF-α were determined using the ELISA kits (Vector-Best, Russia) IL-6 (Catalog No: A-8768), IL-10 (Catalog No: A-8774) and TNF-α (Catalog No: A-8756) following the manufacturers' instructions.

2.2. Determination of the Functional Activity of Platelets. The study of induced platelet aggregation was carried out in platelet-rich plasma. Sodium citrate 3.2% was used as an anticoagulant in a ratio of 9 parts blood to 1 part stabilizer. To obtain platelet-rich plasma, the blood was immediately centrifuged for 10-12 min at 1000 rpm. One part of the resulting plasma was taken into a plastic tube and stored in a thermostat at 37°C until analysis. The second part of the plasma was subjected to further centrifugation at 4000 rpm for 20 minutes, thus obtaining platelet-poor plasma. This plasma was used to zero the optical density of the device and dilute the platelet-rich plasma. For the analysis, we took

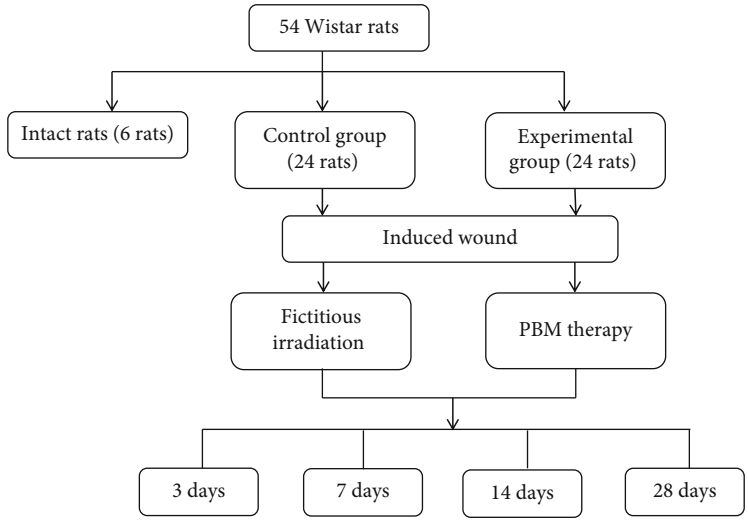

Figure 1: Study design.

Figure 2: The induced injury.

plasma, keeping the concentration of platelets to 200-250 thousand/μl or 43.5–52.5% of light transmission, relative to platelet-poor plasma. The study was carried out on a computerized analyzer of platelet aggregation SOLAR 2110 (Belarus). Adenosine diphosphate (ADP) (Tekhnologiya-Standard, Russia) at concentrations of 2.5, 5, and 10 μmol/l was used to induce aggregation. An aggregatogram recording was carried out for 10 minutes at 37° C. All studies were carried out in plasma obtained no later than 3 hours after blood sampling. The analysis of the aggregatograms included estimating the shape of the curves and determining the following: the degree of aggregation (the maximum level of plasma light transmission after the inductor was introduced), the rate of aggregation (measured over a 30-second segment at the most linear portion of the rise in the aggregation curve), and the aggregation time (the time to reach the maximum light transmission of the plasma).

2.3. Histological Analysis. After euthanasia of the animals, the wound area was surgically removed, fixed in 10% formalin, and embedded in paraffin. Subsequently, serial sections of 5-7 μm in size were obtained and stained with hematoxylin and eosin (H&E). The preparations were analyzed and photographed using a Primostar microscope (Zeiss) and a microocular digital camera.

2.4. Statistical Analysis. Statistical processing of the results was performed using Statistica 6.0 (StatSoft, USA) statistical analysis package. The descriptive data were presented as $M \pm$ SE, where M is the arithmetic mean and SE is the standard error of the arithmetic mean. The significance of differences between groups (statistical significance) was determined using the nonparametric Kruskal–Wallis test for independent samples. The significance $p < 0.05$ was considered statistically significant. Histograms were plotted by GraphPad Prism 9 (GraphPad Software, USA).

3. Results

Indicators of the degree, rate, and time of reaching the maximum rate of platelet aggregation at concentrations of the aggregation inducer 2.5, 5, and 10 μmol/l ADP are shown in Table 2.

A significant decrease in the degree and rate of platelet aggregation was observed in rats with wounds at concentrations of an aggregation inducer of 2.5, 5, and 10 μmol/l on day 3 after surgery, compared to the control group (see Table 2). The time to reach the maximum rate of

Table 1: Laser parameters.

Wavelength (nm)	Mode	Total energy	Power output (mW)	Spot area (cm^2)	Time (sec)	Energy density (J/cm^2)
660	Continuous	3.14	10	3.14	314	1.0

Table 2: . Indicators of functional activity of platelets in animals at various concentrations of adenosine diphosphate (ADP).

Indicators	Groups of animals				
	Int	Con 3 days	Exp 3 days	Con 7 days	Exp 7 days
Aggregation degree (%) 2.5 μmol/l	27.26 ± 2.44	57.73 ± 3.06	20.95 ± 5.89*	28.76 ± 1.61	23.77 ± 5.64
Aggregation time (s) 2.5 μmol/l	61.17 ± 3.46	102.33 ± 7.22	59.00 ± 4.05*	61.40 ± 2.86	66.67 ± 1.98
Aggregation rate for 30 s (%/min) 2.5 μmol/l	56.77 ± 2.05	88.00 ± 2.79	54.10 ± 6.70*	65.20 ± 2.77	52.07 ± 8.15
Aggregation degree (%) 5 μmol/l	42.28 ± 4.54	72.50 ± 0.44	33.50 ± 8.22*	45.34 ± 2.16	44.53 ± 4.96
Aggregation time (s) 5 μmol/l	108.17 ± 7.56	146.00 ± 5.25	106.33 ± 6.45*	100.60 ± 8.33	106.67 ± 3.04
Aggregation rate for 30 s (%/min) 5 μmol/l	62.77 ± 4.87	100.07 ± 2.72	57.25 ± 10.99*	71.60 ± 3.38	69.07 ± 7.05
Aggregation degree (%) 10 μmol/l	60.73 ± 1.45	78.60 ± 1.18	53.98 ± 3.77*	57.86 ± 1.53	55.93 ± 1.85
Aggregation time (s) 10 μmol/l	150.83 ± 5.25	221.67 ± 7.86	153.50 ± 9.93*	163.80 ± 6.84	201.00 ± 9.97**
Aggregation rate for 30 s (%/min) 10 μmol/l	83.05 ± 4.46	104.87 ± 3.01	72.40 ± 5.14*	76.28 ± 2.19	64.47 ± 2.81**

*$p < 0.05$ in comparison with the Con 3-day group, **$p < 0.05$ in comparison with the Con 7-day group.

aggregation, in this case, was shorter than in rats without affecting the wound defect. At the same time, on the 7th day after modeling the wounds, the study of the effect of PBM therapy on the functional activity of rats' platelets did not show any differences in the studied parameters, except for the time to reach the maximum aggregation rate at an ADP concentration of 10 μmol/l (see Table 2). The shapes of the aggregation curves (single-phase reversible aggregation) did not differ in the control and experimental groups (see Figure 3).

The concentrations of ROS, bFGF, and interleukins in the blood serum of animals whose experimental wounds were exposed to PBM therapy compared to animals that did not receive PBM therapy are presented in Figure 4.

Histological studies revealed that wound healing in the animals treated with PBM therapy is characterized by a reduction in the duration of the inflammation phase compared to the control group (see Figure 5). Microscopically, this is expressed in a smaller number of polymorphonuclear leukocytes, fibrin, and tissue detritus on day 3. At the same time, fibroblasts, newly formed collagen fibers, and vessels are noted in sufficient quantities. Such signs are characteristic of the onset of the proliferation phase. In the control group, such signs are noted on day 7 (see Figure 5(b)).

Earlier onset of the remodeling phase in the experimental group of animals is evidenced by the packing of collagen fibers into bundles and their orientation parallel to the wound surface (in accordance with the mechanical load). These signs are noted on day 7. By day 14, the granulation tissue of the animals of the experimental group has signs of transformation into scar tissue, specifically a reduction in the number of vessels and fibroblasts, the transformation of some of the fibroblasts into fibrocytes, and compaction of bundles of collagen fibers (see Figure 5(c)). By day 28 in the experimental group, the structure of the connective tissue at the site of the wound corresponded to the histoarchitectonics of the dermis of normal skin: the thickness and location of collagen fiber bundles, the presence of hair follicles and sebaceous glands, and the absence of newly formed vessels and fibroblast proliferation. Collagen fiber bundles had a greater thickness and packing density compared to the control group. The animals of the control group showed signs of the continuation of the remodeling phase in the central sections of the wound: the presence of a significant number of fibroblasts, newly formed vessels, chaotically located, with thin collagen fibers. That is, the connective tissue was immature, and the remodeling process continued with the formation of first scar tissue and then the dermis.

In general, the results of histological examination indicate a positive effect of PBM therapy with the applied parameters on the repair processes of chronic wounds.

4. Discussion

The choice of radiation parameters for PBM therapy is an important task. An inappropriate choice of parameters leads

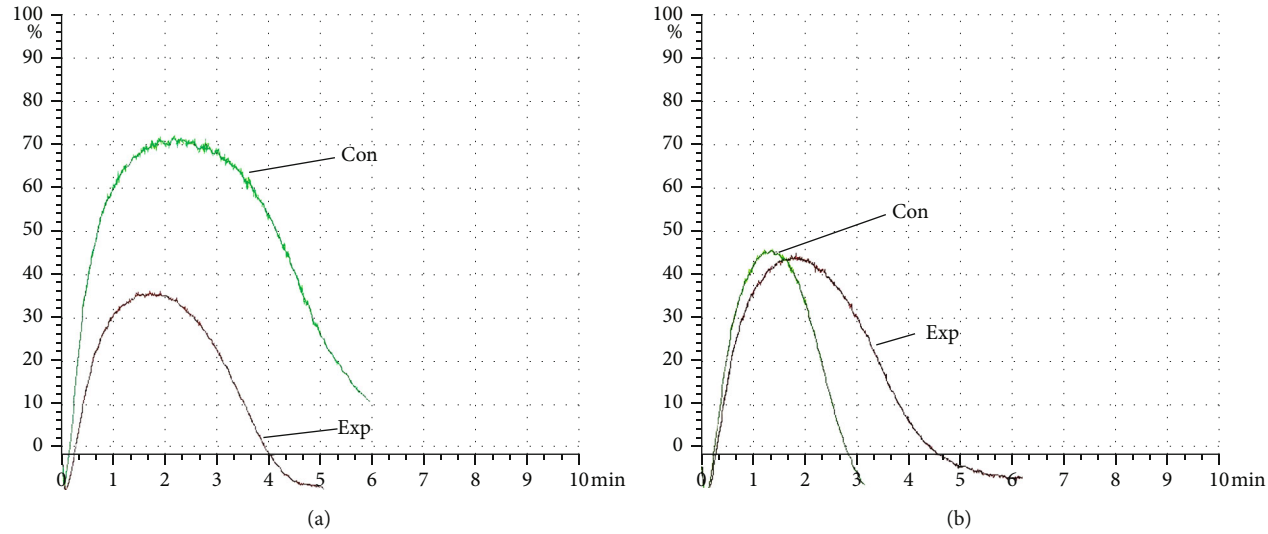

Figure 3: An example of the shape of the aggregation curves for animals in the control and experimental groups on day 3 (a) and day 7 (b) after surgery at an ADP concentration of 5 μmol/l.

to unsatisfactory results or even to a negative therapeutic effect [11].

Considering that the new term "photobiomodulation therapy" is designated as "a form of light therapy…in the visible and infrared spectrum…" [12]; in previously published studies, we analyzed the effects of PBM therapy on wound regeneration processes. Wavelengths in the 600 or 800 nm range with daily laser exposure have been shown to be most beneficial in rodent studies, regardless of health condition or wound type [13]. The optimal therapeutic dose when using laser therapy in an open wound is from 0.5 J/cm^2 to 1 J/cm^2 [14]. Improved healing of experimental wounds in rats has been demonstrated using PBM therapy with a wavelength of 660 nm and energy densities of 1 and 5 J/cm^2 [15].

The frequency and number of PBM therapy sessions vary in the literature from one to several dozen [13]. A review by Ebrahimi et al. showed that the frequency of irradiation sessions is 3–8 times [16]. In our work, PBM therapy was applied daily for 5 days, starting the day after surgery. Literature data indicate that primary effects resulting from laser stimulation, such as an increase in the number of fibroblasts, myofibroblasts, and collagen expression, are present even after interruption of PBM therapy. Thus, after four treatment sessions carried out in the first days after wound induction, a more pronounced expression of collagen fibers was observed in rats receiving PBM therapy, compared with the control group on days 14 and 21 [17]. The results of another study also demonstrate accelerated maturation and increased collagen deposition and better architecture of final fibrous scarring at 21 days after injury, following daily application of PBM therapy during the first 7 days after wound induction [18]. In our work, we investigated the effect of PBM therapy, applied in the first 5 days after wound modeling, on the reparation processes of chronic wounds at all stages of wound healing, including the long-term effects of this method on days 14 and 28.

Taking into account the two-phase dose-effect curve [19], we applied other radiation parameters on the wound model already used in our studies [20]: radiation power of 10 mW at an energy density of 1 J/cm^2 and a wavelength of 660 nm.

Since it is the reaction of the body as an integral system that often determines the outcome of the wound healing process (for example, in patients with diabetes), this study focused on the effect of local exposure by PBM therapy on the features of the body's response. The systemic body response, in turn, affects the local processes in the wound. Many studies have been devoted to the study of local processes directly in the wound, including by methods of immunohistochemistry. But the effect of PBM therapy on the healing of chronic wounds at the systemic level has not been adequately studied, justifying the choice of research methods utilized here.

The first response to tissue damage in the body is hemostasis. Platelets are known to be an integral part of hemostasis, but these cells also function as a physiological trigger to activate inflammation [21]. Therefore, the aggregation activity of platelets was studied in our work at the initial stages of healing. On day 3 after modeling the wound, platelet aggregation activity was increased compared to intact animals. Our results are comparable to the literature data on platelet hyperactivity in mice with impaired wound healing [22]. The platelet aggregation activity in mice was studied in pooled blood samples. We, having the opportunity to obtain a larger volume of blood in rats, investigated the aggregation activity of platelets in each animal. The use of PBM therapy in our study helped to reduce the degree, speed, and time to reach the maximum rate of aggregation for a period of 3 days after wound modeling. This is apparently due to the ability of PBM therapy to activate anti-inflammatory regulatory pathways. In our work, no differences were found in the aggregation activity of platelets between the experimental and control groups 7 days after wound simulation. Similar results were obtained in our previous study on the third day after surgery with the same wound model and similar parameters of the applied radiation (wavelength, energy density), except that the study used a radiation power of

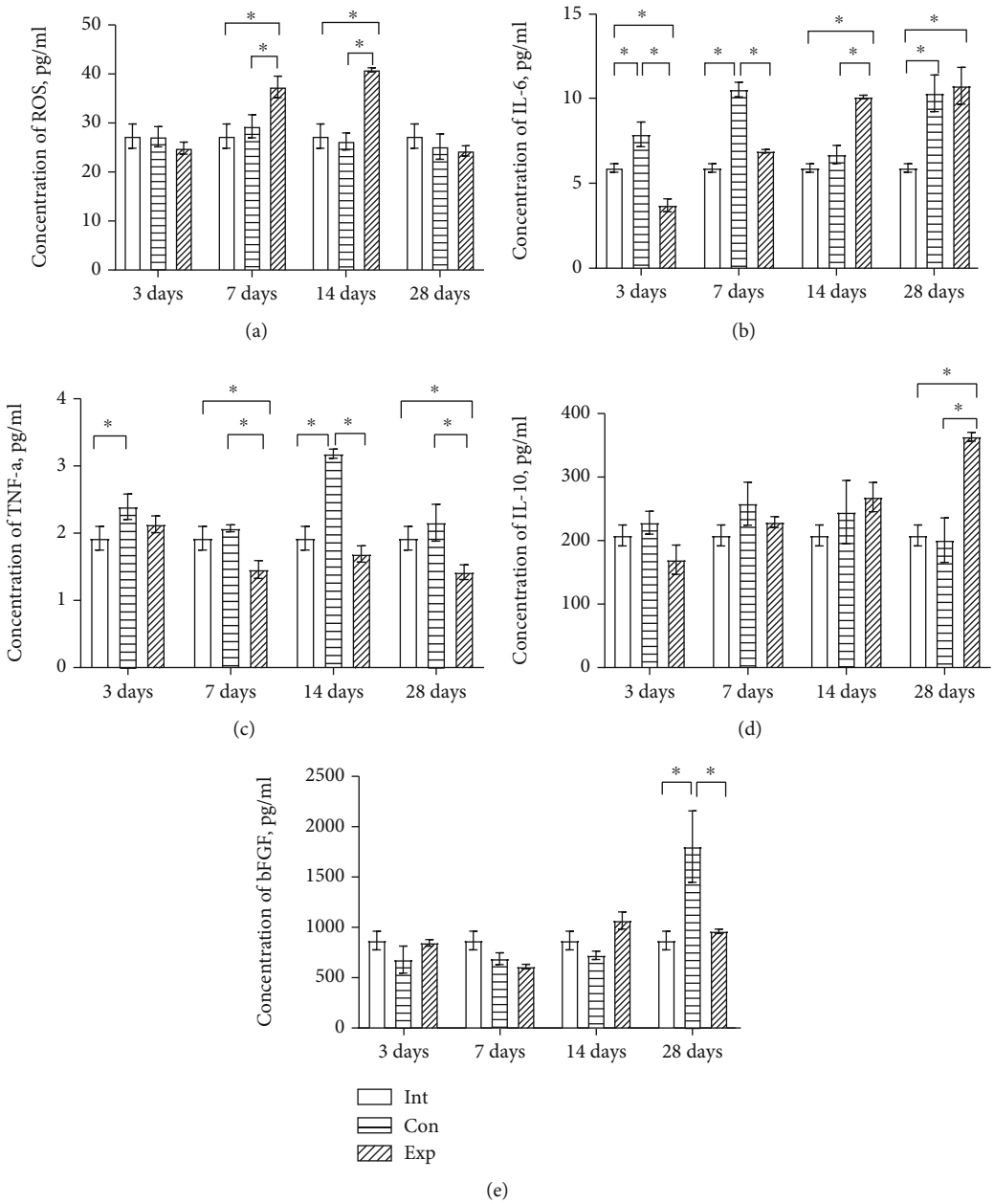

Figure 4: Levels of the studied indicators in the blood serum of animals: (a) ROS, (b) IL-6, (c) TNF-α, (d) IL-10, and (e) bFGF ($^*p < 0.05$). Int: intact animals; Con: control group; Exp: experimental group. The error bars represent the standard error of the arithmetic mean for each indicator ($n = 6$).

50 mW. However, on the 7th day after modeling the wound, an increase in platelet aggregation activity was observed [23]. This effect is apparently associated with the ability of PBM therapy to inhibit or resolve the inflammatory process [24], as well as with the pro- and anti-inflammatory functions of the platelets themselves [25].

In the regulation of platelet function, reactive oxygen species and mitochondria play a key role [26]. In our work, it was found that the action of PBM therapy on a wound defect leads to an increase in ROS levels 7 and 14 days after wound modeling. The literature provides data on an increase in the generation of ROS after PBM therapy at a wavelength of 660 nm [27]. In the same work, it was shown that different wavelengths have an opposite effect on the production of ROS. Many of the biological effects of PBM are attributed to the absorption of photons by chromophores located inside the mitochondria, which leads to an increase in cellular metabolic activity. Moreover, many of the mechanistic pathways for mediating the biological effects of PBM include ROS [28]. The induction of safe ROS levels observed in our study may be one of the mechanisms by which the signaling pathways that regulate cell proliferation, differentiation, and apoptosis are activated.

ROS are also important regulators of inflammation [29]. It was found that the formation of ROS originating from mitochondria induces the activation of proinflammatory

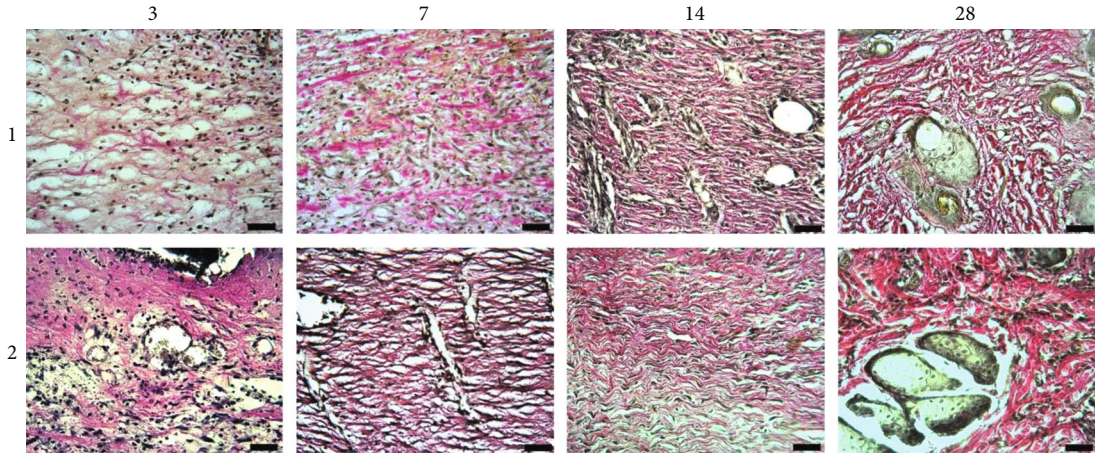

Figure 5: Animal wound sites: 1: control group ((a) on day 3, among fibrins, there are numerous polymorphonuclear leukocytes, single fibroblasts, and collagen fibers; (b) on day 7, young granulation tissue with a moderate number of polymorphonuclear leukocytes, fibroblasts and blood vessels, and chaotic collagen fibers; (c) on the 14th day, granulation tissue with signs of maturation in the form of parallel orientation and thickening of collagen fiber bundles, the presence of fibrocytes, and single vessels; (d) on the 28th day, the newly formed dermis); 2: experimental group ((a) on day 3, young granulation tissue with a moderate number of fibroblasts and polymorphonuclear leukocytes, randomly located collagen fibers, and numerous vessels; (b) on day 7, granulation tissue with a moderate number of fibroblasts, numerous vessels, and parallel bundles of collagen fibers; (c) on the 14th day, maturing granulation tissue with parallel bundles of collagen fibers, fibrocytes, and single vessels; (d) on the 28th day, the newly formed dermis with dense bundles of collagen fibers) (H&E, ×400, scale bar 50 μm).

cytokines IL-1, IL-6, and TNF-α[30]. In our study, the decrease in IL-6 levels in the experimental groups in the initial phases of healing and TNF-α throughout the entire wound healing process appears to be due to the anti-inflammatory effect of PBM therapy at the systemic level.

Proinflammatory cytokines must perform an obligatory part of the inflammatory process because insufficient inflammation can lead to delayed healing. On the other hand, chronic wounds remain indefinitely in the inflammatory stage of wound healing [31]. To continue the healing process, each phase, upon completion of its functions, must be able to initiate the next stage (for example, resolution of inflammation shifts the process towards the proliferation phase), which is then able to turn off the previous one. Phase switching using positive and negative feedback loops is carried out by cytokines and growth factors [32]. Regulation of the levels of these intercellular mediators by PBM therapy can promote the progression of wound healing processes and prevent inhibition of progression into the next phase.

Proinflammatory cytokines are also thought to mediate cell proliferation and differentiation during wound healing. Thus, in our work, when a wound defect was exposed to low-intensity laser radiation, an increase in IL-6 levels was observed at the stage of the transition from proliferation to remodeling, which may be associated with its anti-inflammatory and regenerating properties. The ability of this pleiotropic cytokine to stimulate the formation of granulation tissue, mechanisms of reepithelialization, angiogenesis, infiltration, and cell remodeling has been previously discovered [33]. There are a limited number of studies in the literature demonstrating the effect of PBM therapy on IL-6 levels in cutaneous pathology. The increase in the levels of this cytokine in the early stages of wound healing, demonstrated by Mo et al. [34], and the decrease in IL-6 concentrations after 14 and 30 days of treatment for pressure ulcers, shown by Taradaj et al. [35], do not coincide with our data. This is probably due to the difference in wound models and the studied parameters (local or systemic levels), as well as the parameters of the applied PBM therapy.

TNF-α, like IL-6, has both proinflammatory and immunoregulatory properties. TNF-α provides a wide spectrum of cellular responses including regulation of inflammation, immune response, cell survival, proliferation, and apoptosis [36]. An increase in the formation of granulation tissue and a better arrangement of collagen fibers found in histological studies of wounds in the experimental group may be associated with a decrease in the levels of the cytokine TNF-α observed in our work [37]. Our results are comparable to the literature data, in which exposure to PBM therapy led to a decrease in the levels of the pleiotropic cytokine TNF-α[34, 35, 38, 39].

The anti-inflammatory cytokine IL-10 also facilitates the transition from the inflammatory to the proliferative phase by regulating cytokine expression [40]. PBM therapy used in our work increases the levels of IL-10 in the serum of rats as inflammation decreases. This confirms the ability of PBM, in the absence of inflammation, to provide proinflammatory mediators that could help in tissue remodeling [41].

The improvement in skin regeneration of the animals of the experimental group, observed in our study, is apparently due, inter alia, to the pleiotropic effects of IL-10, including regulation of the formation of the extracellular matrix, modulation of fibroblast function, and differentiation and increased content of endothelial progenitor cells (EPC) in the wound [42]. Considering also the ability of IL-10 to counteract the deposition of collagen in scars [43], the

regulation of levels of this cytokine by PBM therapy promotes better organization of collagen fibers, which is confirmed by our histological analysis.

Collagenogenesis is stimulated by a number of factors, including the fibroblast growth factor (FGF). bFGF is known to be a potent mitogen and chemoattractant for endothelial cells and fibroblasts. This growth factor also accelerates the formation of granulation tissue and induces reepithelialization [41]. The decrease in the maximum concentration of bFGF, observed in the blood of animals of the experimental group on day 28 after exposure to PBM therapy, apparently indicates an earlier transition of the wound healing process in the experimental group of animals to the remodeling phase. At the stage of remodeling, the number of macrophages and fibroblasts decreases due to apoptosis and regression of the new vasculature occurs, with the further transformation of granulation tissue into scar tissue [44]. The literature contains studies on the effect of PBM therapy on bFGF expression: PBM therapy stimulates the release of bFGF from human skin fibroblasts [45] and increases the concentration of this growth factor at the initial stages of wound healing [23]. The change in bFGF levels upon exposure to PMB therapy of 630 nm, an energy density of 3.6 J/cm^2 on wounds of diabetic rats, depending on the radiation power and the timing of the wound defect, was demonstrated by Ma et al. [46].

Thus, in our study, the use of PBM therapy in the treatment of chronic wounds resulted in systemic effects. There was a decrease in platelet aggregation activity in the inflammatory phase. At all phases of the healing process, the use of this method of treatment resulted in a change in the expression of biologically active substances. The impact of PBM therapy applied locally to the wound resulted in the following changes in the central blood flow: a decrease in IL-6 levels and an increase in ROS levels in the inflammatory phase and during the transition from the inflammatory phase to the proliferation phase; an increase in IL-6 levels during the transition from the proliferation phase to the remodeling phase; a decrease in TNF-α levels during the transition from the inflammatory phase to the proliferation phase and further, up to the remodeling phase; and an increase in IL-10 levels and a decrease in bFGF concentration in the remodeling phase.

We believe that optimization of the activity of these biomarkers at the systemic level—as observed in our study—may be one of the mechanisms by which PBM therapy stimulates the processes of chronic wound repair. The study of systemic reactions, we hope, will make it possible in the future to develop approaches to correct violations of the repair process, supplementing the local effect of laser radiation on the wound with correction at the systemic level.

5. Conclusions

The results obtained in our study indicate the ability of PBM therapy to positively influence the reparation processes of chronic wounds.

The results of the histological study indicate a positive effect of PBM therapy with the applied parameters on the healing of chronic wounds, which is expressed in the acceleration of the repair processes at all phases of healing.

PBM therapy can be used to regulate wound healing processes by modulating the levels of ROS; cytokines TNF-α, IL-6, and IL-10; and bFGF.

Further research is needed to optimize radiation parameters.

Data Availability

The authors are ready to provide the main data confirming the results of the study on request.

Conflicts of Interest

The authors declare that there is no conflict of interest regarding the publication of this article.

Acknowledgments

This study was funded by the Ministry of Health of Ukraine from the state budget and was a fragment of the research work "Peculiarities of Cellular-Molecular Mechanisms of Activation of Reparative Processes in Case of Tissue Damage against the Background of a Decrease in Adaptation Reserves Characteristic of Emergency Situations" (state registration number 0120U101408).

References

[1] E. Mester, T. Spiry, B. Szende, and J. G. Tota, "Effect of laser rays on wound healing," *American Journal of Surgery*, vol. 122, no. 4, pp. 532–535, 1971.

[2] F. S. Cardoso, R. Á. B. Lopes Martins, and S. Gomes da Silva, "Therapeutic Potential of Photobiomodulation In Alzheimer's Disease: A Systematic Review: Photobiomodulation in Alzheimer's Disease," *Journal of Lasers in Medical Sciences*, vol. 11, Supplement 1, pp. S16–S22, 2020.

[3] S. S. Tomazoni, L. O. P. Costa, J. Joensen et al., "Photobiomodulation therapy is able to modulate PGE2Levels in patients with chronic non-specific low back pain: a randomized placebo-controlled trial," *Lasers in Surgery and Medicine*, vol. 53, no. 2, pp. 236–244, 2021.

[4] J. Ward, J. Holden, M. Grob, and M. Soldin, "Management of wounds in the community: five principles," *British Journal of Community Nursing*, vol. 24, Supplement 6, pp. S20–S23, 2019.

[5] L. E. Lindley, O. Stojadinovic, I. Pastar, and M. Tomic-Canic, "Biology and biomarkers for wound healing," *Plastic and Reconstructive Surgery*, vol. 138, Supplement 3, pp. 18S–28S, 2016.

[6] L. Deng, C. du, P. Song et al., "The role of oxidative stress and antioxidants in diabetic wound healing," *Oxidative medicine and cellular longevity*, vol. 2021, Article ID 8852759, 11 pages, 2021.

[7] I. Khan and P. Arany, "Biophysical approaches for oral wound healing: emphasis on photobiomodulation," *Advances in Wound Care*, vol. 4, no. 12, pp. 724–737, 2015.

[8] N. Houreld, "Healing effects of photobiomodulation on diabetic wounds," *Applied Sciences*, vol. 9, no. 23, article 5114, 2019.

[9] D. G. Sami, H. H. Heiba, and A. Abdellatif, "Wound healing models: a systematic review of animal and non-animal models," *Wound Medicine*, vol. 24, no. 1, pp. 8–17, 2019.

[10] R. M. Zinatullin, T. R. Gizatullin, V. N. Pavlov et al., "Method for simulating trophic wound in experiment," in *RF patent No. 2510083 C1*, Federal Service for Intellectual Property (Rospatent), Ufa, Russia, 2014.

[11] M. B. Stausholm and J. M. Bjordal, "Neglect of relevant treatment recommendations in the conduct and reporting of a laser therapy knee osteoarthritis trial: letter to the editor," *BMC musculoskeletal disorders*, vol. 22, no. 1, p. 71, 2021.

[12] J. J. Anders, R. J. Lanzafame, and P. R. Arany, "Low-level light/laser therapy versus photobiomodulation therapy," *Photomedicine and Laser Surgery*, vol. 33, no. 4, pp. 183-184, 2015.

[13] A. Lopez and C. Brundage, "Wound photobiomodulation treatment outcomes in animal models," *Journal of Veterinary Medicine*, vol. 2019, Article ID 6320515, 9 pages, 2019.

[14] J. Tunér and L. Hode, *Laser Therapy – Clinical Practice and Scientific Background*, Prima Books AB, Grangesberg, Sweden, 2002.

[15] R. Suzuki and K. Takakuda, "Wound healing efficacy of a 660-nm diode laser in a rat incisional wound model," *Lasers in Medical Science*, vol. 31, no. 8, pp. 1683–1689, 2016.

[16] P. Ebrahimi, M. Hadilou, F. Naserneysari et al., "Effect of photobiomodulation in secondary intention gingival wound healing—a systematic review and meta-analysis," *BMC Oral Health*, vol. 21, no. 1, 2021.

[17] T. Fortuna, A. C. Gonzalez, M. F. Sá, Z. . A. Andrade, S. R. A. Reis, and A. R. A. P. Medrado, "Effect of 670 nm laser photobiomodulation on vascular density and fibroplasia in late stages of tissue repair," *International Wound Journal*, vol. 15, no. 2, pp. 274–282, 2018.

[18] J. L. S. Cunha, F. M. A. de Carvalho, R. N. Pereira Filho, M. A. G. Ribeiro, and R. L. C. de Albuquerque-Júnior, "Effects of different protocols of low-level laser therapy on collagen deposition in wound healing," *Brazilian Dental Journal*, vol. 30, no. 4, pp. 317–324, 2019.

[19] Y. Y. Huang, A. C. Chen, J. D. Carroll, and M. R. Hamblin, "Biphasic dose response in low level light therapy," *Dose–Response*, vol. 7, no. 4, pp. 358–383, 2009.

[20] S. B. Pavlov, N. M. Babenko, M. V. Kumetchko, O. B. Litvinova, N. G. Semko, and R. N. Mikhaylusov, "The influence of photobiomodulation therapy on chronic wound healing," *Romanian reports in physics*, vol. 72, article 609, 2020.

[21] W. R. Parrish and B. Roides, "Physiology of blood components in wound healing: an appreciation of cellular co-operativity in platelet rich plasma action," *Journal of Exercise, Sports & Orthopedics*, vol. 4, no. 2, pp. 1–14, 2017.

[22] S. Dhall, Z. A. Karim, F. T. Khasawneh, and M. Martins-Green, "Platelet hyperactivity inTNFSF14/LIGHTKnockout mouse model of impaired healing," *Advances in Wound Care*, vol. 5, no. 10, pp. 421–431, 2016.

[23] N. Babenko and S. Pavlov, "Effects of low-level laser therapy on reactive oxygen species, platelet aggregation activity, and the expression of growth factors in the process of regeneration of chronic wounds," *Annals of the Romanian Society for Cell Biology*, vol. 25, no. 4, pp. 2226–2234, 2021.

[24] R. A. B. Lopes-Martins, P. S. Leonardo, J. M. Bjordal, and R. L. Marcos, "Photobiomodulation: inhibition or resolution of the inflammatory process?," *Photobiomodulation, photomedicine, and laser surgery*, vol. 38, no. 8, pp. 453-454, 2020.

[25] A. Margraf and A. Zarbock, "Platelets in inflammation and resolution," *Journal of Immunology (Baltimore, Md. : 1950)*, vol. 203, no. 9, pp. 2357–2367, 2019.

[26] E. Masselli, G. Pozzi, M. Vaccarezza et al., "ROS in platelet biology: functional aspects and methodological insights," *International journal of molecular sciences*, vol. 21, no. 14, article ???, 2020.

[27] K. Rupel, L. Zupin, A. Colliva et al., "Photobiomodulation at multiple wavelengths differentially modulates oxidative stress in vitro and in vivo," *Oxidative medicine and cellular longevity*, vol. 2018, Article ID 6510159, 2018.

[28] M. R. Hamblin, "Mechanisms and mitochondrial redox signaling in photobiomodulation," *Photochemistry and Photobiology*, vol. 94, no. 2, pp. 199–212, 2018.

[29] R. Mehling, J. Schwenck, C. Lemberg et al., "Immunomodulatory role of reactive oxygen species and nitrogen species during T cell-driven neutrophil-enriched acute and chronic cutaneous delayed-type hypersensitivity reactions," *Theranostics*, vol. 11, no. 2, pp. 470–490, 2021.

[30] E. Naik and V. M. Dixit, "Mitochondrial reactive oxygen species drive proinflammatory cytokine production," *The Journal of Experimental Medicine*, vol. 208, no. 3, pp. 417–420, 2011.

[31] P. Krzyszczyk, R. Schloss, A. Palmer, and F. Berthiaume, "The role of macrophages in acute and chronic wound healing and interventions to promote pro-wound healing phenotypes," *Frontiers in physiology*, vol. 9, article 419, 2018.

[32] N. B. Menke, K. R. Ward, T. M. Witten, D. G. Bonchev, and R. F. Diegelmann, "Impaired wound healing," *Clinics in Dermatology*, vol. 25, no. 1, pp. 19–25, 2007.

[33] Y. Feng, A. J. Sanders, L. D. Morgan, K. G. Harding, and W. G. Jiang, "Potential roles of suppressor of cytokine signaling in wound healing," *Regenerative Medicine*, vol. 11, no. 2, pp. 193–209, 2016.

[34] S. Mo, P. S. Chung, and J. C. Ahn, "630 nm-OLED accelerates wound healing in mice via regulation of cytokine release and genes expression of growth factors," *Current Optics and Photonics*, vol. 3, no. 6, pp. 485–495, 2019.

[35] J. Taradaj, B. Shay, R. Dymarek et al., "Effect of laser therapy on expression of angio- and fibrogenic factors, and cytokine concentrations during the healing process of human pressure ulcers," *International Journal of Medical Sciences*, vol. 15, no. 11, pp. 1105–1112, 2018.

[36] N. Petryk and O. Shevchenko, "Mesenchymal stem cells anti-inflammatory activity in rats: proinflammatory cytokines," *Journal of Inflammation Research*, vol. Volume 13, pp. 293–301, 2020.

[37] M. B. Serra, W. A. Barroso, N. N. . Silva et al., "From inflammation to current and alternative therapies involved in wound healing," *International journal of inflammation*, vol. 2017, Article ID 3406215, 17 pages, 2017.

[38] G. K. Keshri, A. Gupta, A. Yadav, S. K. Sharma, and S. B. Singh, "Photobiomodulation with pulsed and continuous wave near-infrared laser (810 nm, Al-Ga-As) augments dermal wound healing in immunosuppressed rats," *PLoS One*, vol. 11, no. 11, article e0166705, 2016.

[39] A. N. Otterço, A. L. Andrade, P. Brassolatti, K. N. Z. Pinto, H. S. S. Araújo, and N. A. Parizotto, "Photobiomodulation mechanisms in the kinetics of the wound healing process in

rats," *Journal of Photochemistry and Photobiology B: Biology*, vol. 183, pp. 22–29, 2018.

[40] S. Willenborg and S. A. Eming, "Macrophages – sensors and effectors coordinating skin damage and repair," *Journal of the German Society of Dermatology: JDDG*, vol. 12, no. 3, pp. 214–223, 2014.

[41] L. F. de Freitas and M. R. Hamblin, "Proposed mechanisms of photobiomodulation or low-level light therapy," *IEEE journal of selected topics in quantum electronics: a publication of the IEEE Lasers and Electro-optics Society*, vol. 22, no. 3, article 7000417, 2016.

[42] A. King, S. Balaji, L. D. Le, T. M. Crombleholme, and S. G. Keswani, "Regenerative wound healing: the role of interleukin-10," *Advances in Wound Care*, vol. 3, no. 4, pp. 315–323, 2014.

[43] K. L. Singampalli, S. Balaji, X. Wang et al., "The role of an IL-10/hyaluronan axis in dermal wound healing," *Frontiers in cell and developmental biology*, vol. 8, article 636, 2020.

[44] M. Rodrigues, N. Kosaric, C. A. Bonham, and G. C. Gurtner, "Wound healing: a cellular perspective," *Physiological Reviews*, vol. 99, no. 1, pp. 665–706, 2019.

[45] M. Esmaeelinejad and M. Bayat, "Effect of low-level laser therapy on the release of interleukin-6 and basic fibroblast growth factor from cultured human skin fibroblasts in normal and high glucose mediums," *Journal of cosmetic and laser therapy : official publication of the European Society for Laser Dermatology*, vol. 15, no. 6, pp. 310–317, 2013.

[46] H. Ma, Y. Li, H. Chen, M. Kang, and T. C. Y. Liu, "Effects of low-intensity laser irradiation on wound healing in diabetic rats," *International Journal of Photoenergy*, vol. 2012, Article ID 838496, ll pages, 2012.

Hindawi
International Journal of Photoenergy
Volume 2021, Article ID 5578387, 9 pages
https://doi.org/10.1155/2021/5578387

Research Article

Photodynamic Therapy in the Extracellular Matrix of Mouse Lungs: Preliminary Results of an Alternative Tissue Sterilization Process

Luis Vicente Franco Oliveira,[1] **Nadua Apostólico**,[2] **Juan José Uriarte**,[3] **Renata Kelly da Palma**,[4,5] **Renato A. Prates**,[6] **Alessandro Melo Deana**,[6] **Luis Rodolfo Ferreira**,[6] **João Pedro Ribeiro Afonso**,[1] **Rodolfo de Paula Vieira**,[7,8] **Manoel Carneiro de Oliveira Júnior**,[8] **Daniel Navajas**,[3] **Ramon Farré**,[3] **and Rodrigo Alvaro B. Lopes-Martins**[1,7]

[1]*Human Movement and Rehabilitation (PPGMHR), University Center of Anápolis (UniEVANGÉLICA), Anápolis, GO, Brazil*
[2]*Rehabilitation Sciences, Nove de Julho University (UNINOVE), Sao Paulo, SP, Brazil*
[3]*Unitat de Biofísica i Bioenginyeria, Facultat de Medicina, Universitat de Barcelona (UB), Barcelona, Spain*
[4]*Faculdade de Medicina Veterinária e Zootecnia da Universidade de São Paulo, São Paulo, SP, Brazil*
[5]*Biomimetic Systems for Cell Engineering, Institute for Bioengineering of Catalonia (IBEC), Barcelona, Spain*
[6]*Master's and Doctoral Degree Programs in Biophotonics Applied to Health Sciences, Nove de Julho University (UNINOVE), São Paulo, SP, Brazil*
[7]*Postgraduate Program in Bioengineering, Universidade Brasil, São Paulo, SP, Brazil*
[8]*Brazilian Institute of Teaching and Research in Pulmonary and Exercise Immunology (IBEPIPE), São José dos Campos, SP, Brazil*

Correspondence should be addressed to Luis Vicente Franco Oliveira; oliveira.lvf@gmail.com

Received 12 January 2021; Accepted 21 May 2021; Published 29 May 2021

Academic Editor: Umapada Pal

Copyright © 2021 Luis Vicente Franco Oliveira et al. This is an open access article distributed under the Creative Commons Attribution License, which permits unrestricted use, distribution, and reproduction in any medium, provided the original work is properly cited.

Lung transplantation is one of the most difficult and delicate procedures among organ transplants. For the success of the procedure and survival of the new organ, the sterilization step for acellular lungs prior to recellularization is important to ensure that they are free of any risk of transmitting infections from the donor to the recipient subject. However, there are no available information concerning the lung mechanical parameters after sterilizing photodynamic therapy. The aim of this study was to evaluate the extracellular matrix (ECM) and lung mechanical parameters of decellularized lungs undergoing sterilizing photodynamic therapy (PDT). Besides, we also analyzed the lung after controlled infection with *C. albicans* in order to evaluate the effectiveness of PDT. The lung mechanical evaluation parameters, resistance (R_L) and elastance (E_L), exhibited no significant differences between groups. In addition, there were no PDT-induced changes in lung properties, with maintenance of the viscoelastic behavior of the lung scaffold after 1 h exposure to PDT. The ECM components remained virtually unchanged in the acellular lungs of both groups. We also showed that there was a reduction in fungal infection population after 45 minutes of PDT. However, more studies should be performed to establish and verify the effectiveness of PDT as a possible means for sterilizing lung scaffolds. This manuscript was presented as a master thesis of Nadua Apostólico at the postgraduate program in rehabilitation sciences, University Nove de Julho—UNINOVE.

1. Introduction

According to the World Health Organization (WHO), organ transplantation is frequently the only treatment for end-state organ failure, such as liver, lung, and heart failure. However, as a biomaterial, all implanted or transplanted material from human origin presents serious risks of several disease transmissions. Besides the biological risks, the extremely low availability of organ/tissue donors is the most important restriction for such procedures all over the world. In this scenario, tissue engineering has emerged as an alternative that is aimed at developing functional tissue substitutes with the goal of improving health and quality of life in terminal patients.

Tissue engineering has the specific target of promoting regeneration of structures and functions of tissues/organs compromised by disease or surgery. Research in the field of lung bioengineering has been particularly active in recent years due to the lack of viable lungs designated to transplant and the reduced long-term patient survival after transplantation [1, 2].

An important step in handling acellular lungs before they are subjected to recellularization is sterilization to suppress any risk of transmission of viruses or bacteria from the donor to the receiver of the transplanted tissue/organ. Indeed, potential transmission of infections, such as HIV and hepatitis C, has been reported in tissue engineering applications [3–5]. Therefore, the effects of different sterilization methods on a variety of tissue types have been studied to determine the optimal procedures. To this end, it is imperative to take into account that aggressive sterilization methods that ensure full elimination of pathogens may also deteriorate the structural components of the tissue, specifically its mechanical performance [6, 7].

Not all sterilization methods used in the health industry are applicable to bioscaffolds. At first, sterilization methods, such as those based on gamma irradiation, ethylene oxide, or other chemical agents, could be used. However, all sterilization procedures have their side effects, since any action to destroy infectious microorganisms at the same time can affect the different structures of the molecular scaffold.

It has been reported that both ethylene oxide and irradiation can interact with molecules and scaffolds and potentially degrade their function. It has recently been suggested that peracetic acid (PAA) can be a useful chemical agent for sterilizing scaffolds for tissue engineering [8]. However, it was not fully effective to sterilize pulmonary scaffolds [9].

Thus, appropriate sterilization procedures that preserve the mechanical properties of lung scaffolds after decellularization are essential for safe repopulation. Particularly, photodynamic therapy (PDT) could be a tool for obtaining viable lung scaffolds necessary for the repopulation process [10, 11].

The PDT was discovered in 1900 by Oscar Raab and Hermann Von Tappeiner [12], who found that *Paramecium* spp. protozoans were killed following acridine orange staining and subsequent exposure to bright light [13]. In the 1970's, PDT was initially developed to be used in cancer therapy after it was discovered that porphyrins selectively localized in tumors [14]. Since then, PDT has been clinically used for the treatment of various malignancies and is an approved therapy for the destruction of choroidal neovascularization (CNV) in age-related macular degeneration. Recently, antimicrobial PDT has been proposed as an alternative approach for treating localized infections [12–16].

A photosensitizer plays a key role in the efficacy of PDT. Protoporphyrin IX (PpIX) is actively transported into the cell through an uptake mechanism induced by growth under nutritionally restrictive conditions. For instance, in *C. albicans*, the surface properties and composition are complex and dynamic and hydrophobicity is one of the many potential factors that may influence uptake. Previous studies demonstrated that filamentous forms and biofilms of *Candida albicans* were sensitive to PDT using porphyrin as a photosensitizer [17–19].

Understanding the mechanical consequences of lung scaffold sterilization is particularly relevant since the lung is an organ with high structural and mechanical complexity that is physiologically subjected to continuous deformation cycling during breathing. Therefore, the mechanical properties of the organ scaffold should be preserved as much as possible after sterilization to ensure optimal organ regeneration. However, studies concerning the efficacy of PDT in the sterilization of lung scaffolds and its repercussions on the mechanical properties are lacking. Thus, the aim of this study was to evaluate the extracellular matrix and lung mechanical parameters of decellularized lungs undergoing PDT with the purpose of sterilization and to perform a proof of concept of microbiological analyses of lungs infected with *Candida albicans* to determine the effectiveness of PDT.

2. Material and Methods

2.1. Experimental Animals. Male C57BL/6 mice (7–8 weeks old) were kept under standard housing conditions in ventilated rooms (12 h light-dark cycles, temperature at 23°C, and 60–70% humidity), with food and water provided *ad libitum*. Experimental procedures were carried out after submission and approvals by the Ethical Committee for Animal Research of the Universitat de Barcelona and by the Research Ethics Committee of Universidade Nove de Julho (UNINOVE) (protocol 0038/2011).

2.2. Experimental Setting. This study was divided into two phases: phase 1—decellularized mice lungs were mechanically evaluated and the extracellular matrix morphology was assessed before and after PDT and phase 2—decellularized mice lungs experimentally contaminated with *C. albicans* (ATCC 90028) were submitted to PDT; microbiological analyses were performed to evaluate the efficacy of PDT on *C. albicans* decontamination (Figure 1).

The animals were weighed, intraperitoneally anesthetized with 1.0 g/kg urethane, and sacrificed by exsanguination. Immediately, lungs were perfused via the pulmonary artery with phosphate-buffered saline (PBS) containing 50 U/mL heparin (Sigma-Aldrich, St. Louis, MO, USA) and 1 μg/mL sodium nitroprusside (SNP) (Fluka Analytical, St. Louis, MO, USA) to prevent the formation of blood clots. Then,

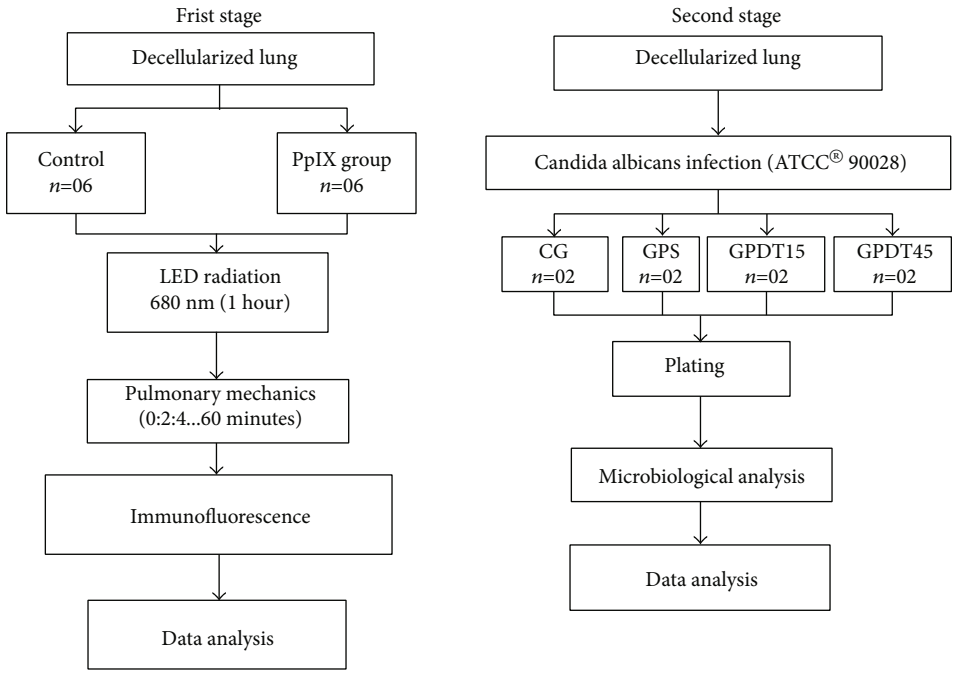

Figure 1: Flowchart of the study.

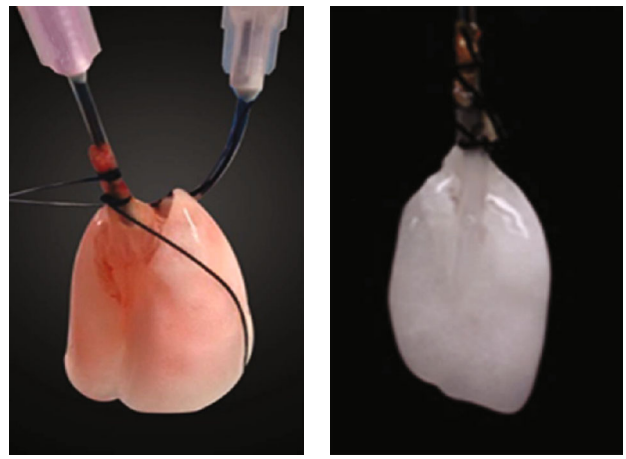

(a) (b)

Figure 2: Decellularization process of the lungs. (a) Perfusion of the lungs with reagents through the trachea and the pulmonary artery. (b) Decellularized lungs.

the lungs and heart were removed together with the trachea and esophagus. The whole block was stored at −80°C until the decellularization protocol was performed.

2.3. Lung Decellularization. At the day of the experiment, the tissues were thawed decellularized as previously described [20]. Briefly, once the trachea and pulmonary artery were cannulated (Figure 2(a)) and placed into the experimental system, the following sequence of reagents was perfused: PBS for 30 min, deionized water (DI) for 15 min, 0.1% triton for 30 min, DI for 5 min, 1% sodium dodecyl sulfate (SDS) for 150 min, and a final wash of PBS for 30 min, resulting in a translucent acellular lung (Figure 2(b)).

2.4. Addition of a Photosensitizer and Sterilization with Red LED (660 nm). The first set of experiments consisted in a test to prove that PDT would be able to quell a controlled infection with *C. albicans*. A number of 12 decellularized mouse lungs were randomly divided into two groups of six animals: a group injected with protoporphyrin IX (group PpIX or GPpIX) and a control group injected with PBS (control). For the second stage, a total of eight decellularized mice lungs were randomly divided into four groups, each containing two animals: a control group of infected mice (CG), a group treated with PpIX (group photosensitizer or GPS), a group treated with PDT for 15 minutes (group PDT 15 minutes or GPDT15), and a group treated with PDT for 45 min

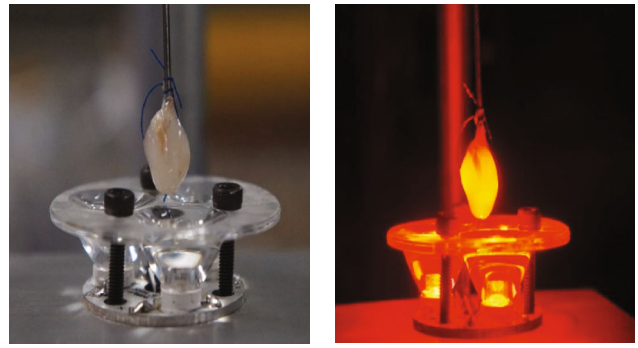

(a) (b)

Figure 3: (a) Setup of the irradiation system with the LED; (b) lungs being irradiated with the LED.

Table 1: Spectroscopic parameters used to irradiate the lungs with the LED.

Wavelength (nm)	660
Operation mode	Continuous wave
Average radiant energy (mW)	2000
Beam area (cm^2)	8.50
Intensity (mW/cm^2)	236
Polarization	Aleatory
Beam profile	Multimode
Exposure time (min)	15, 45, 60
Radiant energy (J)	1808, 5424, 7232
Radiant exposure (J/cm^2)	212.5, 637.5, 850

(group PDT 45 minutes or GPDT45). After decellularization, GPpIX, GPS, GPDT15, and GPDT45 mice were tracheally injected with 1 mL PpIX (10 μM; Sigma-Aldrich), while both control groups were injected with 1 mL PBS. Each stage-one decellularized lung was irradiated for one hour using a light-emitting diode (LED) with a wavelength of 660 nm, controlled by a current source of 1400 mA at 7.5 V (Figure 3). For the second stage, decellularized lungs were irradiated for 15 minutes in GPDT15 and 45 minutes in GPDT45. The parameters of irradiation are showed in Table 1.

2.5. Evaluation of Pulmonary Mechanics. To evaluate the resistance and elastance of acellular lungs, a custom-built system was used. The trachea was cannulated, and the lung was vertically connected to the system. Flow signal was recorded as the pressure drop across a pneumotachograph with a differential pressure transducer (DCXL01DS, range ±2.5 cmH_2O) and tracheal pressure (P_{tr}) was measured using a pressure transducer (176PC14HD2, ±35 cmH_2O) on a side port between the pneumotachograph and the cannula. Acellular lungs were subjected to conventional pressure-controlled ventilation with a quasi-sinusoidal flow pattern at a frequency of 80 breaths/min. A positive end expiratory pressure (PEEP) of 2 cmH_2O was applied through the ventilator to counteract the absence of physiological negative pleural pressure. Flow and pressure signals were recorded with LabView (© 2011 National Instruments Corporation, Austin, Texas, USA) and postanalyzed

Table 2: Values of positive end-expiratory pressure (PEEP) and lung volumes of the control group and protoporphyrin IX group (GPpIX).

	Control		GPpIX	
	Volume (mL)	PEEP (cmH_2O)	Volume (mL)	PEEP (cmH_2O)
Mean	0.15	1.95	0.12	1.93
SD	0.04	0.03	0.01	0.02

with MATLAB (© 1994-2015 The MathWorks Inc., Natick, Massachusetts, USA). Effective lung resistance (R_L) and elastance (E_L) were computed by linear regression of the recorded signals P_{tr} (tracheal pressure), V' (volume), and V (flow), using the conventional respiratory mechanics model $P_{tr} = P_o + (E_L.V) + (R_L.V')$, where P_o is a parameter to account for the external PEEP applied by the ventilator. For each decellularized lung, R_L and E_L were computed from data including five ventilation cycles [21].

2.6. Immunofluorescent Microscopy. For conventional fluorescence microscopy analysis, decellularized lungs were fixed with a mixture of optimal cutting temperature compound (OCT) (Sakura Finetek, Torrance, CA, USA) and PBS in a 3 : 1 ratio and frozen at −80°C. Ten-micrometer sections of lung samples were obtained using an HM 560 CryoStar Cryostat (Thermo Scientific, Waltham, MA, USA). Then, sections were rinsed with PBS to remove the OCT, fixed with 4% paraformaldehyde for 30 minutes at room temperature, and incubated for 10 min with 4′,6-diamidino-2-phenylindole (DAPI). To assess extracellular matrix proteins following PDT, cryosections were rinsed as previously described and incubated with a blocking solution (1% bovine serum albumin, 6% fetal bovine serum, and 0.5% triton in Tris-buffered solution) for 30 minutes, washed with PBS, and incubated overnight with the following primary antibodies: anti-collagen-I (Abcam, Cambridge, UK), anti-laminin (Sigma-Aldrich), anti-collagen-IV (Santa Cruz Biotechnology, Santa Cruz, CA, USA), and anti-elastin (Santa Cruz Biotechnology). The primary antibodies were detected using appropriate secondary antibodies. Images were taken using an Eclipse Ti fluorescence microscope (Nikon, Tokyo, Japan).

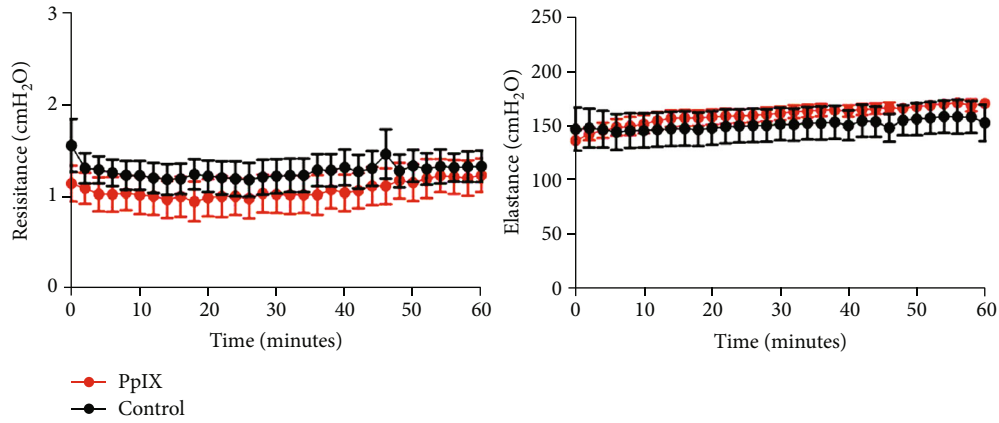

Figure 4: Values of pulmonary resistance and elastance of the control group and protoporphyrin IX group in relation to time during photodynamic therapy.

2.7. Scanning Electron Microscopy (SEM). Decellularized lungs were analyzed by SEM after PDT in both groups. Tissue samples were fixed with 2% glutaraldehyde and 2.5% paraformaldehyde in 0.1 M cacodylate buffer for 2 h at room temperature. Then, samples were rinsed in cacodylate buffer, sliced, and dehydrated over an ethanol gradient. Samples were dehydrated in hexamethyldisilazane for 10 min, dried overnight, coated with a 14.4 nm layer of gold using a sputter coater (SC510; Fisons Instruments, San Carlos, CA, USA), and analyzed using a DSM 940A microscope (Zeiss, Oberkochen, Germany) with an acceleration of 15 kV.

2.8. Candida albicans Growth Conditions and Inoculum Preparation. Candida albicans (ATCC 90028) was cultivated in Sabouraud dextrose agar (SDA) at 37°C for 24 h. Cells were harvested, suspended in PBS, and homogenized in a vortex shaker. The concentration was estimated by the turbidity of the suspension at 15% transmittance [22]. The concentration of the inoculum was confirmed by culture on SDA and CFU/mL count, according to methodology proposed by Jett et al. [23].

2.9. Microbiological Evaluation. For microbiological analysis, we conducted a sagittal cut into the left lung. After slicing, half of the left lung was subjected to manual maceration. After maceration, serial dilutions were performed and plated on SDA and plates were incubated at 37°C for 24 h. After 24 hours, a count colony-forming unit of the plated content (CFU/g) was conducted.

2.10. Statistical Analysis. All rates are expressed as the mean ± standard deviation (SD). To verify the normality of groups, we used the Shapiro-Wilk test. One-way ANOVA was used to test for differences between groups. The group means were analyzed with the Tukey test and Levene test for comparison of variances. Comparisons between the values obtained for R_L and E_L measured in each group pre- and postirradiation were carried out using a paired Student's t-test. The p value was considered statistically significant at the 5% level. For these analyses, we used the Statistical Package for Social Sciences (SPSS) version 21.0 (SPSS Inc., Chicago, IL, USA).

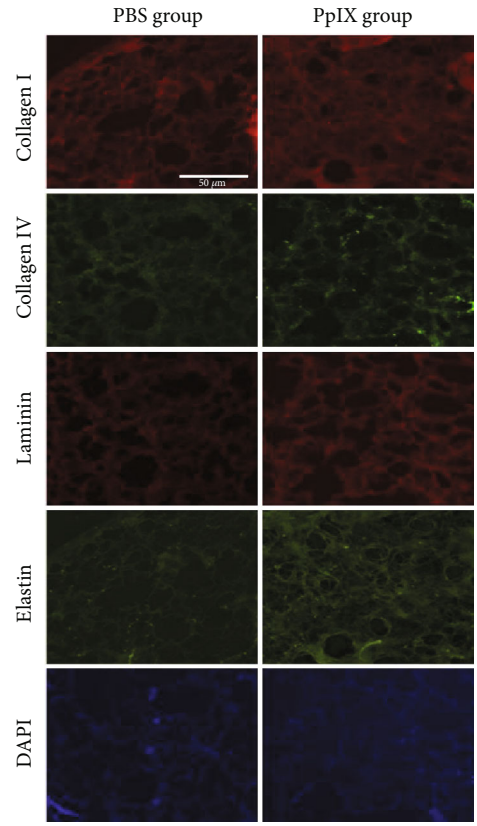

Figure 5: Immunofluorescent images of extracellular matrix components of acellular lung sections of the control group and the protoporphyrin IX group after LED irradiation.

3. Results

Pulmonary mechanics were evaluated in all 12 mice lung scaffolds divided in two groups: the control ($n = 6$) administered 1 mL PBS and GPpIX ($n = 6$) injected with 1 mL PpIX in the lungs, both of which were irradiated with a 660 nm LED. Mean of ventilation volumes and PEEPs are described in Table 2.

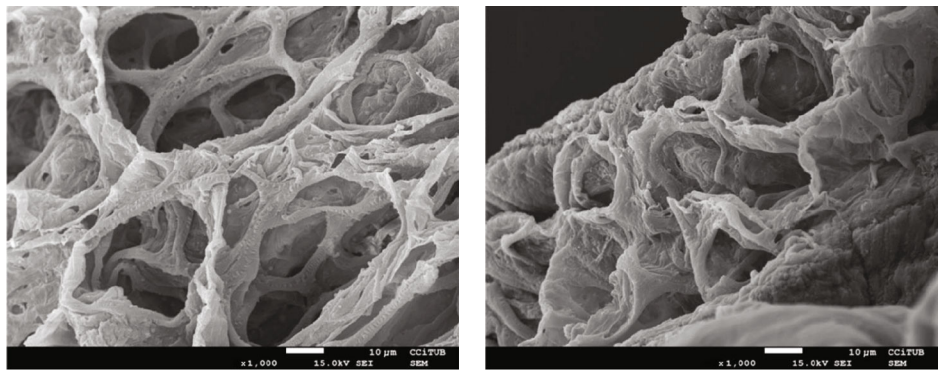

(a) (b)

Figure 6: Scanning electron microscopy images of decellularized lungs submitted to photodynamic therapy for one hour with phosphate-buffered saline (a) or photosensitizer protoporphyrin IX (b).

There were no significant differences between the control and GPpIX groups, which represents an equal ventilation for both evaluations. The lung mechanical evaluation parameters, R_L and E_L, exhibited no significant differences between both PDT intervals (Figure 4). Also, there were no changes observed over time of irradiation, representing the maintenance of the viscoelastic behavior of the lung scaffold after 1 h exposure to LED light.

Figure 5 demonstrates that extracellular matrix components responsible for the maintenance of the 3D lung structure, such as elastin, laminin, and collagens I and IV, remained virtually unchanged in the acellular lungs of both the control and GPpIX groups following application of the LED. The SEM analysis, observed in Figure 6, suggests that the microscopic lung structure has been maintained in both groups (control, Figure 6(a) and PpIX, Figure 6(b)), after application of photodynamic therapy. Also, the pulmonary scaffolds obtained from the decellularization process after irradiation LED compared to acellular lungs subjected to photodynamic therapy showed the absence of cell nuclei assessed by DAPI staining.

For the second stage of this study, eight mouse lungs were decellularized and divided into four groups: CG ($n = 2$), GPS ($n = 2$), GPDT15 ($n = 2$), and GPDT45 ($n = 2$). In the CG, no intervention of any kind was performed. For the group-denominated GPS, there was no application of LED, just addition of the PpIX photosensitizer. We observed that the PDT protocol promoted a reduction in the fungal population by about 1.60 $\log_{10}$ (CFU/g) (4.87 ± 0.16 and 3.27 ± 0.45 for GPDT15 and GPDT45, respectively) when compared to GPS (4.24 ± 0.23; $p < 0.05$). When comparing the CG (4.38 ± 0.31) with the GPS (4.24 ± 0.23), there was no significant reduction in microbial counts observed (Figure 7).

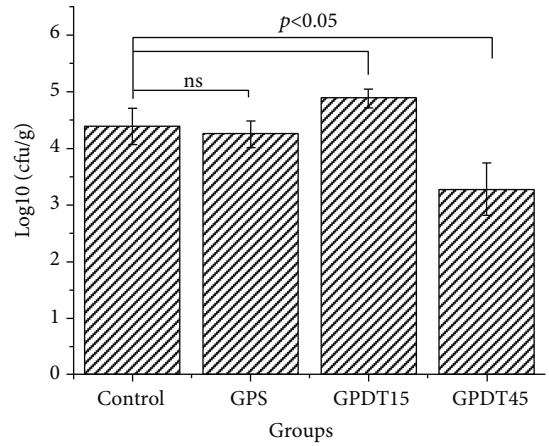

Figure 7: Values of the population of *Candida albicans* according to the protocol of photodynamic therapy with protoporphyrin IX. NS: no significance; control: infected lungs; GPS: infected lungs treated with protoporphyrin IX; GPDT15: infected lungs treated with protoporphyrin IX for 15 minutes; GPDT45: infected lungs treated with protoporphyrin IX for 45 minutes.

4. Discussion

Tissue engineering is a rapidly evolving field that aims at developing functional tissue substitutes with the goal of improving the quality of life in patients by promoting true regeneration of the structure and function of tissue compromised by disease or surgery. Hence, it is especially important that an appropriate sterilization method is chosen to ensure safety and maintain the mechanical properties of the lung scaffolds after sterilization for effective regeneration of the organ. Sterilization is required for bioengineering organs because there is a risk of contamination during the whole process of creation and due to the existence of potentially infectious organisms in the donor tissue. The organism microbiota considered benign in a healthy individual can become pathogenic to scaffolds when submitted to a bioreactor during the repopulation procedure.

In the past few years, researchers have explored alternative methods of sterilization due to the limitations of the conventional ones used for tissue engineering [8, 9, 24]. Siritientong et al. analyzed the effects of sterilization on scaffolds of polyvinyl-alcohol and freeze-dried sericin and came to the conclusion that gamma irradiation degraded the scaffolds by almost 70% after 24 hours, but it was the most appropriate method for sterilization [25]. Rainer et al. remarked that dry heat and autoclave treatments resulted in

an increase in crystallinity, while low-temperature UV and hydrogen peroxide plasma preserved the structural properties [26]. Shearer et al. verified that PAA and antibiotic solutions were effective in sterilizing hollow fiber and flat sheets of poly (lactide: glycolide) but obtained unfavorable changes in morphology [27]. The limitations found in these studies, mentioned previously, included a lack of uniform model organisms tested; many did not specify the source or the identity of the contaminating bacteria or another microorganism, making it difficult to compare sterilization method scaffolds for tissue engineering. Preliminary studies have shown that sterilization of scaffolds in tissue engineering is as much about maintaining the properties of materials and architecture, as about killing microbes [25–27]. Sterilization assumed major significance in scaffolds containing proteins or biological material, where the risk of denaturation is real and can result in the reduction or loss of important biological activity [8].

Finsen, Raab, and Von Tappeiner demonstrated that a combination of light and administration of drugs led to photochemotherapy emergence as a therapeutic tool and isolation of porphyrins and discovery of phototoxic effects on cancer cells led to the development of PDT [12, 28]. The ECM is important for tissue organization in multicellular organisms and is a complex network of macromolecules secreted by the cells, residing between cells as both a barrier and a scaffold on which tissues are built. Studies have demonstrated that PDT alters the extracellular matrix [29]. Pazos et al. demonstrated that ECM components are affected, even when they are not the primary targets [30]. However, we should also keep in mind that the action of PDT on specific molecular pathways depends on the fluence rate and photosensitizer used.

It has been reported that both ethylene oxide and irradiation can interact with molecules and scaffolds and potentially degrade their functions. It has recently been suggested that peracetic acid can be a useful sterilizing chemical agent in the tissue engineering of scaffolds [8, 31]. By contrast, in our study, we demonstrated that there were no apparent changes in the relevant extracellular matrix components of elastin, laminin, and collagens I and IV. These components remained almost unchanged in the acellular lungs of both groups following LED application.

Sterilization methods involving high temperature must obviously be discarded due to the denaturation of proteins and other biomolecules under these conditions. In a study on the impact of gamma radiation, the pulmonary valve scaffolds applied with a dose of 25–40 kGy exhibited great reduction in the collagen content fragmentation of the extracellular matrix, caused by oxidative damage following irradiation. This resulted in considerable biomechanical changes to tissue integrity, causing structural damage of collagen fibers and significant changes in the mechanical behavior [32]. Moreover, Uriarte et al. demonstrated that irradiation of acellular lungs with a typical ^{60}Co gamma sterilization dose for health applications resulted in a significant increase in the mechanical resistance of lung scaffolds [33].

Remarkably, in the present study, we observed that there were no changes in the values of pulmonary elastance (E_L) and pulmonary resistance (R_L) after irradiation by LED for 60 min with addition of photosensitizer. This was in contrast to previous reports on gamma irradiation, which causes degradation and fragmentation of the peptide chain and also damages collagen fibers, resulting in changes to lung mechanical properties [34].

PDT has been used successfully to treat different localized infections [35, 36], and our results are a proof of concept that PDT is also a suitable method to promote the reduction of *C. albicans*. Our study provides evidence that the photosensitizer PpIX does not exhibit any antifungal activity when used alone without the application of LED. It is also well described in the literature that the use of lasers alone, without the addition of a photosensitizer, similarly does not reduce fungal populations. We observed that there was a reduction in the fungal population after 45 min of PDT when compared to only 15 min of PDT. It is supposed that from the moment at which PDT acts, *C. albicans* disintegrates when a part of the cell detaches, forming another cell, which may be confused with a yeast recolonization. Teichert et al. demonstrated that the total reduction in fungal load was dependent on the concentration of the photosensitizer and light parameters, using red and methylene blue lasers in the oral mucosa of a mouse model [37].

5. Conclusion

In summary, this is the first study evaluating the mechanical behavior of lung scaffolds subjected to LED irradiation with a photosensitizer, with the objective of sterilizing lung scaffolds. We found that irradiation doses that effectively can reduce infection do not modify the structural and mechanical properties of decellularized lungs. This study opens the door to further research to confirm the suitability of PDT as a tool for routinely sterilizing lung scaffolds in the process of lung biofabrication.

Data Availability

The data that support the findings of this study are available from the corresponding author, upon reasonable request.

Additional Points

Highlights. The following were highlighted: behavior of the mechanical properties of pulmonary scaffolds submitted to photodynamic therapy, application of photodynamic therapy in the sterilization of pulmonary scaffolds, and use of LED in the process of sterilization of lung scaffolds in regenerative medicine.

Disclosure

This manuscript was presented as a master thesis of Nadua Apostólico at the postgraduate program in rehabilitation sciences, University Nove de Julho—UNINOVE.

Conflicts of Interest

The authors declare no financial or other conflict of interest regarding this article. This manuscript presents the results of the research of a master's thesis by the author Nadua Apostolico defended in the master's degree program in rehabilitation sciences at Universidade Nove de Julho (UNINOVE), São Paulo (SP), Brazil [38]. The results of this study are original and have not been previously published in any manuscript.

Authors' Contributions

LVFO, RF and DN: Conceptualization of the study, project administration and, supervision; NA, JJU, RKP, RABLM, LRF, RAP, AMD, LRF and, RPV: Investigation, Methodology, Data collect and, Formal analysis; RPV, MCOJ, RABLM, RPK, LVFO, RF and, JPRA Interpretation of the data; RKP, RABLM. JJU, LVFO and, NA: wrote the original version of the manuscript; RF, DN, JJU and, LVFO: reviewed the final version of the manuscript; All authors read and agreed with the final version of the manuscript.

Acknowledgments

We would like to thank the technical support offered by the Unitat de Biophysics i Bioenginyeria, Facultat de Medicina, Universitat de Barcelona (UB), Barcelona, Spain. We would like to express a special thanks to Prof. Dr. Paulo de Tarso Camillo de Carvalho for his friendship, opportunity, learning, and participation in this study. This is in memoriam of Paulo de Tarso Camillo de Carvalho, m.d., 1962–2020. This work was supported in part by the Spanish Ministry of Economy and Competitiveness (SAF2011-22576). Luis Vicente Franco de Oliveira receives grants by CNPq Research Productivity modality—PQID protocol number 313053/2014-6. Nadua Apostólico receives national support from "Fundação de Amparo à Pesquisa do Estado de São Paulo," protocol number 2013/21765-5, and was also covered with a "Bolsa de Estágio de Pesquisa no Exterior (BEPE/FAPESP) protocol number 2015/01649-6." The co-authors Nadua Apostolico, Luis Rodolfo Ferreira, and Manoel Carneiro de Oliveira Júnior received support from the Coordination for the Improvement of Higher Education Personnel (local acronym CAPES).

References

[1] R. D. Yusen, T. H. Shearon, Y. Qian et al., "Lung transplantation in the United States, 1999–2008," *American Journal of Transplantation*, vol. 10, no. 4p2, pp. 1047–1068, 2010.

[2] J. E. Nichols, J. A. Niles, and J. Cortiella, "Design and development of tissue engineered lung: progress and challenges," *Organogenesis*, vol. 5, no. 2, pp. 57–61, 2009.

[3] D. Huh, B. D. Matthews, A. Mammoto, M. Montoya-Zavala, H. Y. Hsin, and D. E. Ingber, "Reconstituting organ-level lung functions on a chip," *Science*, vol. 328, no. 5986, pp. 1662–1668, 2010.

[4] T. Eastlund, "Bacterial infection transmitted by human tissue allograft transplantation," *Cell and Tissue Banking*, vol. 7, no. 3, pp. 147–166, 2006.

[5] A.-M. Kajbafzadeh, N. Javan-Farazmand, M. Monajemzadeh, and A. Baghayee, "Determining the optimal decellularization and sterilization protocol for preparing a tissue scaffold of a human-sized liver tissue," *Tissue Engineering Part C: Methods*, vol. 19, no. 8, pp. 642–651, 2013.

[6] S.-S. Gouk, T.-M. Lim, S.-H. Teoh, and W. Q. Sun, "Alterations of human acellular tissue matrix by gamma irradiation: histology, biomechanical property, stability, in vitro cell repopulation, and remodeling," *Journal of Biomedical Materials Research Part B: Applied Biomaterials*, vol. 84B, no. 1, pp. 205–217, 2008.

[7] K. C. McGilvray, B. G. Santoni, A. S. Turner, S. Bogdansky, D. L. Wheeler, and C. M. Puttlitz, "Effects of 60Co gamma radiation dose on initial structural biomechanical properties of ovine bone—patellar tendon—bone allografts," *Cell and Tissue Banking*, vol. 12, no. 2, pp. 89–98, 2011.

[8] S. Yoganarasimha, W. R. Trahan, A. M. Best et al., "Peracetic acid: a practical agent for sterilizing heat-labile polymeric tissue-engineering scaffolds," *Tissue Engineering Part C: Methods*, vol. 20, no. 9, pp. 714–723, 2014.

[9] N. R. Bonenfant, D. Sokocevic, D. E. Wagner et al., "The effects of storage and sterilization on de-cellularized and re- cellularized whole lung," *Biomaterials*, vol. 34, no. 13, pp. 3231–3245, 2013.

[10] F. Gad, T. Zahra, T. Hasan, and M. R. Hamblin, "Effects of growth phase and extracellular slime on photodynamic inactivation of gram-positive pathogenic bacteria," *Antimicrobial Agents and Chemotherapy*, vol. 48, no. 6, pp. 2173–2178, 2004.

[11] M. Wainwright, "Photodynamic antimicrobial chemotherapy (PACT)," *The Journal of Antimicrobial Chemotherapy*, vol. 42, no. 1, pp. 13–28, 1998.

[12] O. Raab, "On the effect of fluorescent substances on infusoria," *Z O Biologico*, vol. 39, pp. 524–526, 1900.

[13] M. Wainwright, "Pathogen inactivation in blood products," *Current Medicinal Chemistry*, vol. 9, no. 1, pp. 127–143, 2002.

[14] M. R. Hamblin, "Antimicrobial photodynamic inactivation: a bright new technique to kill resistant microbes," *Current Opinion in Microbiology*, vol. 33, pp. 67–73, 2016.

[15] F. Freire, C. Ferraresi, A. O. C. Jorge, and M. R. Hamblin, "Photodynamic therapy of oral _*Candida*_ infection in a mouse model," *Journal of Photochemistry and Photobiology B: Biology*, vol. 159, pp. 161–168, 2016.

[16] B. Zeina, J. Greenman, D. Corry, and W. M. Purcell, "Cytotoxic effects of antimicrobial photodynamic therapy on keratinocytes in vitro," *British Journal of Dermatology*, vol. 146, no. 4, pp. 568–573, 2002.

[17] F. Barra, E. Roscetto, A. Soriano et al., "Photodynamic and antibiotic therapy in combination to fight biofilms and resistant surface bacterial infections," *International Journal of Molecular Sciences*, vol. 16, no. 9, pp. 20417–20430, 2015.

[18] H. Homayoni, K. Jiang, X. Zou, M. Hossu, L. H. Rashidi, and W. Chen, "Enhancement of protoporphyrin IX performance in aqueous solutions for photodynamic therapy," *Photodiagnosis and Photodynamic Therapy*, vol. 12, no. 2, pp. 258–266, 2015.

[19] T. Dai, V. J. Bil de Arce, G. P. Tegos, and M. R. Hamblin, "Blue dye and red light, a dynamic combination for prophylaxis and treatment of cutaneous Candida albicans infections in mice," *Antimicrobial Agents and Chemotherapy*, vol. 55, no. 12, pp. 5710–5717, 2011.

[20] R. K. da Palma, N. Campillo, J. J. Uriarte, L. V. F. Oliveira, D. Navajas, and R. Farré, "Pressure- and flow-controlled

media perfusion differently modify vascular mechanics in lung decellularization," *Journal of the Mechanical Behavior of Biomedical Materials*, vol. 49, pp. 69–79, 2015.

[21] S. Kano, C. J. Lanteri, A. W. Duncan, and P. D. Sly, "Influence of nonlinearities on estimates of respiratory mechanics using multilinear regression analysis," *Journal of Applied Physiology*, vol. 77, no. 3, pp. 1185–1197, 1994.

[22] Y. Chabrier-Roselló, T. H. Foster, S. Mitra, and C. G. Haidaris, "Respiratory deficiency enhances the sensitivity of the pathogenic fungus Candida to photodynamic treatment," *Photochemistry and Photobiology*, vol. 84, no. 5, pp. 1141–1148, 2008.

[23] B. D. Jett, K. L. Hatter, M. M. Huycke, and M. S. Gilmore, "Simplified agar plate method for quantifying viable bacteria," *BioTechniques*, vol. 23, no. 4, pp. 648–650, 1997.

[24] M. Martina and D. W. Hutmacher, "Biodegradable polymers applied in tissue engineering research: a review," *Polymer International*, vol. 56, no. 2, pp. 145–157, 2007.

[25] T. Siritientong, T. Srichana, and P. Aramwit, "The effect of sterilization methods on the physical properties of silk sericin scaffolds," *AAPS PharmSciTech*, vol. 12, no. 2, pp. 771–781, 2011.

[26] A. Rainer, M. Centola, C. Spadaccio et al., "Comparative study of different techniques for the sterilization of poly-L-lactide electrospun microfibers: effectiveness vs. material degradation," *The International Journal of Artificial Organs*, vol. 33, no. 2, pp. 76–85, 2010.

[27] H. Shearer, M. J. Ellis, S. P. Perera, and J. B. Chaudhuri, "Effects of common sterilization methods on the structure and properties of poly (D, L lactic-co-glycolic acid) scaffolds," *Tissue Engineering*, vol. 12, no. 10, pp. 2717–2727, 2006.

[28] R. Ackroyd, C. Kelty, N. Brown, and M. Reed, "The history of photodetection and photodynamic therapy," *Photochemistry and Photobiology*, vol. 75, no. 5, pp. 656–669, 2001.

[29] T. F. Linsenmayer and E. D. Hay, "Cell biology of extracellular matrix," in *Collagen*, p. 7, Plenum Press, New York, 1991.

[30] M. D. C. Pazos and H. B. Nader, "Effect of photodynamic therapy on the extracellular matrix and associated components," *Brazilian Journal of Medical and Biological Research*, vol. 40, no. 8, pp. 1025–1035, 2007.

[31] W. A. Rutala, D. J. Weber, and Society for Healthcare Epidemiology of America, "Guideline for disinfection and sterilization of prion-contaminated medical instruments," *Infection Control and Hospital Epidemiology*, vol. 31, no. 2, pp. 107–117, 2010.

[32] P. Sarathchandra, R. T. Smolenski, A. H. Y. Yuen et al., "Impact of γ-irradiation on extracellular matrix of porcine pulmonary valves," *Journal of Surgical Research*, vol. 176, no. 2, pp. 376–385, 2012.

[33] J. J. Uriarte, P. N. Nonaka, N. Campillo et al., "Mechanical properties of acellular mouse lungs after sterilization by gamma irradiation," *Journal of the Mechanical Behavior of Biomedical Materials*, vol. 40, pp. 168–177, 2014.

[34] K. Sun, S.-q. Tian, J.-h. Zhang, C.-s. Xia, C.-l. Zhang, and T.-b. Yu, "ACL reconstruction with BPTB autograft and irradiated fresh frozen allograft," *Journal of Zhejiang University. Science. B*, vol. 10, no. 4, pp. 306–316, 2009.

[35] G. B. Kharkwal, S. K. Sharma, Y.-Y. Huang, T. Dai, and M. R. Hamblin, "Photodynamic therapy for infections: clinical applications," *Lasers in Surgery and Medicine*, vol. 43, no. 7, pp. 755–767, 2011.

[36] P. d. T. C. d. Carvalho, A. P. d. C. Marques, F. A. d. Reis et al., "Photodynamic inactivation of in vitro bacterial cultures from pressure ulcers<A NAME="volta1"></A>," *Acta Cirúrgica Brasileira*, vol. 21, suppl 4, pp. 32–35, 2006.

[37] M. C. Teichert, M. N. Usacheva, M. A. Biel, and M. A. Biel, "Treatment of oral candidiasis with methylene blue-mediated photodynamic therapy in an immunodeficient murine model," *Oral Surgery, Oral Medicine, Oral Pathology, Oral Radiology, and Endodontology*, vol. 93, no. 2, pp. 155–160, 2002.

[38] N. Apostolico and O. LVF, Eds., *Análise das propriedades mecânicas viscoelásticas de pulmões de camundongos descelularizados após o uso da terapia fotodinâmica: uma alternativa para o processo de esterilização*, São Paulo, 2015http://Biliotecatede.uninove.br; [cited 2021 May 20]. Available from: http://bibliotecatede.uninove.br/bitstream/tede/1813/2/Nadua%20Apostolico.pdf.

Hindawi
International Journal of Photoenergy
Volume 2021, Article ID 5519709, 13 pages
https://doi.org/10.1155/2021/5519709

Review Article

A Comprehensive Review on the Effects of Laser Photobiomodulation on Skeletal Muscle Fatigue in Spastic Patients

Sadi F. Stamborowski,[1] **Fernanda Púpio Silva Lima**,[1] **Patrícia Sardinha Leonardo**,[2] **and Mário Oliveira Lima**[1]

[1]*Laboratório de Engenharia de Reabilitação Sensório Motora, Institute of Research and Development (IP&D), Universidade do Vale do Paraíba (UNIVAP), São José dos Campos, 12244-000 São Paulo, Brazil*
[2]*Faculty of Health Sciences, Universidade do Vale do Paraíba (UNIVAP), São José dos Campos, 12244-000 São Paulo, Brazil*

Correspondence should be addressed to Sadi F. Stamborowski; sadifs@gmail.com

Received 14 January 2021; Accepted 23 March 2021; Published 8 April 2021

Academic Editor: Alberto Ãlvarez-Gallegos

Copyright © 2021 Sadi F. Stamborowski et al. This is an open access article distributed under the Creative Commons Attribution License, which permits unrestricted use, distribution, and reproduction in any medium, provided the original work is properly cited.

Peripheral muscle fatigue is a common experience in daily life. Every individual at some point in their life has realized the inability to maintain muscle contraction, a phenomenon known as fatigue. Interestingly, neurological patients with peripheral sequelae such as spastic muscle contraction are able to remain in a pattern of muscle contraction for prolonged periods. The effects of laser therapy are already recognized in muscle contraction to delay skeletal muscle fatigue, prolong physical activity, and reduce delayed onset muscle soreness. However, the effects of photobiomodulation on neurological patients with muscular spasticity are still not well established. The present literature review seeks to recognize articles about the application of laser irradiation, also known as photobiomodulation, to patients with muscle fatigue and/or spastic palsy. To perform a literature review, we used the systematic review methodology for the literature search. The following keywords were searched: (skeletal muscle fatigue) AND (spastic patients) AND (low-level laser therapy OR low intensity laser therapy OR low energy laser therapy OR LLLT OR LILT OR LELT OR infrared laser OR IR laser OR diode laser), and these were used for search on the following databases: PubMed, Embase, Web of Science, BIREME, Scopus, and SciELO. Besides that, a literature review concerning on muscle physiology, fatigue, and LLLT was made. No language filter was applied, and altogether, 689 papers were identified. A group of 3 physiotherapists and 01 pharmaceutical scientist performed the literature review, and every exclusion was confirmed by at least two reviewers. After inclusion and exclusion criteria, 128 studies were included in this review. Conclusion, the LLLT can contribute to the recovery of spastic patients and muscles in fatigue. However, the real effect of laser photobiomodulation on muscle spasticity remains to be established. Only a much reduced number of clinical trials have been performed with a small number of participants. There is a lack of clinical trials from different research groups that could help to understand and elucidate the effects of laser in prolonged muscle contraction in spastic palsy.

1. Introduction

Looking into the past, more specifically since the 1960s, it was consistently seen that low-level laser therapy (LLLT) could present positive effects on the muscle-skeletal system and related diseases such as joint inflammation, sports injuries, muscle fatigue, and lower back and neck pain among other conditions [1]. Photobiomodulation has been covering new areas of study, and with them, there is a range of possibilities for spastic patients, to reduce or eliminate muscle fatigue in some cases, especially in patients with traumatic brain injury, for example [2].

Previously, photomodulation was called a "low-level laser therapy" or LLLT, including light from light-emitting diodes (LEDs), lasers, and other light sources with wavelengths ranging from visible to infrared. It has also become an

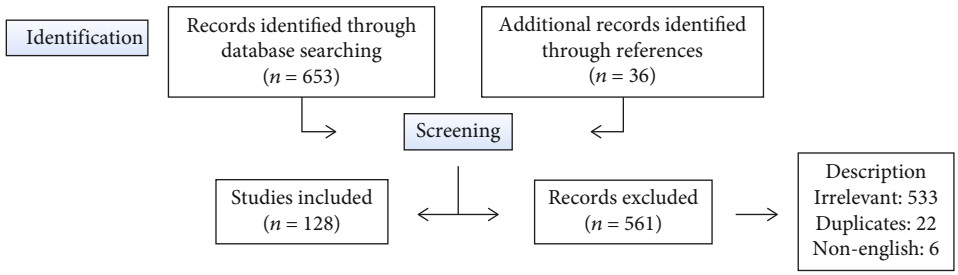

Figure 1: Schematic representation of the study selection to be included in the review.

increasingly mainstream treatment for muscle fatigue, especially in the areas of physical medicine and rehabilitation, in patients with a type of degenerative disease [3].

It is well known that there are dose responses to simultaneous applications of several different wavelengths in some cases, for example, to kill cancer cells and promote significantly faster healing in chronic and diabetic wounds and sports injuries, reduction of pain in arthritic joints and back and neck, reduction of inflammation by increasing the number of fibroblasts and myofibroblast, induction of the accumulation of collagen, and decrease of fatigue in the muscles in spastic patients [4]. Additionally, recent studies indicate that photobiomodulation can also become promising in clinical cases of patients suffering from myocardial infarction, stroke, brain injuries caused by trauma, or degenerative and spinal cord injury, with the last three triggering injuries in motor neurons and ending up directly affecting the muscles, causing spasms and finally fatigue and pain [5].

The wavelengths for photobiomodulation are more regularly used in the 500–700 nm range for treating superficial healing, while wavelengths between 800 and 1000 nm are used for deeper tissues and skeletal muscle fatigue [4].

This review focuses on the efficacy of photobiomodulation in muscle fatigue in spastic patients, its mechanisms of action, and how its efficacy may be increased by using multiple wavelengths. The review examines research related to the induction of muscle fatigue signaling pathways and the elimination of pain by the application of photobiomodulation and their mechanisms of action. Photobiomodulation application is making clear headway toward the development of a reliable and successful set of irradiation parameters for inducing significantly faster and more complete healing of illness related to muscles that does not respond to conventional treatment [3]. However, further work is required to optimize its therapeutic value to determine the integrative nature of fatigue in spastic patients.

2. Methodology

The following bibliographic databases were searched in MEDLINE via PubMed, Embase, Web of Science, BIREME, Scopus, and SciELO. The search strategy was (skeletal muscle fatigue) AND (spastic patients) AND (low-level laser therapy OR low intensity laser therapy OR low energy laser therapy OR LLLT OR LILT OR LELT OR infrared laser OR IR laser OR diode laser). No language filter was applied, and altogether, 689 papers were identified. A group of 3 physiotherapists and 01 pharmaceutical scientist performed the literature review, and each exclusion was confirmed by at least two reviewers. After inclusion and exclusion criteria, 128 studies were included in this review.

Reviewers independently identified titles and abstracts relevant to applying LLLT to patients suffering from muscle fatigue and/or spastic. Full texts of the published articles, unpublished articles, and unpublished data of completely finished and analyzed studies were included. The reference list of full-text articles was also reviewed. Figure 1 illustrates the selection process for including studies.

3. Homeostasis

In the human body, one of the most plastic and dynamic tissues is the skeletal muscle. There is about 40% of the human total body weight in humans that is made up of skeletal muscle and is composed of 50–75% of all body proteins and accounts for 30–50% of the whole-body protein turnover. The composition of the muscle is mainly of water (75%), protein (20%), and other substances including inorganic salts, minerals, fats, and carbohydrates (5%) [6].

The muscle mass depends on the conditional nutrition, hormonal condition, and the balance between physical activity/exercise and illness or injury. In addition, the balance between protein synthesis and degradation is extremely sensitive to factors that deregulate the different cellular compartments (structural, contractile, and regulatory); for this reason, it has received significant scientific attention because of their important contribution to mobility, contractility capacity, and functioning [7].

Skeletal muscle contributes significantly to multiple bodily functions, since mechanical function for converting chemical energy into mechanical energy to generate force and power, walking motion, or stand, besides allowing participation in social and sportive settings, maintains a possibility of functional independence. From a metabolic point of view, several skeletal muscle functions include a contribution to basal energy metabolism, like storage for important substrates such as amino acids and carbohydrates used by other tissues such as the skin, brain, and heart, and the production of heat for the maintenance of core temperature, and it is responsible for the consumption of the majority of oxygen and energy during physical activity and exercise [8].

Furthermore, amino acid release from muscle contributes to the maintenance of blood glucose levels during conditions

of starvation, in that case, a person with a reduced muscle mass impairs the body's ability to respond to stress and chronic illness [9].

The architecture of skeletal muscle is characterized by myofibers or muscle cells and associated connective tissue. The structure of muscle is characterized by the number and size of individual muscle fibers, but any pathological infiltration by fat and connective tissue may alter this relationship [10, 11].

Observing the cellular level, the muscle fibers are multinucleated and postmitotic, and some part of each nucleus within a muscle fiber controls the type of protein synthesized in that specific region of the cell; these regions are known as nuclear domains and have a highly regulated, but not uniform, size [12]. Protein expression found in the adjacent domains of a single fiber appears to be coordinated in such a way that the type of protein, in this case, the myosin produced, is almost the same across the length of the fiber [13].

In the human body, there are several cell storage sites with stem cell potential; knowing this, it is important to note that skeletal muscle has cells of this nature, which are known as satellite cells and are located between the sarcolemma and the basal lamina and contribute to muscle growth, repair, and regeneration [12, 14]. When these cells are activated by myogenic factors, satellite cells proliferate and differentiate into new muscle fibers and repair the local injury.

The functional unit of the muscle is divided into compatibilities and is separated by a dense connective tissue called a sarcolemma. The outermost layer that contemplates the bundles of muscular fibers is called epimisio. The perimeter consists of the grouping of fibers within and surrounded by another layer of connective tissue. In addition, there is a complex of several proteins associated with the sarcolemma and are usually connected to the myofilament of actin. A single-muscle fiber has approximate dimensions of 100 μm in diameter and 1 cm in length [15].

The contractile units of skeletal muscle are composed of grouped and organized myofilaments, called sarcomeres. These myofilaments are actin and myosin proteins (70–80% of the total proteins present). Myosin is the main driver of the muscle fiber and is present in a total of eleven sarcomere myosin genes, but only a few can be described in humans, and at least two of these genes are expressed in cardiac muscle. There are many other proteins present in the sarcomere and sarcoplasm, which act as the coupling of the processes of excitation and contraction, release of energy, structuring of the cytoskeleton, and generation of strength and power [16]. Among them, in particular, we can mention the regulatory proteins that form the calcium-dependent troponin complex, which are troponins C, I, and T. Tropomyosin plays an essential role in the activation process that leads to slippage and the creation of force, which is directly associated with the actin filament [17].

In addition to the proteins mentioned above, there are other proteins that contribute to the physiological and mechanical properties of muscle, titin, and nebulin [18]. The titin is able to bind to the Z disk of the sarcomere and to the myosin, to provide stability and alignment to the thick filament, and this is only possible thanks to its large width. Nebulin proteins, on the other hand, are integrated with other proteins in the thin filaments that contain actin, in which they help to maintain the sarcomere integrity [19] and influence the cell stiffness and tension that proportionally influence the formation of myofibrils and signaling local cell . In addition, in vitro studies suggest that titin may assist in muscle contraction and strength generation [20]. In the sarcomere, disk Z has several proteins; among them, the one that fixes the actin myofilament is called actinin. There are other proteins that also connect the Z disk to the sarcolemma and the extracellular matrix, called desmin [20].

Sarcoplasm is composed of several cellular elements, among them, a transverse tubular system (T tubule), the sarcoplasmic reticulum, and a mitochondrial network; based on each type of fiber, the amount of these elements can be estimated. Detailing the cellular elements above, the T tubule system is nothing more than an invagination of the sarcolemma and its important role in driving the nerve action potential into the cell is of utmost importance for local homeostasis [21]. This network of tubules is in contact with the exterior of the cell and ensures that the excitation can spread uniformly throughout the fiber and the change in the calcium concentration was detected by the protein Dysferlin located in the membrane of the T tubule system [22].

The concept that mitochondria, in isolation, provide the necessary energy for muscle fibers, according to some studies, is not applicable. It was seen that there is the formation of a three-dimensional network around the cell and generates the necessary energy for muscle action when oxygen is available [23]. In this way, some mitochondria remain close to the sarcolemma to decrease the time of diffusion of oxygen through the capillaries; thus, during aerobic exercise, when the oxygen demand increases, other mitochondria, located in the intermyofibrillar space, are recruited to supply the new demand [24].

It is well known that several neuromuscular pathologies, the practice of physical exercises, and even aging directly influence the structure and function of myofilaments and the surroundings. For example, training with resistance exercises induces the production of mitochondria through the activation of the coactivator-1a of the c-receptor, activated by the peroxisome proliferator [25]. The number and size of mitochondria increase with resistance training programs/type of aerobic exercise. On the other hand, observing muscle aging, the sarcoplasmic reticulum shows a fragmented aspect and this impairs calcium release and muscle activation, so we can understand why there is muscle weakness in this population, specifically [26].

Due to the heterogeneity of human skeletal muscle in the biochemical, mechanical, and metabolic phenotypes of the individual fibers, it is possible to highlight the presence of different muscle fibers with different properties with each one specifically imposed by its respective motor neuron [27]. Through this, several physiological properties of muscle allow the plasticity capacity of the muscle according to various metabolic and mechanical demands, such as the architecture of capillary supply networks, which varies according to the type of fiber [28].

The three basic ways of obtaining energy for muscle fiber are the stocks of ATP and CP, anaerobic glycolysis, and oxidative phosphorylation. This obtaining in the form of ATP is of extreme importance, because according to the metabolic pathway, the production of energy varies and this must supply the energy requirement of the muscle during the period and the intensity of the activity or exercise [26].

Muscle contraction is related to the extension of the development of the sarcoplasmic reticulum, so that its contraction speed is directly proportional to this development, looking from another angle, or the oxidative capacity also directly influences this speed, but it is more observed in fatigue. The most used classifications for muscle in adults are three types of fibers: type I (slow, oxidative, and fatigue resistant), IIA (fast, oxidative, and intermediate metabolic properties), and IIx (fastest, glycolytic, and fatigable) [26, 27].

In the muscle, an activity that uses the stocks of ATP and CP assists high-intensity short-duration (few seconds) activities because the reserves in muscle fibers are just few. Looking into anaerobic glycolysis, it produces ATP quickly to sustain muscle actions for a couple of minutes but the end products (H^+ and lactate) are associated with muscle fatigue and consequently damage the muscle. Eventually, the energy obtained by oxidative phosphorylation is carried out within the mitochondrial network, which is able to supply the energy demand for an intense activity or activity lasting minutes and even hours [28–30].

Obtaining the raw material for energy production can be done through carbohydrates and free plasma fatty acids and muscle triglycerides, in addition to the use of amino acid metabolism, but the percentage obtained is small compared to the energy production total [31, 32].

4. Muscle Fatigue

Muscle fatigue is usually defined as a loss of strength or power in response to contractile activity. These can occur as a result of injury or physiological or pathological adaptations [33].

In order to understand the nature of skeletal muscle fatigue, we must take into account external factors such as injuries and disuse that somehow influence the fatigue mechanism and the internal factors, which include cell signaling, vascular function, neurophysiology, bioenergetics, and molecular mechanics [34, 35].

Observing the loss of maximum strength or capacity to generate energy during a muscle contraction, this would be a physiological response to all muscle contractions; however, in the shortest, this cannot occur [36].

The contractions can be sustained or repetitive, and the intensity of these contractions can vary from submaximal to maximum, and from a mechanical point of view, they can be concentric, eccentric, and isometric [37, 38]. That way, according to researchers, the magnitude of loss of force or power in response to fatigue in the muscle can occur in a continuous way or only for a few moments [39].

Following this line of thought, quantifying fatigue as a single continuous contraction or a series of contractions with submaximal tension, further studies are needed. However, the study of fatigue recovery proves to be valuable, in particular, for detecting and understanding low-frequency fatigue (LFF) associated with loss of strength due to low activation frequencies and failure of the excitation and contraction coupling (ECC) of skeletal muscle [40–43].

In general, the causes of fatigue vary widely, depending on the model studied, the experimental conditions, and the tasks imposed on the muscle. In in vitro studies, it is typical to manipulate the conditions to directly determine the cause(s) of the contractile failure and fatigue is quickly observed as the drop in strength or power of a single cell or group studied. In situ studies also usually use this approach, to mimic physiological conditions and compare them by proceeding in more basic ways compared to the in vitro study.

In vivo, usually, the mechanisms of muscle fatigue magnitude vary according to the animal model and the task imposed, this is called "task specificity," and to demonstrate these mechanisms, it is common to use approaches that can cover and evaluate directly and indirectly the location(s) of failure in muscle strength and power [44–47].

5. Fatigue in Cells

Studies using a material that mimics fine muscle fibers to observe motility in vitro have provided insights into how actin (thin filament) interacting with myosin (thick filaments) is capable of generating strength, speed, and power [48–50]. From these studies, it was possible to observe that the main stages related to fatigue are the transition from the state of low strength to the state of high strength of the actin-myosin (AM) cross-bridge and the step of dissociation of adenosine diphosphate (ADP) from the cross-bridge AM. The first stage would be associated with the release of inorganic phosphate (Pi) and hydrogen (H^+) ions; this stage is being considered as limiting because the rate of force development and the force inhibition site immediately begin to accumulate these ions and fatigue starts during the exercise, being of high or low intensity [45, 51]. It has been known for years that a high rate of ATP utilization accelerates the reaction of creatine kinase (CK) and this can be seen in the last step, the release of ADP, in which the loaded contractions limit the speed of the AM cross-bridge cycle and therefore the speed of the fiber [52].

Due to the high turnover of ATP and the increase in anaerobic metabolism, as a result of the intense contractile activity, $[H^+]$ also increases, causing the decrease in intracellular pH in fast glycolytic fibers (FG) from 7.0 to 6.2 and for the end resulting in the decline of cellular phosphocreatine (Pi) [45, 53]. However, other studies indicate that the increases of Pi decrease the isometric strength and fiber stiffness proportionally, indicating that the cross-bridge strength remains constant and that the strength decline is directly connected with the transition period from a bonding state of the fibers and these are also affected by the concentration of Pi and H^+ [52, 54–56].

Adversely, studies show that a low pH in the presence of Ca^{2+} decreases the strength and this may be related to the hypothesis that a high $[H^+]$ limits the amount of high-strength AM cross-bridges, inhibiting the direct velocity

constant for the transition from the weak to the strong link state of the cross-bridge AM [57–59].

The Westerblad and Allen studies demonstrated that when the fast fibers of the mouse flexor digitorum brevis (FDB) are stimulated in vitro, the initial decline in strength occurs before any detectable change in intracellular [Ca^{2+}] [60, 61]. The hypothesis of some authors was that the early loss of strength was mediated by increased pi, which was confirmed by the observation that fibers isolated from CK knockout mice, which when stimulated, did not show an increase in pi or loss of strength during the initial phase of muscle contraction [62, 63].

In the stimulus phase, with the high contraction rate, it was observed that the initial drop in strength would be mediated by the combined effects of the increase in [Pi] and [H^+] and that the effects of these ions on the myofilaments have been shown to involve additives that involve a direct inhibition of strength and reduced sensitivity to Ca^{2+} and that at the beginning of fatigue, the amplitude of intracellular Ca^{2+} is high, causing local sensitivity to be impaired and preventing fatigue from ceasing [62–64].

However, a subsequent decline in the amount of Ca^{2+} that had been released by the sarcoplasmic reticulum (RS) and was impairing local sensitivity causes muscle fatigue as the muscle needs to recover from this uncoordinated imbalance, resulting in more loss of strength during peak saturation and less close to physiological temperatures compared to muscle temperatures that did not contract [50, 65].

It is important to note that studies have shown that the [Ca^{2+}], necessary to elicit half the maximum strength in the muscle of mice, was significantly increased by 30 mM pi and that the effect was two times greater on slow fibers and was performed at temperatures of 30°C and 15°C [66]. The mechanism of sensitivity to Ca^{2+} is not yet fully understood; however, at a pH of approximately 6.2, it is partially mediated by the competitive inhibition of Ca^{2+} binding to troponin-C [67, 68].

One factor that contributes to the certain change in the ratio of [Ca^{2+}] and strength is the decline in coarse filament cooperative, which is a direct result of the reduced number of high-strength cross-bridges [69–71]. In addition to the high [H^+], the micromolar increases in cell ADP, due to intense contractile activity, depress the fiber speed, but the strength increases; this is probably due to the increase in the amount and type of cross-bridges in the high-strength peaks, these being cross-bridges AM-ADP-Pi, and cross-bridges AM-ADP [72, 73]. The most important role for increases in cellular ADP in eliciting fatigue seems to be related to the inhibition of the Ca^{2+} pump present in the sarcoplasmic reticulum, causing direct effects on the AM cross-bridge.

Looking at the effects of low pH in conjunction with high pi and high [ADP], on slow fibers and fast fibers, it is not entirely clear how it can influence fatigue [74–77]. However, recent studies have shown that the effects of low pH and high ADP and pi have been investigated at the molecular level using the in vitro motility assay to assess the slip speed of actin filaments without the regulatory proteins tropomyosin and troponin in myosin [78, 79].

To confirm that using single-fiber studies, the high Pi had no effect on the sliding speed, while at pH 6.4, the speed of the actin filament showed a 36% reduction. The increase in ADP from a low resting value of 0.02 mM to a fatigue level of 0.3 mM caused an 18% drop in filament speed and with phosphorylation of the N-terminal region of the myosin light chain demonstrating that the inhibition increased to 34% [79, 80].

Thus, both high [H^+] and ADP seem to decrease the sliding speed of the filament without load, increasing the affinity of ADP for the myosin head, thus decreasing the rate of ADP release. Besides that, the additional inhibition of speed caused by phosphorylation of the N-terminal region of the myosin regulatory light chain can be explained by the high affinity for ADP observed in phosphorylated myosin compared to nonphosphorylated myosin.

This suggests that, although high ADP can reduce the maximum shortening speed without load, ADP may have little or no effect on fiber speeds during peak power generation at the high intensity of force. However, it is worth mentioning that phosphorylation in the N-terminal region of the myosin light chain reduced the inhibitory effects of conditions similar to fatigue on the decrease in speed by only 28% [81–83].

6. Excitation-Contraction Coupling Failure

The first step for excitation-contraction (ECC) coupling to occur is the generation and propagation of the sarcolemma (SL) action potential and the proper functioning of the neuromuscular junction in nonfatigued muscle cells. It is well known that the SL membrane potential at rest is approximately −80 mv and, during activation, the peak action potential approaches +20 mv. The duration of the action potential is short, varying from 1 to 1.5 milliseconds (ms), and the membrane is capable of responding to stimulation frequencies even greater than 150 Hz [84–87].

With the development of fatigue induced by high rates of muscle contraction, the surface membrane potential, both at rest and in action, demonstrates characteristic changes, as the resting potential becomes depolarized in 10 to 20 mv and the height of the peak of the action potential decreases proportionately; however, the duration of the action potential becomes prolonged [84, 85].

The great lack of information about how and when these changes about the extent to which the tubular membrane T is changed and how these changes can be mitigated during exercise is still a challenge, but the hypothesis would be that the changes observed in the T tube should probably be greater compared to the changes observed in SL [86, 87].

The depolarization of the SL and T tube membranes interferes in two processes: first, they interfere with the generation and propagation of the action potential due to reduced activation and slower inactivation kinetics of the voltage-dependent Na^+ channels. Second, they interfere with the inactivation of the intramembranous T tubular protein, more specifically the voltage sensor, called the 1,4-dihydropyridine receptor (DHPR), obtaining the reduction in the peak of the action potential as a direct result of the

inactivation induced by the depolarization of the voltage-regulated Na^+ channels and, now, by the reduced electrochemical gradient and inducing the influx of Na^+ in the T system, so that the extracellular [Na^+] decreases and intracellular [Na^+] increases [88–90].

For inactivation of the Na^+ channel and DHPR, depolarization is necessary if the cell has an intracellular [K^+] reduction and an extracellular [K^+] increase. Studies have shown that small increases in [K^+] increase the subtetan strength, while large increases reach a critical level where it causes tetany and an abrupt decrease in the contraction force. Besides that, the malfunction of the Na^+ K^+ pump may result in unregulated pH-free energy of ATPase hydrolysis by increasing ADP/Pi intracellular and extracellular [91, 92].

In order for the processes to work correctly, the following are required: maintaining the ideal rate of activation of motor activity, diversified recruitment of motor units carried out in the CNS and β-adrenergic stimuli, stimuli for the Na^+ K^+ pump to function, and an increase in [Cl^-] to control the influx of K^+ to prevent it from reaching a critical level, resulting in fatigue [93–95].

Checking the amount of K^+ used by muscle cells during contraction and the amount of efflux released by the sarcolemma during action potentials, we can conclude that the account is far from closing. Thus, studies suggest that the depolarization observed in fatigued muscle cells is the result of the effects of high K^+ contractions, both intracellular and extracellular, and of the increase in their conductance. The increase in K^+ conductance can cause the activation of K^+ channels, which depend on ATP or dependent on Ca^{2+}, and the activation of these channels can directly influence the local pH, making it more basic, creating a cascading effect that would contribute to fatigue by cell depolarization or an attempt to return homeostasis [96–98].

Studies suggest that the infusion of nonspecific antioxidant N-acetylcysteine prolongs fatigue time and reduces the decline in Na^+ K^+ pump activity by approximately half, but the mechanisms of pump inactivation are not yet known; however, data suggest it that can be related with reactive oxygen species (ROS) [99].

Studies suggest that the main evidence that disturbances in eccentric contraction (ECC) contribute to fatigue is the low transient Ca^{2+} amplitude and that the greatest decline in Ca^{2+} release tends to occur late in fatigue. From this, we can observe that changes in the amplitude of Ca^{2+} also influence the strength, because when inducing metabolic factors signaled by the concentration of Ca^{2+} in CPB, fatigue becomes early and is characterized by an increase in ATP turnover during the initial stage of contractile activity and consequently by an increase in pi and H^+. Thus, so that there is a release of Ca^{2+} by SL, it has become quantitatively more important in the process of developing fatigue independently if the Ca^{2+} ions act on the AM cross-bridge [97, 100].

Furthermore, there is strong evidence that Ca^{2+} plays an important role in cell signaling that triggers fatigue; however, the nature and how it occurs are still unknown. Studies suggest that in ECC, fatigue can be compensated by activating the Ca^{2+}/ATPase pumps present in the T tubes, in which they can move the Ca^{2+} from the cytoplasm to the extracellular space; from that, it is expected that local factors can activate mechanisms to correct this deregulation, such as the activation of the local [Ca^{2+}] pumps due to the modification of the local pH, and thus inhibit the activity of ATPase. However, [Ca^{2+}] can interfere with DHPR and thus decrease the likelihood of ATPase inactivation, consequently changing the threshold of the action potential in the lumen of the T tube to increasingly positive values, making it deeply difficult for the muscle to leave the stage of contraction for relaxation [101–103].

Once knowing that recovery from fatigue usually occurs within minutes to an hour, we must understand that some studies theorize that part of the fatigue problem is actually related to cell signaling, more precisely, in the direct inhibition of the Ca^{2+} channel released by SL, called RyR1, because the content of intracellular Ca^{2+} depends on the activity of this channel, both for entry and removal, mainly in fast fibers. The permeability of the channel is directly regulated by Ca^{2+} already released in the SR, so that the ion itself, with the smallest fluctuation in concentration, regulates the RyR1 channel [104, 105].

Beyond that, considering that the intensity of the force is intracellular [Ca^{2+}] related and that in turn depends on the release of Ca^{2+} and the self-regulation of some channels for removal or influx, it is important to note that the decrease in [Ca^{2+}], even if is it physiological, tends to prolong the relaxation period, the opposite being also possible, and the increase in [Ca^{2+}] tends to prolong the contractile period of the fibers, even when the reduction of the Ca^{2+} of the SR during the contractile activity remains due to the binding of increased Ca^{2+} intracellular fast fiber proteins and the SR pump, thus consequently removing more slowly. In summary, the cell signaling that controls the period and the place where Ca^{2+} must be maintained during the contraction time and the relaxation time after tetanus contraction in the muscle are essential to understand muscle fatigue [106, 107].

Comparatively, the mechanism for the development of muscle fatigue also depends on the amount of ATP recruited by the muscle, from which it will then be degraded into ADP + pi, as well as the extent of phosphocreatine depletion. Studies suggest that muscle fibers have the ability to sustain ADP decline without opening Ca^{2+} channels and flooding the muscle with these ions, so that action potentials with 0.5 mM cell decline did not activate Ca^{2+} release. However, when injected with Mg^{2+} ion in the declining action potential, an inhibition of Ca^{2+} channels was observed, due to the competition of intracellular Mg^{2+} by ATP, resulting in the fall of free ATP, which was possible to be released after intense exercise [108, 109].

7. Fatigue in Organs

Fatigue occurs in whole muscles when there is a loss of peak strength, speed, and power, in which the time course of change in function depends on the intensity of activation and the composition of the type of muscle fiber [92, 109]. The human body has some muscles made up of slow muscle fibers, so they are called slow muscles, such as the sole of the calf. These fibers are composed mainly of slow type I or slow

oxidative fibers, that is, they generate ATP mainly from oxidative phosphorylation and are kept tonically active and are extremely resistant to fatigue. On the other hand, muscles made up of fast fibers usually have greater capacity to obtain ATP from glycolysis and other energy sources, are not kept tonically active, and are not resistant to fatigue [79, 96].

Going deeper into the types of fibers present in the human body. There are two types of fast fibers: IIa or fast-oxidizing glycolytic fibers and IIx or glycolytic fibers. In addition to the hybrid fast fibers that contain myosin are IIa and IIx. The hybrid fiber IIx has the highest maximum speed and glycolytic capacity, while the hybrid fiber IIa has properties between fast IIx and slow type I fibers. Additionally, there is a third fast type IIb fiber, which is the fastest of all the fibers, but is expressed, in extremely inactive muscles [108, 110].

Studies have shown that understanding the isometric contraction properties before and after fatigue has helped to identify cell fatigue sites. For example, postfatigue muscle contractions show reduced muscle tension and prolonged contraction and relaxation times. The duration of the contraction depends on the detachment rate of the AM cross-bridge and the duration of the transient intracellular Ca^{2+}; therefore, the prolongation of fatigue-induced contraction is an indication that the Ca^{2+}/ATPase reuptake by the SR may have been inhibited; note as well that the duration of relaxation after a peak of contraction in tetany is limited by the activity of the Ca^{2+}/ATPase/SR pump [50, 105].

According to studies that analyzed the initial phase of relaxation of a muscle in tetany, the lengths of the sarcomere remain constant and it is believed that the relaxation rate depends directly on the detachment rate of the AM cross-bridge, so that this phase showed a longer fatigue time compared to the second relaxation phase and should probably be limited by the activity of the Ca^{2+}/ATPase/SR pump [23].

Another point to be considered would be that the development of fatigue would be a force-frequency relationship. If the strength continuously decreases and relatively less frequently compared to the high ones, a solution would be that the transient Ca^{2+} induces in the prolongation of fatigue with low injections, however, continuous so that the muscular strength in fatigued muscles also decreases [78].

Along with the slowing of relaxation, α-motoneuron firing rates decline with fatigue in vivo. This response is consistent with studies that observe that the optimal stimulation frequency for peak force showed a decline in muscle with fatigue [39].

Some studies show that the aim should be the muscle contractile process and should include disturbances in cross-bridge AM interactions caused by increases in pH and Pi and alterations in SR function or in the Ca^{2+}/ATPase pump, besides the changes that can occur in cross-bridge AM. Therefore, the force, velocity, and power all are reduced. In addition, the hydrolysis of ATP produces an increase in free Mg^{2+} and inhibition of the RyR1 and Ca^{2+} release [106].

It is well known that in cases of prolonged exercise, fatigue is inevitable, as this is correlated with muscle glycogen depletion and hypoglycemia. Currently, studies are needed to explain this mandatory carbohydrate oxidation; it is hypothesized that the decrease in muscle glycogen and the increased dependence on fat oxidation end up limiting the ability of mitochondria to provide important components for oxidative phosphorylation such as NADH, before the muscle suffers; in addition, it was also observed that glycogen has a greater affinity with DHPR and RyR1, thus making the alternatives to meet the need for the muscle obsolete [102, 111].

A reduced uptake of SR Ca^{2+} without alteration in ATPase activity suggests a decoupling of the transport or leaking vesicle, through which Ca^{2+} escapes into the intracellular medium and changes the concentration and local pH. Another organelle that can be damaged due to prolonged physical exercise would be the mitochondria, in which studies indicate that it may present some edema, but there is no evidence that it can impair its function; however, it was observed that the fibers showed some wear after prolonged exercise [105, 109].

The oxidative phosphorylation that occurs in the mitochondria produces ATP and consumes O_2; this process is also capable of generating ROS, such as hydrogen peroxide (H_2O_2) and superoxide anion (O_2^-). The rate of production of ROS increases according to the intensity of work and the rate of respiration in skeletal muscle, and it is commonly recognized that ROS play a role in muscle fatigue by the oxidation of critical cellular proteins, such as the Na^+ K^+ pump, myofilaments, DHPR, and RyR1. The oxidation of ROS at critical RyR1 cysteine residues and/or myofibril serine groups can assist in the development of low-frequency fatigue and inhibit the release of Ca^{2+} from SR and the sensitivity of Ca^{2+} in myofibrils [91, 103, 112].

It is believed that there is a mechanism that involves a structural alteration of the Ca^{2+} SR release channel and/or associated proteins, since the amplitude of the Ca^{2+} transient is decreased for all stimulus frequencies, so that the concentration ratio of Ca^{2+} and strength is increasingly observed, and it can be concluded that Ca^{2+} mediators probably involve calmodulin (CaM), calcium-activated proteases, or ROS [64, 89, 104].

Ryr1 is part of a multiprotein complex that includes proteins involved in phosphorylation/dephosphorylation, linked to different types of cell signaling, such as cAMP-dependent protein kinase (PKA), Ca-Calmodulin-dependent protein kinase (CaMKII), phosphodiesterase-4-D-3 (PDE4D3), protein phosphatase 1 (PP1), the Ca^{2+} binding protein CaM, and modulation of Ca^{2+} activation of the channel [23, 105, 113].

It is well established that CaM plays a dual role in the regulation of the Ca^{2+} in SR release channels. CaM binding activates or inhibits the opening of the Ca^{2+} channel in the cytoplasm whose concentration is low and high. In a nonfatigued muscle fiber, this process probably contributes to the cyclic activation and inactivation of the release channel. There is no evidence linking Ca^{2+} with CaM to an altered RyR1 function. However, there is a possibility that the elevated cytoplasmic Ca^{2+} associated with fatigue leads to an altered CaM binding, so that the channel becomes more difficult to activate. The increase in cytoplasmic Ca^{2+} can lead to prolonged elevation of CaMKII and cause excessive phosphorylation of DHPR and/or RyR1. Looking from another point, prolonged β-adrenergic activity with exercise can also

lead to an increase in PKA activity and result in hyperphosphorylation of RyR1. In addition, the inhibition of the PP1 and/or PDE4D3 protein can also lead to excess phosphorylation of RyR1, which can directly reduce the probability of its opening or mediate the dissociation of the stabilizing protein from the FKBP12 channel [7, 48, 106].

The exact mechanisms and relative importance of RyR1 and the Ca^{2+}/ATPase/SR pump are not completely understood and represent an important area for future research [78, 102, 107].

8. Photobiomodulation

Low-level laser therapy (LLLT) or laser therapy has been used for more than 40 years. The idea came up in 1960 after the invention of the laser, making it a widespread treatment with a variety of clinical applications. Scholars of the time decided to use different tools and models to be used according to their functions, the expressions like "photobioactivation" and "biostimulation" are often related to the stimulation effect that the LLT was used for. However, a few years later, it was possible to verify that the LLT also has an inhibitory effect; from that, it was established to coin the term "biomodulation" [108, 110].

Therapeutic treatments are based on three principles: first, minimize inflammation, edema, and chronic disorders of the joints, brain, skin, etc; second, promote wound healing in superficial and deep tissues, etc; and third, treating neurological disorders and pain [108, 111].

Recent studies indicate that the most used wavelengths for photobiomodulation therapy (PBM) are infrared (IR) and 700 nm to near infrared (NIR), in which they have shown more beneficial impacts than light-red in many medical conditions [109, 111].

In general, the laser therapy involves portions of the electromagnetic spectrum (390–1600 nm and 1013–1015 Hz), which is red until NIR, and they are absorbed according to the specific application for each biological tissue and the appropriate wavelengths [4, 112].

Unlike high-power "hard" lasers, LLLT provides low energy, just enough to induce a response in body tissue. In addition, it has a wavelength-dependent shape capable of altering cell function in the absence of significant heating. Thus, LLLT is also called "soft" laser therapy or cold laser, as it has low energy without thermal effects [114, 115].

Studies show that the wide range of laser therapy includes effects at the molecular, cellular, and tissue levels and the ways in which LLLT works can vary according to different application factors [116]. For the LLLT, to produce a photobiological effect, it is necessary for the photon absorption of the laser radiation to occur; the photons are captured by the initial photoreceptor molecules, which can be endogenous or exogenous chromophores. The energy absorbed from a photon can be transferred to another molecule, which can then cause a chemical reaction without changing the temperature in the surrounding tissue and consequently triggers local biochemical reactions without any discomfort [109, 117].

Several studies have suggested that mitochondria are the cellular component most sensitive to visible light and NIR; this stimulus results in increased ATP production, increased deoxyribonucleic acid (DNA) synthesis, ROS modulation, and nitric oxygen species (NOS) and in the induction of transcription factors. In addition, PBM at red and NIR wavelengths stimulates an increase in intracellular ionic Ca^{2+}. However, recent studies emphasize that blue (420 nm) and green (540 nm) lights are more effective in increasing intracellular Ca^{2+}. Researchers also suggest the use of blue or green light for better interaction with light-dependent ion channels, which allows light to control electrical excitability, intracellular acidity, and calcium influx, among other processes. The most likely ion channel is the rhodopsin of the light-gated channel, because the spectrum of action of the rhodopsin family exhibits peaks in the blue-green spectral region. However, the mechanism of laser-tissue interaction has not yet been fully described [118–120].

At the cellular and molecular levels, there are still open arguments and responses about the effectiveness of lasers in producing the desired responses [121]. Photobiomodulation is a form of phototherapy, which is designed to apply light with specific wavelengths from red to NIR with output powers of up to 500 mW. One of the great advantages of LLLT is the use of photon energy at low levels to alter biological activity without thermal reactions, since there is little increase in the temperature of the irradiated tissue, in addition to being nontoxic and nonallergic, and due to the ease of application that its study has been spreading increasingly [122].

Studies indicate that clinical treatment with LLLT in various intensities has a stimulating effect on cellular processes [123]. Recently, it has been reported that at low levels of red or infrared light, LLLT can prevent cell apoptosis; stimulate mitochondrial activity; increase in cell recruitment, proliferation, and renewal; and modulate cell metabolites. In addition, it has also been suggested that LLLT may promote changes in the cell's redox state, playing an important role in ion homeostasis and consequently in cellular activity and induce photobiostimulation processes. Besides that, preexposure of PBM has a protective effect against many external agents, such as hydrogen peroxide (H_2O_2) and UV radiation [124, 125].

9. Discussion

Studies suggested that the implementation of low-level laser therapy (LLLT) may cause biomodulatory, biochemical, bioelectrical, and bioenergetic effects. That is why we can use it in the repair of fatigued muscles, muscular disorders, and improved muscle performance in specific muscles already treated with LLLT. According to [126], the experimental study with 15 volunteers including female and male stroke patients who presented with poststroke spasticity, the LLLT (diode laser, 100 mW, 808 nm, beam spot area 0.0314 cm^2, 127.39 J/cm^2/point, 40 s) was applied mainly in areas where spasticity was present like the *rectus femoris* muscle and to the *vastus medialis* muscle. After LLLT, intervention was observed to contribute to the increase in the recruitment of muscle fibers, reduction in the scale for pain intensity

because of its anti-inflammatory effect in stroke patients with spasticity, time delay to the fatigue onset, improvement of muscle performance, and increase in peak torque. The study also observed that LLLT provided major breakthroughs in the treatment of muscular disorders and prevention of muscle fatigue.

The literature shows that positive results were found with a single application of LLLT on tissue regeneration and decreased neurological injury but there are not enough information about laser therapy related to spastic muscle and it shows increased resistance to passive stretching that can be explained by changes in muscle tissue properties and early onset of muscle fatigue. In addition, the authors found that the application of laser photobiomodulation in spastic muscle prior to isometric exercise contributes to the decrease in blood lactate concentration after exercise possibly because laser radiation increases microcirculation, increases metabolite removal, and prevents local ischemia. Besides, it seems that the vascular effects of PBM may be due to the nitric oxide release, leading to smooth muscle relaxation and increased peripheral microcirculation. Considering the bioenergetic effects, the LLLT application is related to mitochondrial function and light interacts with the mitochondria and promotes cellular changes that also may contribute to delay muscle fatigue [127].

Impairment of basic motor functions, such as muscle weakness in limbs affected by spasticity, leads to peripheral fatigue and impaired functionality. According to [128], the clinical use of PBM has provided major advances in the treatment of muscular disorders and prevention of muscle fatigue. Their study were structured with 10 sessions of PBMT (laser 100 mW, 808 nm, 159.24 J/cm^2/point, 5 J/point); PBM active or placebo was associated with exoskeleton-assisted functional treatment. A double-blind, placebo-controlled sequential clinical trial was conducted with 12 healthy volunteers and 15 poststroke patients who presented upper limb spasticity. Ultimately, it suggests that the application of PBM may contribute to an increased range of elbow motion and muscle fiber recruitment, increases in muscle strength, and, hence, increases in signal conduction on spastic muscle fibers in spastic patients.

10. Conclusion

It could be concluded that LLLT may contribute to an increased range of muscle motion and fiber recruitment and increased strength to increase signal conduction on spastic muscle fibers in spastic patients. However, further studies are needed to understand how fatigued fibers behave in these patients, since clinical studies used different laser wavelengths and numerous illumination parameters, which influence the determination of different biological parameters.

In addition, the literature is not explicit about the application of PBM in spastic patients but that this possibility could reduce pain and fatigue regarding biochemical and neuromotor mechanisms that may represent a new therapeutic use for neurological patients.

Conflicts of Interest

The authors declare that they have no conflicts of interest.

References

[1] C. M. França, C. M. França, S. C. Núñez et al., "Low-intensity red laser on the prevention and treatment of induced-oral mucositis in hamsters," *Journal of Photochemistry and Photobiology B: Biology*, vol. 94, no. 1, pp. 25–31, 2009.

[2] M. T. B. R. Santos, M. da Silva Pinto, K. S. Do Nascimento, and S. C. Maciel, "Efeito da fotobiomodulação no músculo masseter de criança com paralisia cerebral: relato de caso," *Revista Acta Fisiátrica*, vol. 22, no. 1, pp. 39–42, 2015.

[3] C. Kara, T. Demir, and E. Özbek, "Evaluation of low-level laser therapy in rabbit oral mucosa after soft tissue graft application: a pilot study," *Journal of Cosmetic and Laser Therapy*, vol. 15, no. 6, pp. 326–329, 2013.

[4] T. Agrawal, G. K. Gupta, V. Rai, J. D. Carroll, and M. R. Hamblin, "Pre-conditioning with low-level laser (light) therapy: light before the storm," *Dose-Response*, vol. 12, no. 4, pp. -dose–response.1, 2014.

[5] D.-H. Choi, J. H. Lim, K.-H. Lee et al., "Effect of 710-nm visible light irradiation on neuroprotection and immune function after stroke," *Neuroimmunomodulation*, vol. 19, no. 5, pp. 267–276, 2012.

[6] W. R. Frontera and J. Ochala, "Skeletal muscle: a brief review of structure and function," *Calcified Tissue International*, vol. 96, no. 3, pp. 183–195, 2015.

[7] M. Marini and A. Veicsteinas, "The exercised skeletal muscle: a review," *European Journal of Translational Myology*, vol. 20, no. 3, 2010.

[8] R. R. Wolfe, "The underappreciated role of muscle in health and disease," *The American Journal of Clinical Nutrition*, vol. 84, no. 3, pp. 475–482, 2006.

[9] S. B. Heymsfield, M. Adamek, M. C. Gonzalez, G. Jia, and D. M. Thomas, "Assessing skeletal muscle mass: historical overview and state of the art," *Journal of Cachexia, Sarcopenia and Muscle*, vol. 5, no. 1, pp. 9–18, 2014.

[10] R. Javan, J. J. Horvath, L. E. Case et al., "Generating color-coded anatomic muscle maps for correlation of quantitative magnetic resonance imaging analysis with clinical examination in neuromuscular disorders," *Muscle & Nerve*, vol. 48, no. 2, pp. 293–295, 2013.

[11] M. Fortin, T. Videman, L. E. Gibbons, and M. C. Battie, "Paraspinal muscle morphology and composition," *Medicine and Science in Sports and Exercise*, vol. 46, no. 5, pp. 893–901, 2014.

[12] R. S. Hikida, "Aging changes in satellite cells and their functions," *Current Aging Science*, vol. 4, no. 3, pp. 279–297, 2011.

[13] L. Zhao, X. Zhang, Q. Luo, C. Hou, J. Xu, and J. Liu, "Engineering nonmechanical protein-based hydrogels with highly mechanical properties: comparison with natural muscles," *Biomacromolecules*, vol. 21, no. 10, pp. 4212–4219, 2020.

[14] F. Macaluso and K. H. Myburgh, "Current evidence that exercise can increase the number of adult stem cells," *Journal of Muscle Research and Cell Motility*, vol. 33, no. 3-4, pp. 187–198, 2012.

[15] A. Bareja, J. A. Holt, G. Luo et al., "Human and mouse skeletal muscle stem cells: convergent and divergent mechanisms of myogenesis," *PloS one*, vol. 9, no. 2, article e90398, 2014.

[16] G. D. Thomas, "Functional muscle ischemia in Duchenne and Becker muscular dystrophy," *Frontiers in Physiology*, vol. 4, p. 381, 2013.

[17] C. A. Ottenheijm and H. Granzier, "Lifting the nebula: novel insights into skeletal muscle contractility," *Physiology*, vol. 25, no. 5, pp. 304–310, 2010.

[18] C. Gelfi, M. Vasso, and P. Cerretelli, "Diversity of human skeletal muscle in health and disease: contribution of proteomics," *Journal of Proteomics*, vol. 74, no. 6, pp. 774–795, 2011.

[19] J. A. Monroy, K. L. Powers, L. A. Gilmore, T. A. Uyeno, S. L. Lindstedt, and K. C. Nishikawa, "What is the role of titin in active muscle?," *Exercise and Sport Sciences Reviews*, vol. 40, no. 2, pp. 73–78, 2012.

[20] S. M. Greising, H. M. Gransee, C. B. Mantilla, and G. C. Sieck, "Systems biology of skeletal muscle: fiber type as an organizing principle," *Wiley Interdisciplinary Reviews: Systems Biology and Medicine*, vol. 4, no. 5, pp. 457–473, 2012.

[21] T. R. Leonard and W. Herzog, "Regulation of muscle force in the absence of actin-myosin-based cross-bridge interaction," *American Journal of Physiology-Cell Physiology*, vol. 299, no. 1, pp. C14–C20, 2010.

[22] I. D. Jayasinghe and B. S. Launikonis, "Three-dimensional reconstruction and analysis of the tubular system of vertebrate skeletal muscle," *Journal of Cell Science*, vol. 126, no. 17, pp. 4048–4058, 2013.

[23] J. P. Kerr, C. W. Ward, and R. J. Bloch, "Dysferlin in transverse tubules regulates Ca^{2+} homeostasis in skeletal muscle," *Frontiers in Physiology*, vol. 5, p. 89, 2014.

[24] R. Dahl, S. Larsen, T. L. Dohlmann et al., "Three-dimensional reconstruction of the human skeletal muscle mitochondrial network as a tool to assess mitochondrial content and structural organization," *Acta Physiologica*, vol. 213, no. 1, pp. 145–155, 2015.

[25] C. R. Lamboley, R. M. Murphy, M. J. McKenna, and G. D. Lamb, "Sarcoplasmic reticulum Ca2+uptake and leak properties, and SERCA isoform expression, in type I and type II fibres of human skeletal muscle," *The Journal of Physiology*, vol. 592, no. 6, pp. 1381–1395, 2014.

[26] Z. Yan, V. A. Lira, and N. P. Greene, "Exercise training-induced regulation of mitochondrial quality," *Exercise and sport sciences reviews*, vol. 40, no. 3, pp. 159–164, 2012.

[27] N. Weisleder, M. Brotto, S. Komazaki et al., "Muscle aging is associated with compromised Ca^{2+} spark signaling and segregated intracellular Ca^{2+} release," *The Journal of Cell Biology*, vol. 174, no. 5, pp. 639–645, 2006.

[28] S. Schiaffino and C. Reggiani, "Fiber types in mammalian skeletal muscles," *Physiological Reviews*, vol. 91, no. 4, pp. 1447–1531, 2011.

[29] A. J. Galpin, U. Raue, B. Jemiolo et al., "Human skeletal muscle fiber type specific protein content," *Analytical Biochemistry*, vol. 425, no. 2, pp. 175–182, 2012.

[30] E. R. Weibel, "The structural conditions for oxygen supply to muscle cells: the Krogh cylinder model," *Journal of Experimental Biology*, vol. 216, no. 22, pp. 4135–4137, 2013.

[31] O. Baum and M. Bigler, "Pericapillary basement membrane thickening in human skeletal muscles," *American Journal of Physiology-Heart and Circulatory Physiology*, vol. 311, no. 3, pp. H654–H666, 2016.

[32] S. L. Lindstedt, "Body size, time and dimensions of oxygen diffusion," *Comparative Biochemistry and Physiology Part A: Molecular & Integrative Physiology*, vol. 252, article 110847, 2021.

[33] G. R. Steinberg and B. E. Kemp, "AMPK in health and disease," *Physiological Reviews*, vol. 89, no. 3, pp. 1025–1078, 2009.

[34] F. Karpe, J. R. Dickmann, and K. N. Frayn, "Fatty acids, obesity, and insulin resistance: time for a reevaluation," *Diabetes*, vol. 60, no. 10, pp. 2441–2449, 2011.

[35] A. Houdusse and H. L. Sweeney, "How myosin generates force on actin filaments," *Trends in Biochemical Sciences*, vol. 41, no. 12, pp. 989–997, 2016.

[36] D. M. Callahan, S. A. Foulis, and J. A. Kent-Braun, "Age-related fatigue resistance in the knee extensor muscles is specific to contraction mode," *Muscle & Nerve: Official Journal of the American Association of Electrodiagnostic Medicine*, vol. 39, no. 5, pp. 692–702, 2009.

[37] T. Paillard, "Effects of general and local fatigue on postural control: a review," *Neuroscience & Biobehavioral Reviews*, vol. 36, no. 1, pp. 162–176, 2012.

[38] B. C. Clark and T. M. Manini, "What is dynapenia?," *Nutrition*, vol. 28, no. 5, pp. 495–503, 2012.

[39] S. K. Hunter, H. M. Pereira, and K. G. Keenan, "The aging neuromuscular system and motor performance," *Journal of Applied Physiology*, vol. 121, no. 4, pp. 982–995, 2016.

[40] M. Tieland, I. Trouwborst, and B. C. Clark, "Skeletal muscle performance and ageing," *Journal of Cachexia, Sarcopenia and Muscle*, vol. 9, no. 1, pp. 3–19, 2018.

[41] J. A. Kent-Braun, R. H. Fitts, and A. Christie, "Skeletal muscle fatigue," *Comprehensive Physiology*, vol. 2, no. 2, pp. 997–1044, 2011.

[42] C. Byrne, C. Twist, and R. Eston, "Neuromuscular function after exercise-induced muscle damage," *Sports Medicine*, vol. 34, no. 1, pp. 49–69, 2004.

[43] D. E. Rassier and B. R. Macintosh, "Coexistence of potentiation and fatigue in skeletal muscle," *Brazilian Journal of Medical and Biological Research*, vol. 33, no. 5, pp. 499–508, 2000.

[44] J. A. Kent-Braun, A. V. Ng, J. W. Doyle, and T. F. Towse, "Human skeletal muscle responses vary with age and gender during fatigue due to incremental isometric exercise," *Journal of Applied Physiology*, vol. 93, no. 5, pp. 1813–1823, 2002.

[45] R. H. Fitts, "The cross-bridge cycle and skeletal muscle fatigue," *Journal of Applied Physiology*, vol. 104, no. 2, pp. 551–558, 2008.

[46] R. M. Enoka and J. Duchateau, "Muscle fatigue: what, why and how it influences muscle function," *Journal of Physiology*, vol. 586, no. 1, pp. 11–23, 2008.

[47] M. Cifrek, V. Medved, S. Tonković, and S. Ostojić, "Surface EMG based muscle fatigue evaluation in biomechanics," *Clinical biomechanics*, vol. 24, no. 4, pp. 327–340, 2009.

[48] B. M. Kluger, L. B. Krupp, and R. M. Enoka, "Fatigue and fatigability in neurologic illnesses: proposal for a unified taxonomy," *Neurology*, vol. 80, no. 4, pp. 409–416, 2013.

[49] S. M. Marcora and W. Staiano, "The limit to exercise tolerance in humans: mind over muscle?," *European Journal of Applied Physiology*, vol. 109, no. 4, pp. 763–770, 2010.

[50] D. G. Allen, G. D. Lamb, and H. Westerblad, *Skeletal Muscle Fatigue: Cellular Mechanisms*, Physiological reviews, 2008.

[51] P. Steinbacher and P. Eckl, "Impact of oxidative stress on exercising skeletal muscle," *Biomolecules*, vol. 5, no. 2, pp. 356–377, 2015.

[52] R. Cooke, "Modulation of the actomyosin interaction during fatigue of skeletal muscle," *Muscle & Nerve: Official Journal of the American Association of Electrodiagnostic Medicine*, vol. 36, no. 6, pp. 756–777, 2007.

[53] M. J. Greenberg and J. R. Moore, "The molecular basis of frictional loads in the in vitro motility assay with applications to the study of the loaded mechanochemistry of molecular motors," *Cytoskeleton*, vol. 67, no. 5, pp. 273–285, 2010.

[54] E. Debold, "Recent insights into the molecular basis of muscular fatigue," *Medicine & Science in Sports & Exercise*, vol. 44, no. 8, pp. 1440–1452, 2012.

[55] H. Wolfenson, A. Bershadsky, Y. I. Henis, and B. Geiger, "Actomyosin-generated tension controls the molecular kinetics of focal adhesions," *Journal of Cell Science*, vol. 124, no. 9, pp. 1425–1432, 2011.

[56] M. Caremani, J. Dantzig, Y. E. Goldman, V. Lombardi, and M. Linari, "Effect of inorganic phosphate on the force and number of myosin cross-bridges during the isometric contraction of permeabilized muscle fibers from rabbit psoas," *Biophysical Journal*, vol. 95, no. 12, pp. 5798–5808, 2008.

[57] M. Linari, M. Caremani, and V. Lombardi, "A kinetic model that explains the effect of inorganic phosphate on the mechanics and energetics of isometric contraction of fast skeletal muscle," *Proceedings of the Royal Society B: Biological Sciences*, vol. 277, no. 1678, pp. 19–27, 2010.

[58] T. Driss and H. Vandewalle, "The measurement of maximal (anaerobic) power output on a cycle ergometer: a critical review," *BioMed Research International*, vol. 2013, 40 pages, 2013.

[59] H. Westerblad and D. G. Allen, "Changes of myoplasmic calcium concentration during fatigue in single mouse muscle fibers," *Journal of General Physiology*, vol. 98, no. 3, pp. 615–635, 1991.

[60] B. Grassi, H. B. Rossiter, and J. A. Zoladz, "Skeletal muscle fatigue and decreased Efficiency," *Exercise and Sport Sciences Reviews*, vol. 43, no. 2, pp. 75–83, 2015.

[61] J. J. Wan, Z. Qin, P. Y. Wang, Y. Sun, and X. Liu, "Muscle fatigue: general understanding and treatment," *Experimental & Molecular Medicine*, vol. 49, no. 10, pp. e384–e384, 2017.

[62] A. J. Dahlstedt, A. Katz, and H. Westerblad, "Role of myoplasmic phosphate in contractile function of skeletal muscle: studies on creatine kinase-deficient mice," *Journal of Physiology*, vol. 533, no. 2, pp. 379–388, 2001.

[63] D. G. Allen, G. D. Lamb, and H. Westerblad, "Impaired calcium release during fatigue," *Journal of Applied Physiology*, vol. 104, no. 1, pp. 296–305, 2008.

[64] S. P. Cairns, "Lactic acid and exercise performance," *Sports Medicine*, vol. 36, no. 4, pp. 279–291, 2006.

[65] A. M. Jones, D. P. Wilkerson, F. DiMenna, J. Fulford, and D. C. Poole, "Muscle metabolic responses to exercise above and below the "critical power" assessed using 31P-MRS," *American Journal of Physiology Regulatory, Integrative and Comparative Physiology*, vol. 294, no. 2, pp. R585–R593, 2008.

[66] H. Westerblad, J. D. Bruton, and A. Katz, "Skeletal muscle: energy metabolism, fiber types, fatigue and adaptability," *Experimental Cell Research*, vol. 316, no. 18, pp. 3093–3099, 2010.

[67] E. P. Debold, J. Romatowski, and R. H. Fitts, "The depressive effect of Pi on the force-pCa relationship in skinned single muscle fibers is temperature dependent," *American Journal of Physiology-Cell Physiology*, vol. 290, no. 4, pp. C1041–C1050, 2006.

[68] C. R. Nelson and R. H. Fitts, "Effects of low cell pH and elevated inorganic phosphate on the pCa-force relationship in single muscle fibers at near-physiological temperatures," *American Journal of Physiology-Cell Physiology*, vol. 306, no. 7, pp. C670–C678, 2014.

[69] E. Debold, "Recent insights into muscle fatigue at the cross-bridge level," *Frontiers in Physiology*, vol. 3, p. 151, 2012.

[70] G. P. Farman, E. J. Allen, K. Q. Schoenfelt, P. H. Backx, and P. P. De Tombe, "The role of thin filament cooperativity in cardiac length-dependent calcium activation," *Biophysical Journal*, vol. 99, no. 9, pp. 2978–2986, 2010.

[71] R. D. Mateja, M. L. Greaser, and P. P. de Tombe, "Impact of titin isoform on length dependent activation and cross-bridge cycling kinetics in rat skeletal muscle," *Biochimica et Biophysica Acta (BBA)-Molecular Cell Research*, vol. 1833, no. 4, pp. 804–811, 2013.

[72] A. S. Cornachione, F. Leite, M. A. Bagni, and D. E. Rassier, "The increase in non-cross-bridge forces after stretch of activated striated muscle is related to titin isoforms," *American Journal of Physiology-Cell Physiology*, vol. 310, no. 1, pp. C19–C26, 2016.

[73] R. A. Bassit, C. H. da Justa Pinheiro, K. F. Vitzel, A. J. Sproesser, L. R. Silveira, and R. Curi, "Effect of short-term creatine supplementation on markers of skeletal muscle damage after strenuous contractile activity," *European Journal of Applied Physiology*, vol. 108, no. 5, pp. 945–955, 2010.

[74] E. Prochniewicz, D. A. Lowe, D. J. Spakowicz et al., "Functional, structural, and chemical changes in myosin associated with hydrogen peroxide treatment of skeletal muscle fibers," *American Journal of Physiology-Cell Physiology*, vol. 294, no. 2, pp. C613–C626, 2008.

[75] W. A. Macdonald and D. G. Stephenson, "Effect of ADP on slow-twitch muscle fibres of the rat: implications for muscle fatigue," *Journal of Physiology*, vol. 573, no. 1, pp. 187–198, 2006.

[76] R. M. Murphy, N. T. Larkins, J. P. Mollica, N. A. Beard, and G. D. Lamb, "Calsequestrin content and SERCA determine normal and maximal Ca2+storage levels in sarcoplasmic reticulum of fast- and slow-twitch fibres of rat," *The Journal of Physiology*, vol. 587, no. 2, pp. 443–460, 2009.

[77] S. M. Norris, E. Bombardier, I. C. Smith, C. Vigna, and A. R. Tupling, "ATP consumption by sarcoplasmic reticulum Ca2 +pumps accounts for 50% of resting metabolic rate in mouse fast and slow twitch skeletal muscle," *American Journal of Physiology-Cell Physiology*, vol. 298, no. 3, pp. C521–C529, 2010.

[78] S. Gehlert, W. Bloch, and F. Suhr, "Ca2+-dependent regulations and signaling in skeletal muscle: from electromechanical coupling to adaptation," *International Journal of Molecular Sciences*, vol. 16, no. 1, pp. 1066–1095, 2015.

[79] E. P. Debold, S. E. Beck, and D. M. Warshaw, "Effect of low pH on single skeletal muscle myosin mechanics and kinetics," *American Journal of Physiology-Cell Physiology*, vol. 295, no. 1, pp. C173–C179, 2008.

[80] M. Amann and J. A. Calbet, "Convective oxygen transport and fatigue," *Journal of Applied Physiology*, vol. 104, no. 3, pp. 861–870, 2008.

[81] O. Friedrich, M. B. Reid, G. Van den Berghe et al., *The Sick and the Weak: Neuropathies/Myopathies in the Critically Ill*, Physiological reviews, 2015.

[82] M. Maffei, E. Longa, R. Qaisar et al., "Actin sliding velocity on pure myosin isoforms from hindlimb unloaded mice," *Acta Physiologica*, vol. 212, no. 4, pp. 316–329, 2014.

[83] M. Yamaguchi, M. Kimura, Z. B. Li et al., "X-ray diffraction analysis of the effects of myosin regulatory light chain phosphorylation and butanedione monoxime on skinned skeletal muscle fibers," *American Journal of Physiology-Cell Physiology*, vol. 310, no. 8, pp. C692–C700, 2016.

[84] H. Jungbluth, S. Treves, F. Zorzato et al., "Congenital myopathies: disorders of excitation-contraction coupling and muscle contraction," *Nature Reviews Neurology*, vol. 14, no. 3, pp. 151–167, 2018.

[85] G. Cherednichenko, R. Zhang, R. A. Bannister et al., "Triclosan impairs excitation–contraction coupling and Ca^{2+} dynamics in striated muscle," *Proceedings of the National Academy of Sciences*, vol. 109, no. 35, pp. 14158–14163, 2012.

[86] R. T. Rebbeck, Y. Karunasekara, P. G. Board, N. A. Beard, M. G. Casarotto, and A. F. Dulhunty, "Skeletal muscle excitation-contraction coupling: Who are the dancing partners?," *The International Journal of Biochemistry & Cell Biology*, vol. 48, pp. 28–38, 2014.

[87] H. Manring, E. Abreu, L. Brotto, N. Weisleder, and M. Brotto, "Novel excitation-contraction coupling related genes reveal aspects of muscle weakness beyond atrophy—new hopes for the treatment of musculoskeletal diseases," *Frontiers in Physiology*, vol. 5, p. 37, 2014.

[88] G. Santulli, D. R. Lewis, and A. R. Marks, "Physiology and pathophysiology of excitation–contraction coupling: the functional role of ryanodine receptor," *Journal of Muscle Research and Cell Motility*, vol. 38, no. 1, pp. 37–45, 2017.

[89] O. Delbono, "Expression and regulation of excitation-contraction coupling proteins in aging skeletal muscle," *Current Aging Science*, vol. 4, no. 3, pp. 248–259, 2011.

[90] R. Zalk and S. E. Lehnart, "Modulation of the ryanodine receptor and intracellular calcium," *Annual Review of Biochemistry*, vol. 76, no. 1, pp. 367–385, 2007.

[91] M. J. McKenna, J. Bangsbo, and J. M. Renaud, "Muscle K^+, Na^+, and Cl–disturbances and Na+-K+pump inactivation: implications for fatigue," *Journal of Applied Physiology*, vol. 104, no. 1, pp. 288–295, 2008.

[92] J. C. Calderón, P. Bolaños, and C. Caputo, "The excitation–contraction coupling mechanism in skeletal muscle," *Biophysical Reviews*, vol. 6, no. 1, pp. 133–160, 2014.

[93] A. Polster, B. R. Nelson, E. N. Olson, and K. G. Beam, "Stac3 has a direct role in skeletal muscle-type excitation–contraction coupling that is disrupted by a myopathy-causing mutation," *Proceedings of the National Academy of Sciences*, vol. 113, no. 39, pp. 10986–10991, 2016.

[94] M. Quinonez, F. González, C. Morgado-Valle, and M. DiFranco, "Effects of membrane depolarization and changes in extracellular $[K^+]$ on the Ca^{2+} transients of fast skeletal muscle fibers. Implications for muscle fatigue," *Journal of Muscle Research and Cell Motility*, vol. 31, no. 1, pp. 13–33, 2010.

[95] T. Clausen, "Quantification of Na^+, K^+ pumps and their transport rate in skeletal muscle: functional significance," *Journal of General Physiology*, vol. 142, no. 4, pp. 327–345, 2013.

[96] P. Manoharan, T. L. Radzyukevich, H. Hakim Javadi et al., "Phospholemman is not required for the acute stimulation of Na^+-K^+-ATPase α2-activity during skeletal muscle fatigue," *American Journal of Physiology-Cell Physiology*, vol. 309, no. 12, pp. C813–C822, 2015.

[97] B. D. Perry, V. L. Wyckelsma, R. M. Murphy et al., "Dissociation between short-term unloading and resistance training effects on skeletal muscle Na+,K+-ATPase, muscle function, and fatigue in humans," *Journal of Applied Physiology*, vol. 121, no. 5, pp. 1074–1086, 2016.

[98] B. Gong, D. Legault, T. Miki, S. Seino, and J. M. Renaud, "KATPchannels depress force by reducing action potential amplitude in mouse EDL and soleus muscle," *American Journal of Physiology-Cell Physiology*, vol. 285, no. 6, pp. C1464–C1474, 2003.

[99] T. Clausen and O. B. Nielsen, "Potassium, Na+,K+-pumps and fatigue in rat muscle," *The Journal of Physiology*, vol. 584, no. 1, pp. 295–304, 2007.

[100] O. B. Nielsen and F. V. de Paoli, "Regulation of Na+–K+homeostasis and excitability in contracting muscles: implications for fatigue," *Applied Physiology, Nutrition, and Metabolism*, vol. 32, no. 5, pp. 974–984, 2007.

[101] M. Hostrup, A. Kalsen, N. Ørtenblad et al., "β2-Adrenergic stimulation enhances Ca2+release and contractile properties of skeletal muscles, and counteracts exercise-induced reductions in Na+–K+-ATPaseVmaxin trained men," *The Journal of Physiology*, vol. 592, no. 24, pp. 5445–5459, 2014.

[102] V. L. Wyckelsma, I. Levinger, R. M. Murphy et al., "Intense interval training in healthy older adults increases skeletal muscle [3H]ouabain-binding site content and elevates Na+,K+-ATPase α2isoform abundance in Type II fibers," *Physiological reports*, vol. 5, no. 7, article e13219, 2017.

[103] V. L. Wyckelsma, B. D. Perry, J. Bangsbo, and M. J. McKenna, "Inactivity and exercise training differentially regulate abundance of Na^+-K^+-ATPase in human skeletal muscle," *Journal of Applied Physiology*, vol. 127, no. 4, pp. 905–920, 2019.

[104] D. Christiansen, "Molecular stressors underlying exercise training-induced improvements in $^{K⁺}$ regulation during exercise and Na⁺ ,K⁺ -ATPase adaptation in human skeletal muscle," *Acta physiologica*, vol. 225, no. 3, article e13196, 2019.

[105] D. Watanabe and M. Wada, "Fatigue-induced change in T-system excitability and its major cause in rat fast-twitch skeletal musclein vivo," *Journal of Physiology*, vol. 598, no. 22, pp. 5195–5211, 2020.

[106] S. Trappe, D. Costill, P. Gallagher et al., "Exercise in Space: Human Skeletal Muscle after 6 Months aboard the International Space Station," *Journal of applied physiology*, vol. 106, no. 4, pp. 1159–1168, 2009.

[107] M. Murgia, L. Toniolo, N. Nagaraj et al., "Single muscle fiber proteomics reveals fiber-type-specific features of human muscle aging," *Cell Reports*, vol. 19, no. 11, pp. 2396–2409, 2017.

[108] N. Ørtenblad, J. Nielsen, B. Saltin, and H. C. Holmberg, "Role of glycogen availability in sarcoplasmic reticulum Ca^{2+} kinetics in human skeletal muscle," *The Journal of Physiology*, vol. 589, no. 3, pp. 711–725, 2011.

[109] F. Ginani, D. M. Soares, and C. A. G. Barboza, "Effect of low-level laser therapy on mesenchymal stem cell proliferation: a systematic review," *Lasers in Medical Science*, vol. 30, no. 8, pp. 2189–2194, 2015.

[110] N. Ørtenblad, H. Westerblad, and J. Nielsen, "Muscle glycogen stores and fatigue," *The Journal of Physiology*, vol. 591, no. 18, pp. 4405–4413, 2013.

[111] V. Eisner, G. Lenaers, and G. Hajnóczky, "Mitochondrial fusion is frequent in skeletal muscle and supports excitation–contraction coupling," *Journal of Cell Biology*, vol. 205, no. 2, pp. 179–195, 2014.

[112] Y. H. Wu, J. Wang, D. X. Gong, H. Y. Gu, S. S. Hu, and H. Zhang, "Effects of low-level laser irradiation on mesenchymal stem cell proliferation: a microarray analysis," *Lasers in Medical Science*, vol. 27, no. 2, pp. 509–519, 2012.

[113] M. J. Greenberg, T. R. Mealy, M. Jones, D. Szczesna Cordary, and J. R. Moore, "The direct molecular effects of fatigue and myosin regulatory light chain phosphorylation on the actomyosin contractile apparatus," *American Journal of Physiology-Regulatory, Integrative and Comparative Physiology*, vol. 298, no. 4, pp. R989–R996, 2010.

[114] F. Salehpour and S. H. Rasta, "The potential of transcranial photobiomodulation therapy for treatment of major depressive disorder," *Reviews in the Neurosciences*, vol. 28, no. 4, pp. 441–453, 2017.

[115] R. A. Mussttaf, D. F. Jenkins, and A. N. Jha, "Assessing the impact of low level laser therapy (LLLT) on biological systems: a review," *International Journal of Radiation Biology*, vol. 95, no. 2, pp. 120–143, 2019.

[116] H. Chung, T. Dai, S. K. Sharma, Y. Y. Huang, J. D. Carroll, and M. R. Hamblin, "The nuts and bolts of low-level laser (light) therapy," *Annals of Biomedical Engineering*, vol. 40, no. 2, pp. 516–533, 2012.

[117] M. Bayat, A. Virdi, R. Jalalifirouzkouhi, and F. Rezaei, "Comparison of effects of LLLT and LIPUS on fracture healing in animal models and patients: a systematic review," *Progress in Biophysics and Molecular Biology*, vol. 132, pp. 3–22, 2018.

[118] L. F. de Freitas and M. R. Hamblin, "Proposed mechanisms of photobiomodulation or low-level light therapy," *IEEE Journal of Selected Topics in Quantum Electronics*, vol. 22, no. 3, pp. 348–364, 2016.

[119] Y. Wang, Y. Y. Huang, Y. Wang, P. Lyu, and M. R. Hamblin, "Photobiomodulation (blue and green light) encourages osteoblastic- differentiation of human adipose-derived stem cells: role of intracellular calcium and light-gated ion channels," *Scientific Reports*, vol. 6, no. 1, p. 33719, 2016.

[120] J. Kulbacka, A. Choromańska, J. Rossowska, J. Weżgowiec, J. Saczko, and M. P. Rols, "Cell membrane transport mechanisms: ion channels and electrical properties of cell membranes," *In Transport across Natural and Modified Biological Membranes and Its Implications in Physiology and Therapy, Springer, Cham*, pp. 39–58, 2017.

[121] F. G. Basso, C. F. Oliveira, C. Kurachi, J. Hebling, and C. A. de Souza Costa, "Biostimulatory effect of low-level laser therapy on keratinocytes in vitro," *Lasers in Medical Science*, vol. 28, no. 2, pp. 367–374, 2013.

[122] K. M. AlGhamdi, A. Kumar, and N. A. Moussa, "Low-level laser therapy: a useful technique for enhancing the proliferation of various cultured cells," *Lasers in Medical Science*, vol. 27, no. 1, pp. 237–249, 2012.

[123] P. Avci, A. Gupta, M. Sadasivam et al., "Low-level laser (light) therapy (LLLT) in skin: stimulating, healing, restoring," in *Seminars in Cutaneous Medicine and Surgery*, p. 41, NIH Public Access, 2013.

[124] K. S. Canuto, L. P. S. Sergio, O. R. Guimarães, M. Geller, F. Paoli, and A. S. Fonseca, "Low-level red laser therapy alters effects of ultraviolet C radiation on Escherichia coli cells," *Brazilian Journal of Medical and Biological Research*, vol. 48, no. 10, pp. 939–944, 2015.

[125] L. P. D. S. Sergio, A. P. A. D. Silva, P. F. Amorim et al., "DNA damage in blood cells exposed to low-level lasers," *Lasers in Surgery and Medicine*, vol. 47, no. 4, pp. 361–368, 2015.

[126] M. F. das Neves, M. C. Dos Reis, E. A. de Andrade et al., "Effects of low-level laser therapy (LLLT 808 nm) on lower limb spastic muscle activity in chronic stroke patient," *Lasers in Medical Science*, vol. 31, no. 7, pp. 1293–1300, 2016.

[127] M. C. R. dos Reis, E. A. F. de Andrade, A. C. L. Borges et al., "Immediate effects of low-intensity laser (808 nm) on fatigue and strength of spastic muscle," *Lasers in Medical Science*, vol. 30, no. 3, pp. 1089–1096, 2015.

[128] M. F. das Neves, D. C. Aleixo, I. S. Mendes et al., "Long-term analyses of spastic muscle behavior in chronic poststroke patients after near-infrared low-level laser therapy (808 nm): a double-blinded placebo-controlled clinical trial," *Lasers in Medical Science*, vol. 35, no. 7, pp. 1459–1467, 2019.

Hindawi
International Journal of Photoenergy
Volume 2021, Article ID 6641358, 14 pages
https://doi.org/10.1155/2021/6641358

Review Article

Photodynamic Therapy for Oral Squamous Cell Carcinoma: A Systematic Review and Meta-Analysis

Jiao Lin, Guangcheng Ni, Tingting Ding, Shangxue Lei, Liang Zhong, Na Liu, Keran Pan, Ting Chen, Xin Zeng, Hao Xu, Taiwen Li, and Hongxia Dan

State Key Laboratory of Oral Diseases, National Clinical Research Center for Oral Diseases, Chinese Academy of Medical Sciences Research Unit of Oral Carcinogenesis and Management, West China Hospital of Stomatology, Sichuan University, Chengdu, Sichuan 610041, China

Correspondence should be addressed to Taiwen Li; litaiwen@scu.edu.cn and Hongxia Dan; hxdan@foxmail.com

Received 22 October 2020; Revised 14 January 2021; Accepted 28 January 2021; Published 16 February 2021

Academic Editor: Rodrigo Alvaro Lopes-Martins

Copyright © 2021 Jiao Lin et al. This is an open access article distributed under the Creative Commons Attribution License, which permits unrestricted use, distribution, and reproduction in any medium, provided the original work is properly cited.

To assess the efficacy of photodynamic therapy (PDT) for oral squamous cell carcinoma (OSCC), literature on this topic from Embase, PubMed, and Web of Science were obtained and analyzed. The response and recurrence rates with 95% confidence intervals (CI) were calculated using the DerSimonia–Laird method. The pooled complete response (CR) rate from the included studies was 0.799 (95% CI: 0.708–0.867), while the overall response (OR) rate was 0.967 (95% CI: 0.902–0.989). The recurrence rate (RR) was 0.158 (95% CI: 0.090–0.264). A subgroup analysis of lesion site, photosensitizer, laser type, radiant exposure, and power density revealed no statistically significant differences. In general, PDT is effective for the treatment of early OSCC. Investigations on the influence of PDT on the survival of OSCC patients, optimization of the treatment regimen, and evaluation of response after treatment are still needed.

1. Introduction

Oral squamous cell carcinoma (OSCC) is the main type of oral cancer and accounts for more than 90% of all malignant tumors in the oral cavity. At present, its main treatment is surgical treatment, supported by radiotherapy and chemotherapy; however, the efficacy is still unsatisfactory, and adverse reactions are quite common owing to the low selectivity of these treatment options [1–3]. Photodynamic therapy (PDT) is a minimally invasive treatment with high efficacy and selectivity, and it has a low risk of systemic side effects and deformities [4]. The basic elements of PDT are oxygen, photosensitizer, and visible light at specific wavelengths [5]. Photosensitizers are often given locally or intravenously, which subsequently are preferentially concentrated in overproliferative cells with membrane structural defects, such as cancer cells. In the presence of oxygen, a light source of an appropriate wavelength is applied to the target tissue to activate the excited state of the photosensitizer and produce oxygen reactive species with cytotoxic activities [6]. At present, one of the most important clinical applications of PDT is as second-line therapy for primary cancers or recurrent early and superficial cancers of the oral cavity, pharynx, and larynx [7].

In 2015, Cerrati et al. [8] conducted a meta-analysis on the efficacy between PDT and surgical treatment, which included studies published before 2010. In the last 10 years, more studies on this subject have been published. Therefore, to gain a better understanding of the outcome of PDT in the treatment of OSCC, we conducted this meta-analysis to update the cure rate and RR of PDT for OSCC treatment and to explore their relationship with lesion site, photosensitizer, laser type, radiant exposure, and power density and other related factors.

2. Materials and Methods

A systematic review and meta-analysis were performed according to the PRISMA statement [9]. The review protocol was registered on PROSPERO (CRD42020190166).

2.1. Study Identification and Selection. PubMed, Embase, and Web of Science databases were systematically searched until August 1, 2019, to identify all relevant studies using different combinations of the following keywords: "photodynamic therapy" or "photodynamic chemotherapy" and "oral cancer," "oral squamous cell carcinoma," "oral neoplasms," "head and neck tumors," and "head and neck squamous cell carcinoma."

Studies enrolled in the meta-analysis met the following criteria: (A) original study; (B) clinical study; (C) published in English; (D) articles meeting the standard of PICO, in short, all patients were diagnosed with OSCC through clinical manifestations and histological examination (P); the lesions were treated by PDT (I); comparison of lesions of patients before and after treatment (C), response was used as the primary outcome, and recurrence was used as a secondary outcome (O).

The exclusion criteria were as follows: (A) reviews, conference summaries, case reports, and commentaries; (B) animal experiments; (C) efficacy evaluation criteria were inconsistent; (D) publications of nonoriginal studies or based on the same cohort; (E) studies in which the specific sites of the lesion were not recorded.

2.2. Data Extraction. Two investigators (J. Lin and G.C. Ni) independently assessed the titles and abstracts initially to determine whether they met the inclusion criteria and then read the full text of the study. The following information was collected from all studies: first author's name, year of publication, mean age of patients, sample size, lesion locations, female-to-male ratio, light source, type and application method of photosensitizer, laser parameters (wavelength, radiant exposure, and power density), exposure time, number of sessions, follow-up time, adverse reactions, and recurrence status. If two reviewers disagreed on whether a study met the inclusion and exclusion criteria, a third reviewer would join the discussion and resolve discrepancies.

2.3. Statistical Analysis. All statistical analyses were performed using the Meta-Analyst [10] and STATA statistical software 15.1. The response rate with 95% confidence intervals (CI) for PDT in the treatment of OSCC was calculated.

Heterogeneity of meta-analysis ($I^2$and Q test): the heterogeneity of studies was assessed using I^2 and Q tests; if the heterogeneity was statistically significant (I^2 >50% or P value of Q test was <0.05), then a random effect model was used for the data analysis.

Pooled estimates calculation: for discrete variables, the proportion was calculated, and logit transformation was carried out. The inverse variance method was used in the fixed effect model, while the DerSimonia–Laird method was used in the random effect model.

Publication bias: a funnel chart was drawn to evaluate publication bias; publication bias was considered when the funnel chart was asymmetrical or the P value of Egger's test was <0.05.

Quality assessment: nonrandomized studies were assessed by using the Downs–Black Checklist with 26 items [11]. A quality assessment was independently performed by two authors (J. Lin and G.C. Ni), and a full discussion was undertaken when conflicts existed. The corresponding author (Prof. Dan) made the final decision.

Sensitivity analysis: subgroup analyses were performed, and the influence of a single study on the overall result was analyzed by omitting them one by one.

3. Results

3.1. Search Results and Study Selection. Figure 1 shows the selection process; 69 articles were included through a preestablished literature retrieval strategy. First, 10 articles were excluded because of repetition. The titles and abstracts were screened, and 29 articles of reviews, case reports, animal experiments, or basic experiments were excluded. In the subsequent full-text screening, 9 articles were excluded because of inconsistencies in the efficacy evaluation criteria. The remaining 21 articles were used for data extraction. Two studies [12, 13] were excluded because squamous cell carcinoma and dysplasia were not distinguished. One study [14] was excluded because it was based on the same cohort as another study [15]. Finally, a total of 18 studies [15–32] with 900 OSCC patients were included in the meta-analysis. The basic characteristics of the included studies are listed in Table 1.

3.2. Quality Assessment of Included Studies. The results of the Downs–Black Checklist are listed in Table 2. The majority of the non-RCT studies showed high quality in five fields: study quality, external validity, study bias, confounding, and power of study.

3.3. Meta-Analysis Results

3.3.1. Complete Response Rate of OSCC to PDT. A total of 18 articles involving 900 lesions were included in this study. Detailed information of the studies is provided in Table 1. The response rate with 95% CIs was used to evaluate the lesion complete response (CR) after PDT. The P value of the Q test was <0.001, I^2 was 80.03%, a random effect model was recommended, and the DerSimonia–Laird method was used. The pooled CR was 0.799 (95% CI:0.708–0.867), indicating that 79.9% of the lesions achieved a CR (Figure 2).

The funnel plot (Supplementary Figure 1A) and Egger's test indicated no publication bias ($P = 0.345$, 95% CI = -2.932–1.091; $P > 0.05$).

Moreover, a sensitivity analysis (Supplementary Figure 2A) showed that the results were robust.

3.3.2. Overall Response of OSCC to PDT. Seven articles involving 507 cases were included in the analysis. The OR result is shown in Figure 3, where the P value of the Q test was 0.035 and $I^2 = 55.69\%$. A random effects model was adopted, and the pooled OR was 0.967 (95% CI:0.902–0.989), indicating that 96.7% of the lesions achieved an overall response (OR).

The funnel plot (Supplementary Figure 1B) and Egger's test indicated no publication bias ($P = 0.813$, 95% CI = -17.969–17.131; $P > 0.05$).

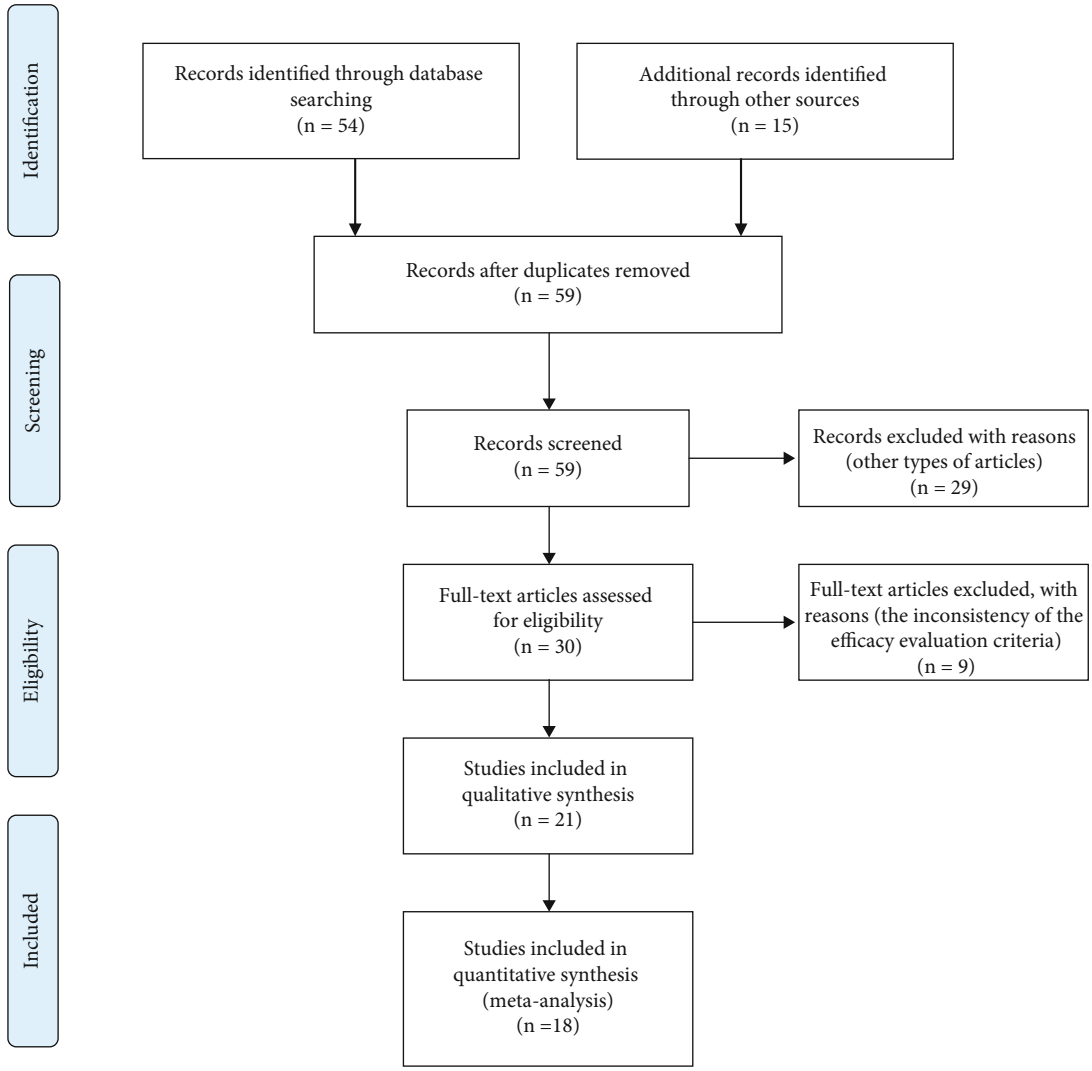

Figure 1: Flow diagram of literature search and study selection process.

Moreover, a sensitivity analysis (Supplementary Figure 2B) showed that the results were robust.

3.3.3. Impact of PDT on the Recurrence Rate of OSCC. Nine articles reported the RR, involving 376 cases. The RR results are shown in Figure 4. Heterogeneity among studies was significant ($I^2 = 67.32\%$, P of Q test = 0.002), and the random effect model and DerSimonia–Laird method were used. The pooled RR was 0.158 (95% CI:0.090–0.264), indicating that 15.8% of the lesions relapsed.

A funnel plot (Supplementary Figure 1C) and Egger's test indicated no publication bias ($P = 0.621$, 95% CI = -4.049 - 2.627; $P > 0.05$).

Moreover, a sensitivity analysis (Supplementary Figure 2C) showed that the results were robust.

3.4. Subgroup Analysis

3.4.1. Lesion Sites. Eight studies were included in the subgroup analysis of the influence of lesion location on the CR of OSCC. They were divided into two groups: the lips and/or buccal mucosa and/or tongue and/or floor of the mouth (BM/L/T/FM) group and gingiva and/or palate (G/P) group. There was no statistically significant difference between the groups (Figure 5).

3.4.2. Photosensitizers. Eighteen studies were included in the subgroup analysis of the influence of the photosensitizer types on the CR of OSCC, including five types of photosensitizers: m-Tetra(hydroxyphenyl) chlorin (m-THPC), chlorin-based compound, 3-(1'-hexyloxyethyl) pyropheophorbide (HPPH), hematoporphyrin derivative (HPD), talaporfin sodium, and porfimer sodium. They were administered intravenously. The results are shown in Figure 6(a). The curative effects were all at the average level, and the differences between the different types of photosensitizers were not statistically significant.

Seven studies were included in the subgroup analysis of the influence of photosensitizer type on the OR of OSCC, including three types of photosensitizers. The results are

Table 1: Parameters of the studies included.

Author	Year	Mean age (year)	Female/male	Types of PS	Laser type	Radiant exposure (J/cm^2)	Power density (mW/cm^2)	Wavelength (nm)	Method of administration	Sample size	CR	OR	RR	Lesion locations	Sample size	CR	OR	Mean follow-up(month)	Exposure time(min)	Number of sessions	Adverse site
Ikeda H	2018	75.2 (55-94)	6/2	Talaporfin sodium	Diode laser	100	150	664	Intravenous	8	6	N/A	1	G/P[a] L/BM/T/FM[b]	1 7	0 6	N/A N/A	48	55-176	1	N/A
Toratani S	2016	70.8	22/12	Porfimer sodium	Dye laser	100-150	160	630	Intravenous	34	30	33	9	N/A	N/A	N/A	N/A	105	N/A	1	Sunburn and sequestrum formation of alveolar bone
Rigual N	2013	N/A	N/A	HPPH[d]	Dye laser	Firstly:50-75/100-125. Then:100-125/140	N/A	665	Intravenous	20	16	N/A	N/A	N/A	N/A	N/A	N/A	5-40	N/A	≥1	Expected pain and edema
Karakullukcu B	2013	60 (38-92)	22/33	mTHPC[c]	N/A	N/A	N/A	630	N/A	55	49	N/A	N/A	N/A	N/A	N/A	N/A	24	N/A	1	N/A
Ikeda H	2013	73.7	N/A	Porfimer sodium	N/A	N/A	N/A	N/A	Intravenous	18	17	N/A	2	G/P L/BM/T/FM	7 11	6 11	N/A N/A	48	30-150	N/A	Swelling and edema
deVisscher S A	2013	61.1	N/A	mTHPC	Diode laser	N/A	100	630	Intravenous	156	127	N/A	N/A	N/A	N/A	N/A	N/A	33	N/A	1	N/A
Karakullukcu B	2011	60.5	N/A	mTHPC	N/A	N/A	100	652	Intravenous	126	86	114	N/A	G/P L/BM/T/FM	26 100	17 69	23 91	60	N/A	N/A	Scar formation
Jerjes W	2011	58	12/26	mTHPC	N/A	10-20	100	652	Intravenous	38	12	N/A	6	N/A	N/A	N/A	N/A	60	N/A	1	Pain and swelling
Merrill A. Biel	2010	N/A	N/A	Porfimer sodium	Dye laser	N/A	150	630	Intravenous	190	190	190	13	N/A	N/A	N/A	N/A	N/A	N/A	N/A	N/A
Vanessa Gayl	2010	N/A	N/A	Porfimer sodium	Pumped laser or a diode laser	50-100	100-200	630	Intravenous	26	22	26	4	N/A	N/A	N/A	N/A	N/A	N/A	≥1	N/A
KAI Johannes	2009	58.8 (48-62)	N/A	mTHPC	N/A	20	100	652	Intravenous	8	4	N/A	N/A	G/P L/BM/T/FM	4 4	2 2	N/A N/A	N/A	N/A	N/A	N/A
Rigual N R	2009	61.2 (36-85)	N/A	Porfimer sodium	Argon pumped dye laser or a diode laser	50-75	N/A	630	Intravenous	11	10	11	11	N/A	N/A	N/A	N/A	15	N/A	≥1	Pain edema itching, weight loss transient hoarseness
Hopper C	2004	64 (33-99)	N/A	mTHPC	Diode laser	20	100	652	Intravenous	114	97	114	N/A	G/P L/BM/T/FM Others	7 103 4	6 87 4	N/A N/A N/A	N/A	N/A	N/A	N/A
Copper M P	2003	N/A	N/A	mTHPC	Diode laser	20	100	652	Intravenous	26	22	N/A	4	G/P L/BM/T/FM	5 21	3 19	N/A N/A	37	N/A	N/A	N/A
Kubler A C	2001	64 (44-99)	6/19	mTHPC	N/A	20	100	652	Intravenous	25	24	N/A	2	G/P L/BM/T/FM	N/A 25	N/A 24	N/A N/A	14	N/A	N/A	Swelling and local pain
Kathleen F M	1997	66.5 (30-80)	N/A	Porfimer sodium	Dye laser	5-20	250	652	Intravenous	25	14	N/A	N/A	G/P	N/A	N/A	N/A	N/A	N/A	≥1	N/A
Yoshida T	1996	60.2 (51-67)	1/4	HPD[e]	Argon or excimer dye laser	200	200-500	630	Intravenous	6	2	5	N/A	L/BM/T/FM	N/A	N/A	N/A	153	N/A	1	Inflammation swelling
Grant W E	1993	N/A	N/A	Porfimer sodium	Dye laser	50-100	150	630	Intravenous	14	13	N/A	N/A	G/P L/BM/T/FM	3 9	3 8	N/A N/A	10.63	N/A	N/A	N/A

G/P[a]: gingiva and/or palate; L/BM/T/FM[b]: lips and/or buccal mucosa and/or tongue and/or floor of the mouth. m-THPC[c]: m-Tetra(hydroxyphenyl) chlorin; HPPH[d]: chlorin-based compound, 3-(1'-hexyloxyethyl) pyropheophorbide; HPD[e]: hematoporphyrin derivative. N/A: not applicable.

Table 2: Results of bias risk assessment for each included non-RCT (score).

Included studies	Reporting	External validity	Bias	Confounding	Power	Overall score
Ikeda H 2018	7	2	3	2	5	19
Toratani S 2016	8	1	3	2	5	19
Rigual N 2013	7	1	3	2	5	18
Karakullukcu B2013	8	1	2	2	5	18
Ikeda H 2013	9	2	3	2	5	21
deVisscher S A2013	8	1	4	3	5	21
Karakullukcu B 2011	8	3	4	2	5	22
Jerjes W2011	9	2	4	2	5	22
Vanessa G S2010	6	1	3	2	5	17
KAI Johannes2009	7	1	4	2	5	19
Merrill A. Biel2010	8	1	4	2	5	20
Rigual N R2009	9	1	3	2	5	20
Hopper C2004	8	1	4	2	5	20
Copper M P2003	7	1	4	2	5	19
Kubler A C2001	8	1	4	2	5	20
Kathleen FM 1997	7	1	3	2	5	18
Yoshida T1996	9	1	4	2	5	21
Grant W E1993	8	1	4	2	5	20

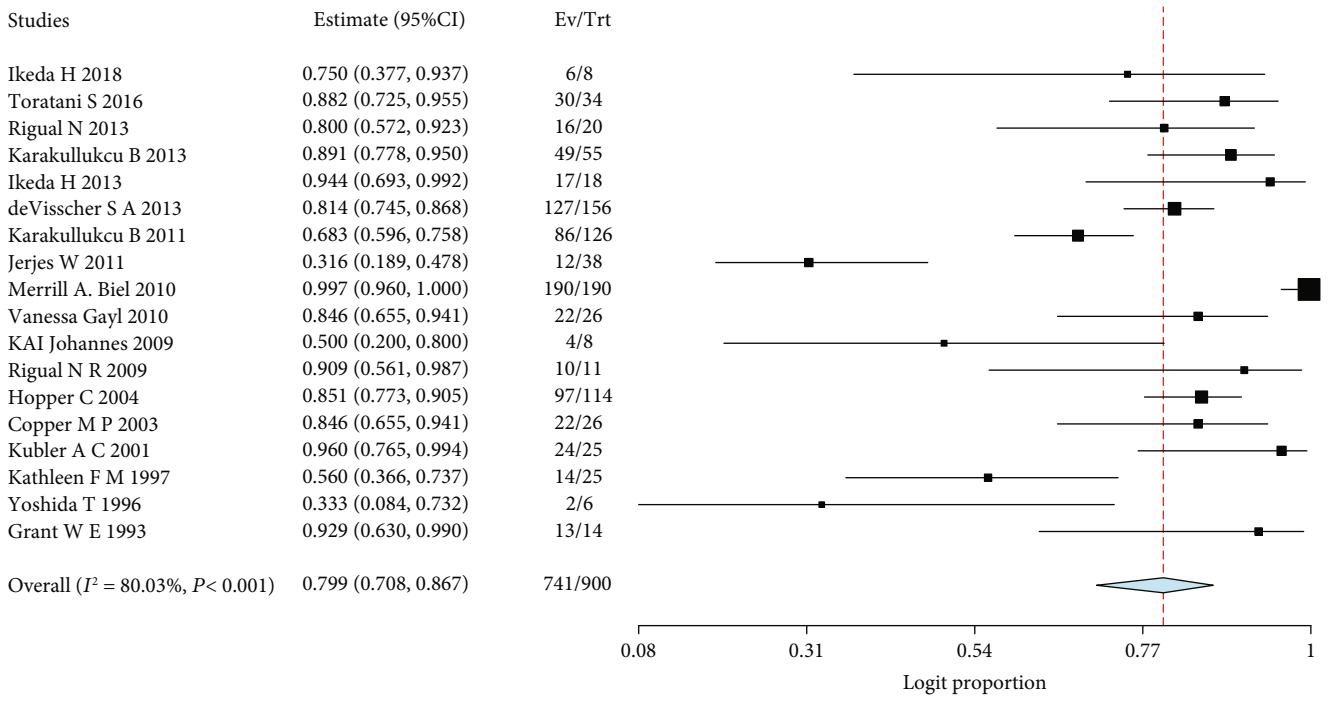

Figure 2: Forest plots of proportions of CR after PDT.

shown in Figure 6(b). There was no statistically significant difference between the different types of photosensitizers.

Nine studies were included in the subgroup analysis of the influence of photosensitizer types on the RR of OSCC, and the results are shown in Figure 6(c). The differences between the different types of photosensitizers were not statistically significant.

3.4.3. Laser Types. Eleven studies were included in the subgroup analysis of the influence of laser type on the CR of OSCC. They were divided into two groups: diode laser and dye laser. As shown in Figure 7(a), there was no significant statistical difference between the different laser types.

Five studies were included in the subgroup analysis of the influence of laser type on the OR of OSCC. The results are

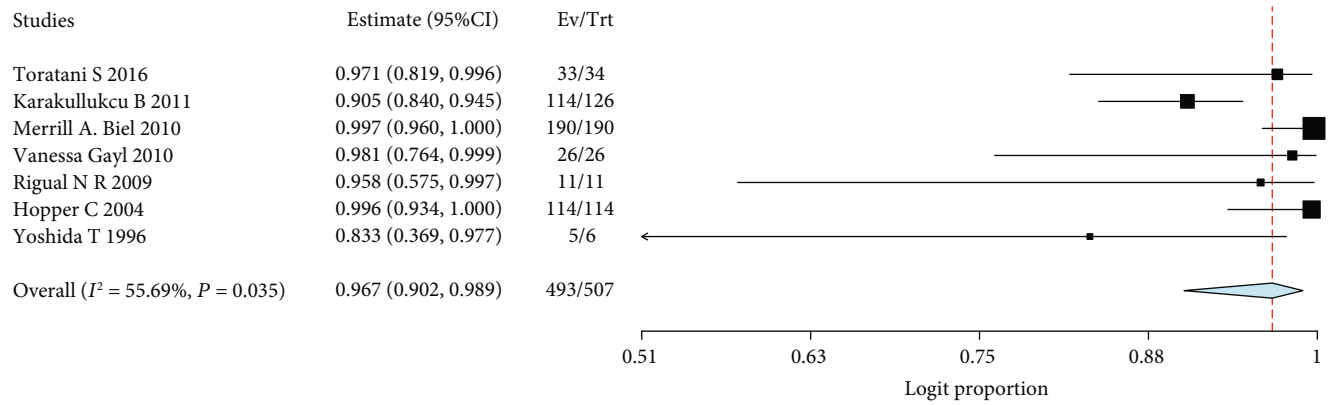

Figure 3: Forest plots of OR rate after PDT.

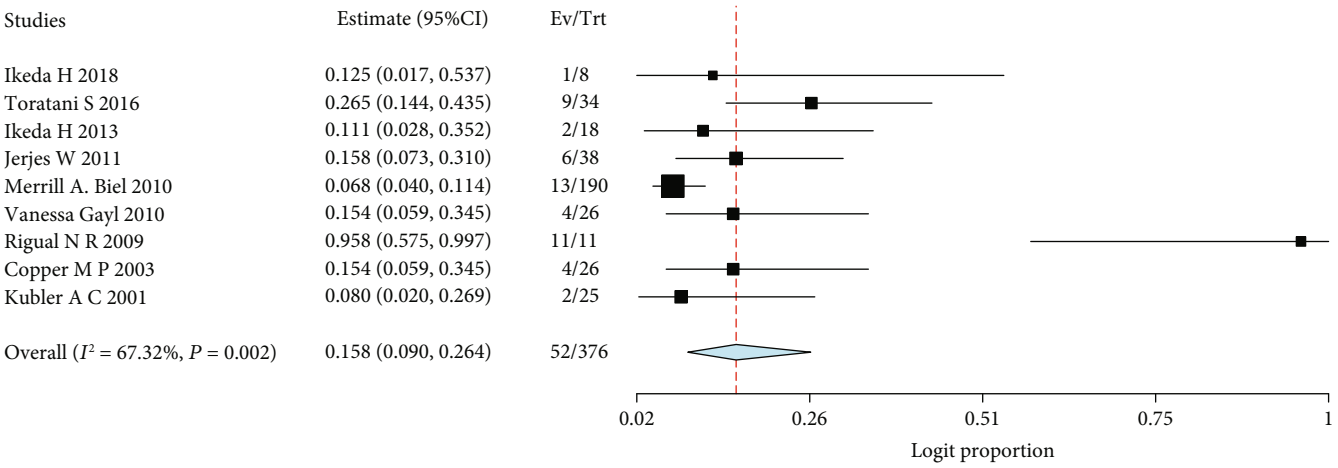

Figure 4: Forest plots of proportions of RR after PDT.

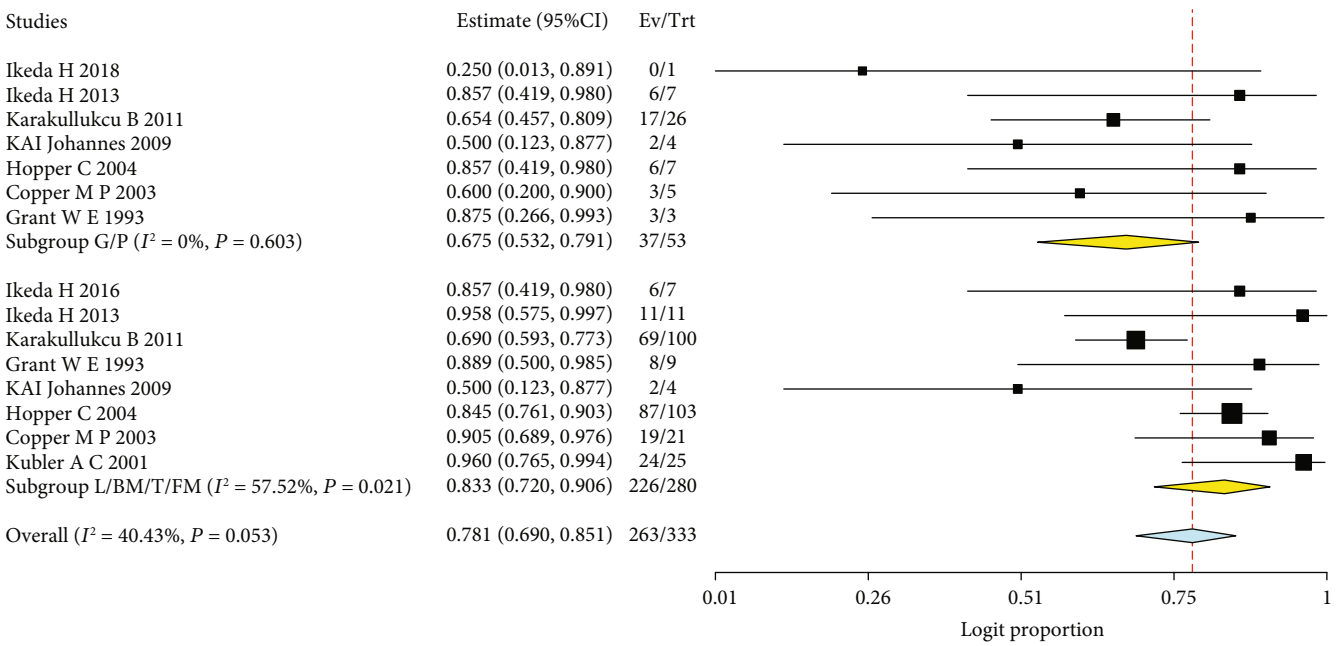

Figure 5: Forest plot of subgroup analysis of complete rate in cases at different lesion sites.

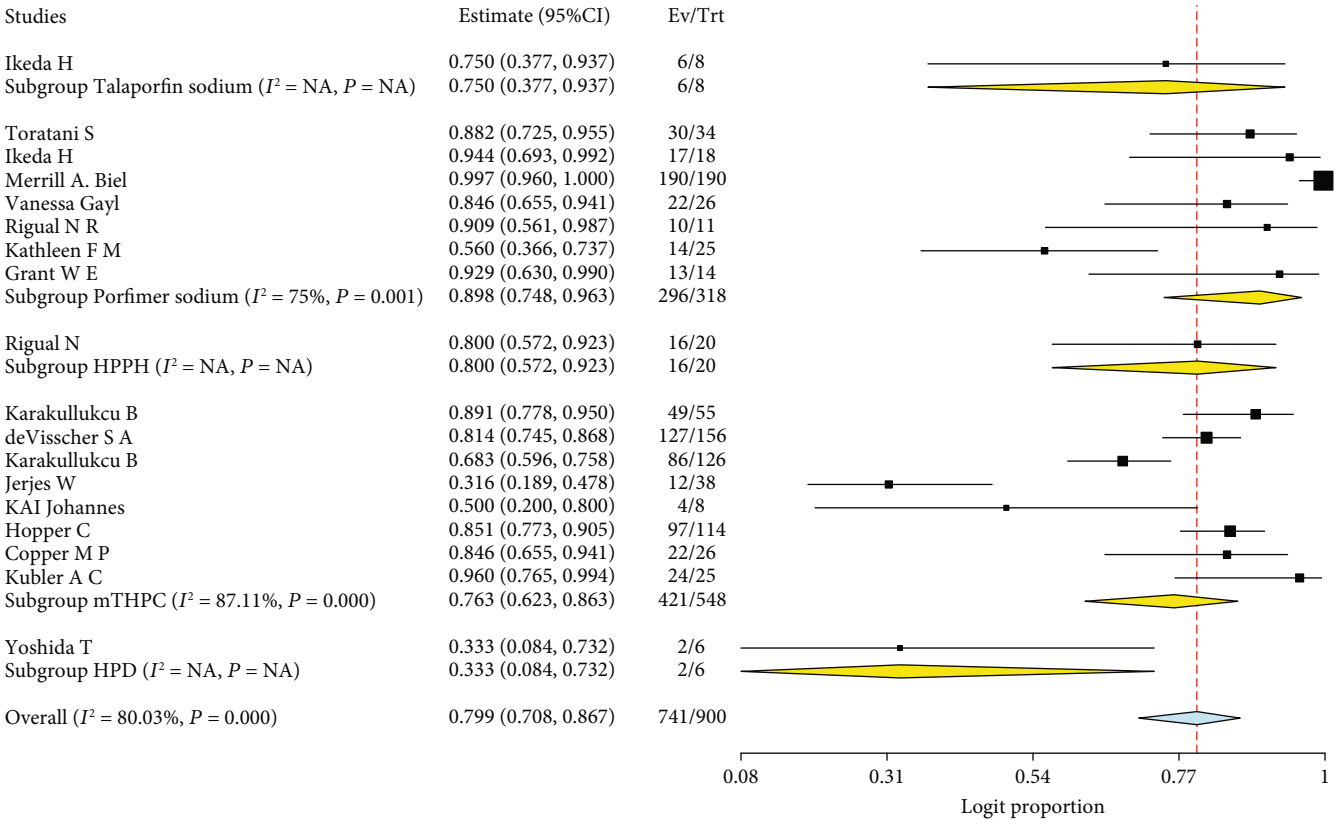

(a)

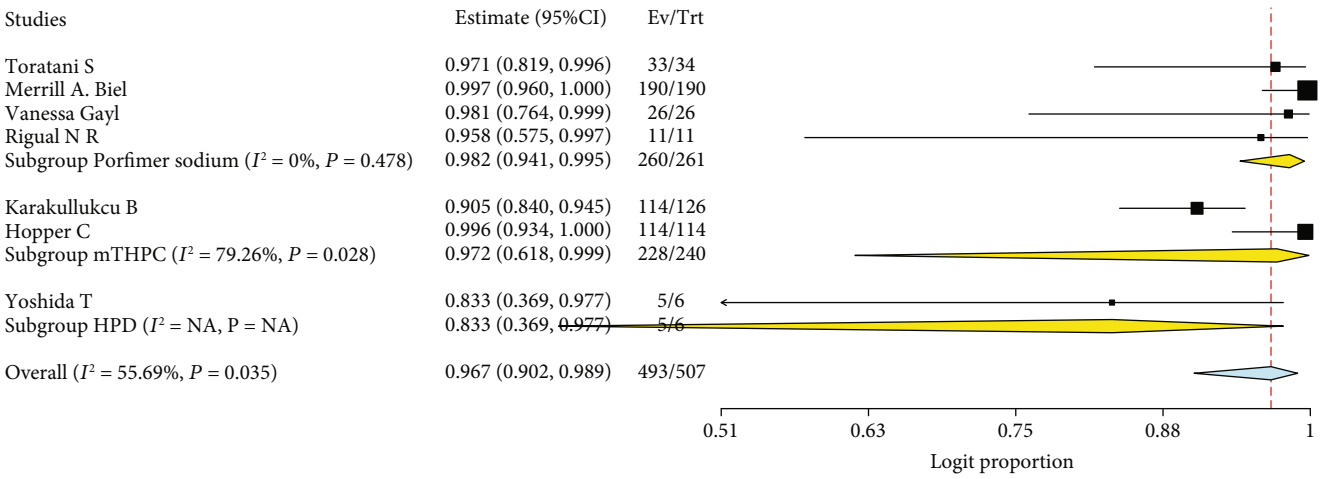

(b)

Figure 6: Continued.

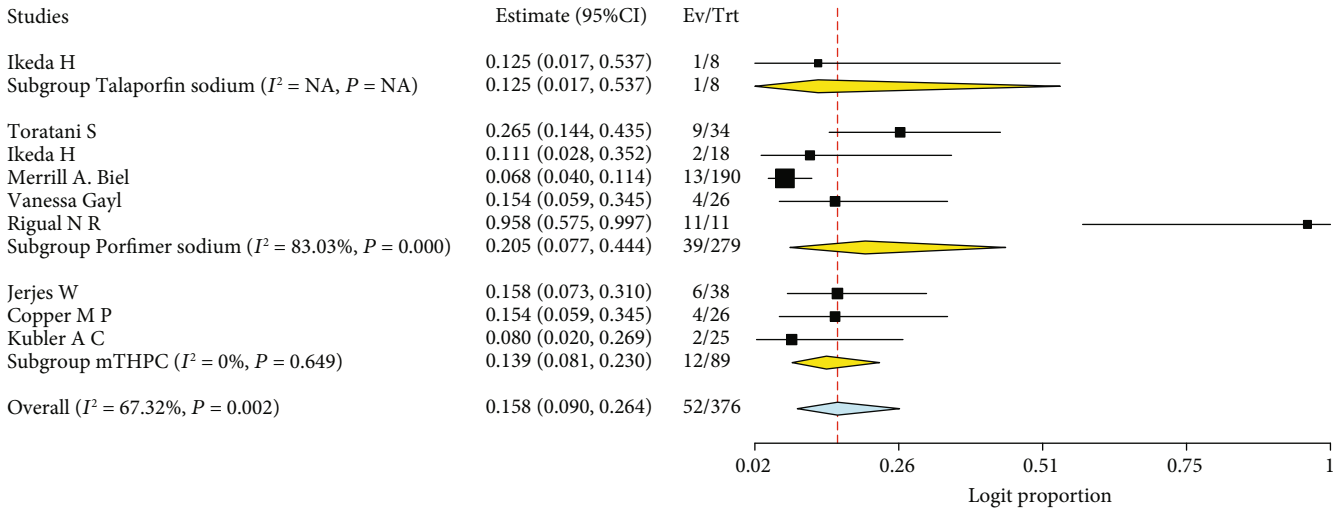

(c)

Figure 6: Forest plot of subgroup analysis of (a) CR, (b) OR, and (c) RR in cases using different types of photosensitizers.

shown in Figure 7(b); there was no significant statistical difference between the different laser types.

Five studies were included in the subgroup analysis of the influence of laser type on the RR of OSCC. The results are shown in Figure 7(c), and the difference between the different laser types was not statistically significant.

3.4.4. Radiant Exposure. Twelve studies were included in the subgroup analysis of the influence of radiant exposure on the CR of OSCC. They were divided into three groups: 0–50 joules per square centimeters (J/cm^2), 50–100 J/cm^2, and 100–200 J/cm^2. The results are shown in Figure 8(a); there was no significant statistical difference between the different groups.

Five studies were included in the subgroup analysis of the influence of radiant exposure on the OR of OSCC. The results are shown in Figure 8(b), and there was no statistically significant difference between the groups.

Seven studies were included in the subgroup analysis of the influence of radiant exposure on the RR of OSCC. The results are shown in Figure 8(c), and there was no statistically significant difference between the groups.

3.4.5. Power Density. Thirteen studies were included in the subgroup analysis of the influence of power density on the CR of OSCC. They were divided into three groups: 100–150 milliwatt per square centimeters (mW/cm^2), 150–200 mW/cm^2, and ≥200 mW/cm^2. The results are shown in Figure 9(a); there was no statistically significant difference between the groups.

Five studies were included in the subgroup analysis of the influence of power density on the OR of OSCC. The results are shown in Figure 9(b); there was no statistically significant difference between the groups.

Six studies were included in the subgroup analysis of the influence of power density on the RR of OSCC. The results are shown in Figure 9(c), and there was no statistically significant difference between the groups.

3.5. Other Factors in PDT Process in all Studies (Table 1). In all studies included, wavelengths of 630–665 nm were used. Most of the patients had no obvious discomfort or only mild discomfort (local pain and inflammatory edema); some patients had scar formation, itching, and weight loss. A small number of patients had alveolar bone sunburns and dead bone formation.

4. Discussion

OSCC is a common type of cancer in the head and neck region [33]. The annual incidence rate is 3.90/100,000, and the mortality rate is 1.94/100,000 [34]. Owing to the high mortality rate and potential damage to the appearance and function of the oral and maxillofacial region caused by the cancer itself as well as the treatment, OSCC has a very negative influence on the physical and mental health of patients [35]. Currently, surgery is still the first-line treatment for OSCC [36] and is supported by radiotherapy and chemotherapy. The advantage of surgery is that the lesion can be removed completely, and neck dissection can be performed at the same time; however, delayed wound healing is commonly seen, and scar formation is almost inevitable. When the lesion is large or located at a special anatomic site (such as the angle of the mouth, frenum linguae, or pterygomandibular fold), surgery often results in impairment of the mouth opening, mastication, language, and appearance. If recurrence occurs, repeated surgery will further exacerbate the situation [8].

PDT has been used for managing many malignant tumors including OSCC. Compared with surgical treatment, it is highly selective, minimally invasive, and easily accepted by patients, with mild adverse reactions and no cumulative toxicity [37]. Unlike radiotherapy and surgery, treatment can be repeated at the same site as needed [5]. According to a previous meta-analysis, PDT can achieve a response rate similar to that of surgical treatment. In that study,

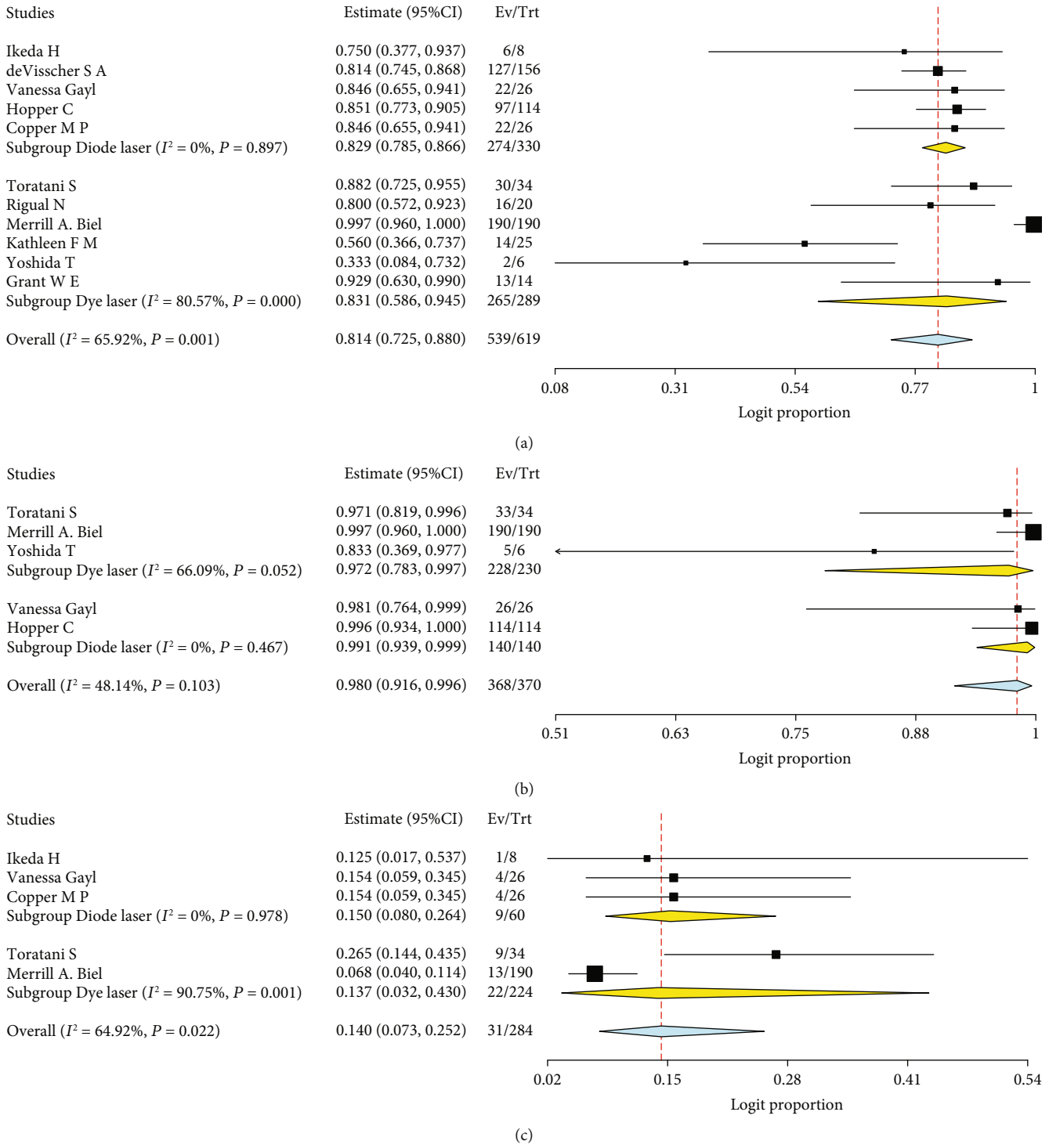

Figure 7: Forest plot of subgroup analysis of (a) CR, (b) OR, and (c) RR in cases using different laser types.

leukoplakia and dysplasia were also included in the calculation of oral cancer, which might have affected the final results.

In this study, only patients diagnosed with OSCC were included. The standards for calculating response rates were set. OR means tumor size reduction of 50% or more after PDT; CR refers to no evidence of tumor both clinically or pathologically. According to these standards, the CR of OSCC treated with PDT was 79.9%. The OR rate, which was the sum of the CR and partial response, was 96.7%. These results indicated that the efficiency, especially the short-term efficiency of PDT in the treatment of early OSCC, was high. At the same time, PDT was highly selective with mild adverse reactions, which made it preferable to surgery when the protection of appearance and function of the target site was needed. However, it should also be noted that PDT had little

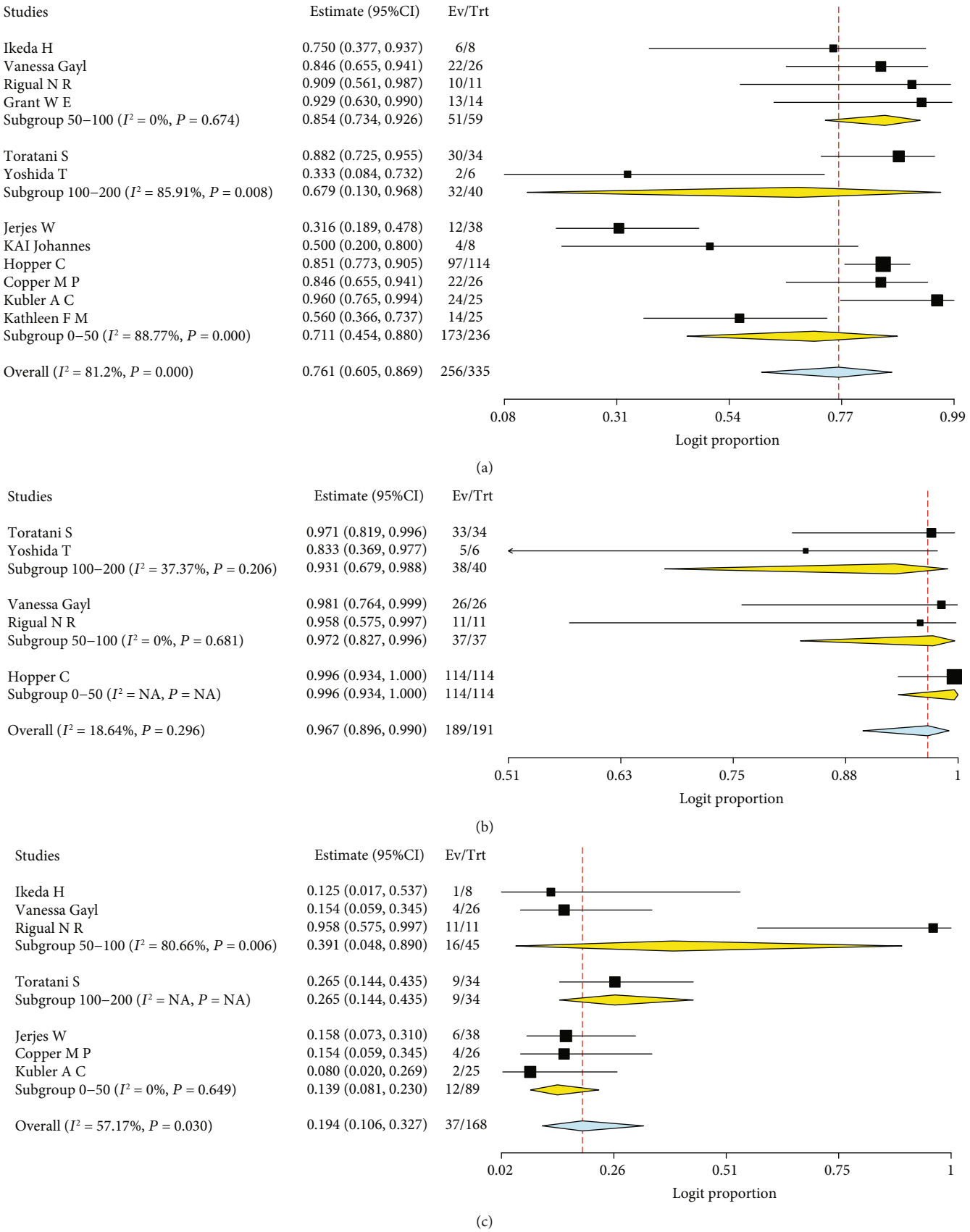

Figure 8: Forest plot of subgroup analysis of (a) CR, (b) OR, and (c) RR in cases about different radiant exposures.

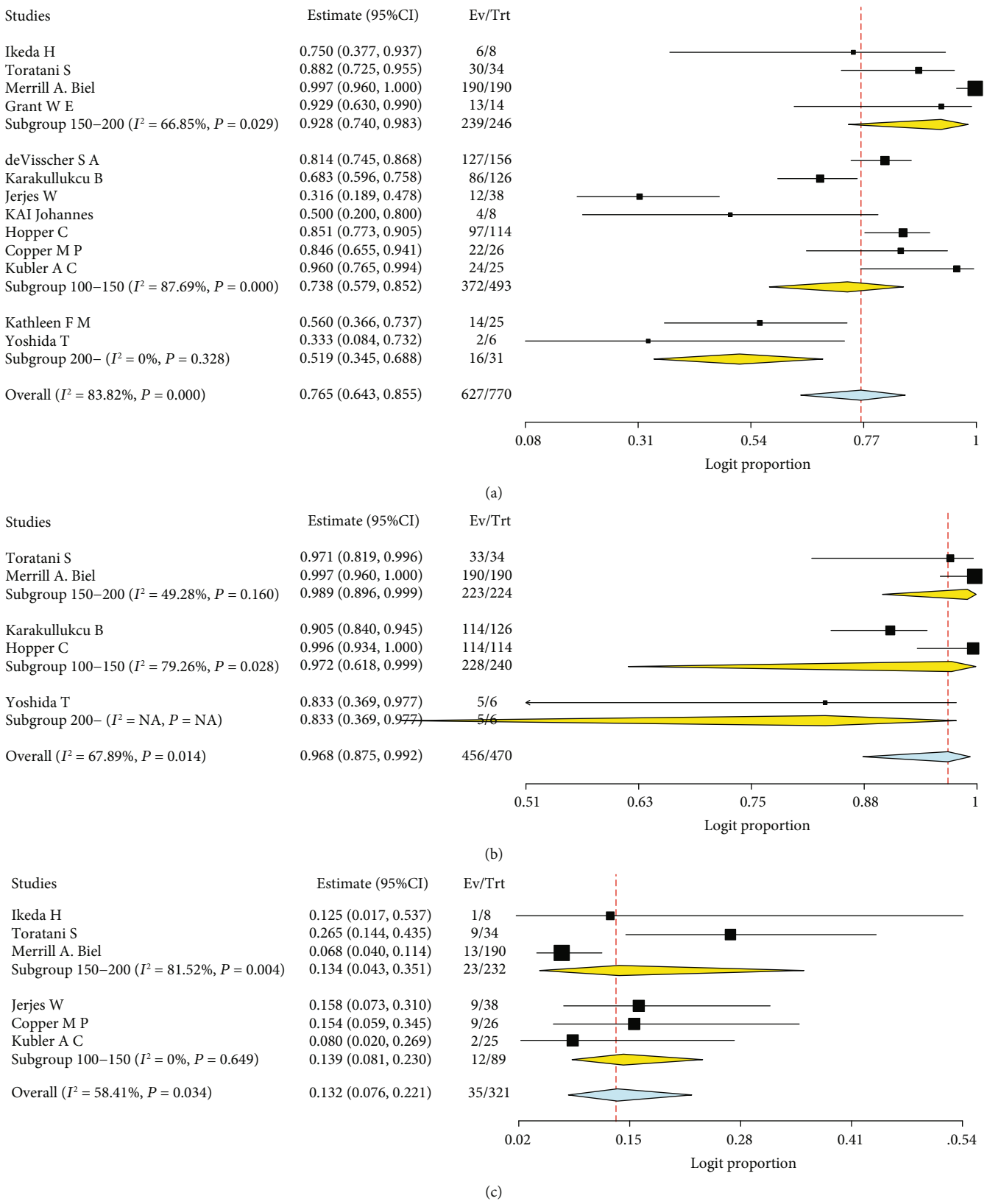

Figure 9: Forest plot of subgroup analysis of (a) CR, (b) OR, and (c) RR in cases using different power densities.

effect on metastatic lesions; therefore, patients with OSCC should be carefully selected (patients at the T1N0M0/T2N0M0 stage in most cases) before PDT treatment. Optional treatment plans should be suggested when a CR could not be achieved. In the current study, the pooled RR of OSCC after PDT was 15.8%, indicating that even when CR was achieved, frequent follow-up should be applied to monitor recurrence.

To determine whether the effect of PDT was affected by different factors, several subgroup analyses were performed, including sites of the lesion, photosensitizers, light sources, radiant exposure, and power density.

As for the sites of lesions, the effect of PDT on OSCC lesions on lining mucosa and masticatory mucosa was compared. The lining mucosa is different from the masticatory mucosa in structure; the latter bears greater masticatory forces and has a keratinized layer that is thicker than the former. In the lining mucosa, less keratin, less fiber, and more vascular connective tissue is formed, while the masticatory mucosa contains connective tissue components with higher density and fewer blood vessels [38]. The subgroup analysis showed that the CR rate of lesions on the lining mucosa was slightly higher than that of the masticatory mucosa, probably owing to the higher infiltration of photosensitizers in lesions on the lining mucosa; however, there was no significant statistical difference.

The ideal photosensitizer should be easy to prepare, stable in storage, highly selective to tumor lesions, and have a significant absorbance band at longer wavelengths [39]. Different photosensitizers have different properties and characteristics. Porfimer sodium is the first-generation photosensitizer, and its depth of action is limited to 5 mm. For thicker tumors, temoporfin, which is a second-generation photosensitizer, can achieve a CR rate of up to 93% [40]. The therapeutic effect of temoporfin is similar to that of porfimer sodium, but the former has better selectivity for early cancer [41]. HPD is the first photosensitizer with water solubility, sufficient affinity for tumors, and low toxicity to normal tissues [39]. However, its metabolism in the body is slow, and patients need to be protected from bright light for weeks after intravenous administration of HPD [42]. HPPH, a compound that strongly absorbs light at 665 nm, has a higher penetration in tumor tissue and less skin photosensitivity [43]. Talaporfin sodium is a second-generation photosensitizer that can be easily eliminated from the body [16]. In the current meta-analysis, there was no significant difference in the response rate among different photosensitizers. Clinicians may consider the availability, incidence, and severity of adverse reactions, cost-performance ratio, and local medical insurance policy when choosing an appropriate photosensitizer.

Different lasers are used for different wavelengths, including diode lasers (630–1100 nm) and dye lasers (390–1000 nm) [44]. Near-infrared lasers with longer wavelengths have deeper penetration, minimal thermal effects, and spatial selectivity than visible lasers, which may be important in the treatment of brain cancer. The properties of the photosensitizer, tissue properties, and matching absorption wavelength should be considered when choosing laser types [44, 45].

In a typical clinical PDT scheme, a radiant exposure of the laser of approximately 50–100 J/cm^2 is typically used. There was no significant difference in the subgroup analysis of the radiant exposure, which might be associated with the fact that the combination of photosensitizer and light was an effective method to destroy tissue based on chemical damage caused by photosensitive reaction rather than heating [45]. Because PDT consumes oxygen, it is important to use an appropriate power density. High power density can accelerate the consumption of oxygen molecules; if oxygen cannot be transferred to the treatment area in time, the PDT efficiency can be reduced. In general, it should be maintained between 150 and 200 mW/cm^2 to avoid hypoxia in tissues [46, 47]. Adverse reactions are inevitable, but their incidence can be reduced by adjusting the light dose, interval time between photosensitizer administration and irradiation, irradiation area, administration method, etc. [48].

The current study still has several limitations. Most studies included did not count the survival time of the patients. In future studies of OSCC treated with PDT, attention should be paid to the follow-up of patients' survival time to provide more powerful evidence for the efficacy of PDT in the treatment of OSCC. Almost all studies included in this meta-analysis were retrospective studies, and there was no control group. The number of treatments and reexamination times of PDT in each study were different, and the results might be inconsistent. Through subgroup analysis, we found that there was no statistically significant difference among the different sites, photosensitizers, and therapy parameters, but this did not mean that the above factors had no influence on efficacy. A possible reason is that these factors are not consistent in different studies, and different factors may interfere with each other. Therefore, it may be necessary to further explore the effects of different factors on the efficacy of PDT through randomized controlled trials to optimize the treatment regimen of PDT for OSCC.

5. Conclusions

Although surgical treatment is still the first choice for the treatment of OSCC, PDT for OSCC has great potential as an adjuvant therapy. Investigations on the influence of PDT on the survival of OSCC patients, optimization of the treatment regimen, and evaluation of response after treatment are still needed.

Abbreviations

PDT:	Photodynamic therapy
OSCC:	Oral squamous cell carcinoma
CI:	Confidence intervals
CR:	Complete response
OR:	Overall response
RR:	Recurrence rate
G/P:	Gingiva and/or palate
L/BM/T/FM:	Lips and/or buccal mucosa and/or tongue and/or floor of the mouth
m-THPC:	m-Tetra(hydroxyphenyl) chlorin
HPPH:	Chlorin-based compound, 3-(1'-hexyloxyethyl) pyropheophorbide
HPD:	Hematoporphyrin derivative
N/A:	Not applicable.

Conflicts of Interest

The authors have no conflict of interest to declare.

Acknowledgments

This study was supported by the National Natural Science Foundation of China (grant numbers: U19A2005, 82071125, 81572663, 81972551), Sichuan Science and Technology Program (grant numbers: 2020YFS0044, 2020YFSY009), and Research and Develop Program, West China Hospital of Stomatology, Sichuan University (grant numbers: LCYJ2019-11).

Supplementary Materials

Supplementary 1. Figure 1: funnel plot of proportions of (A) CR, (B) OR, and (C) RR after PDT.

Supplementary 2. Figure 2: sensitivity analysis of proportions of (A) CR, (B) OR, and (C) RR after PDT.

References

[1] J. J. Kain, A. C. Birkeland, N. Udayakumar et al., "Surgical Margins in Oral Cavity Squamous Cell Carcinoma: Current Practices and Future Directions," *The Laryngoscope*, vol. 130, no. 1, pp. 128–138, 2019.

[2] P. J. Lamey, "Management Options in Potentially Malignant and Malignant Oral Epithelial Lesions," *Community Dental Health*, vol. 10, Supplement 1, pp. 53–62, 1993.

[3] C. Scully, "Oral precancer: preventive and medical approaches to managementOral precancer: Preventive and medical approaches to management," *European Journal of Cancer. Part B, Oral Oncology*, vol. 31, pp. 16–26, 1995.

[4] Q. Chen, H. Dan, F. Tang et al., "Photodynamic therapy guidelines for the management of oral leucoplakiaPhotodynamic Therapy Guidelines for the Management of Oral Leucoplakia," *International Journal of Oral Science*, vol. 11, 2019.

[5] C. Hopper, "Photodynamic therapy: a clinical reality in the treatment of cancerPhotodynamic Therapy: a Clinical Reality in the Treatment of Cancer," *The Lancet Oncology*, vol. 1, pp. 212–219, 2000.

[6] P. Agostinis, K. Berg, K. A. Cengel et al., "Photodynamic Therapy of Cancer: An Update," *CA: a Cancer Journal for Clinicians*, vol. 61, no. 4, pp. 250–281, 2011.

[7] J. Meulemans, P. Delaere, and V. Vander Poorten, "Photodynamic therapy in head and neck cancer: indications, outcomes, and future prospectsPhotodynamic Therapy in Head and Neck Cancer," *Current Opinion in Otolaryngology & Head and Neck Surgery*, vol. 27, no. 2, pp. 136–141, 2019.

[8] E. W. Cerrati, S. A. Nguyen, J. D. Farrar, and E. J. Lentsch, "The Efficacy of Photodynamic Therapy in the Treatment of Oral Squamous Cell Carcinoma: A Meta-Analysis," *Ear, Nose & Throat Journal*, vol. 94, pp. 72–79, 2019.

[9] PRISMA-P Group, D. Moher, L. Shamseer et al., "Preferred reporting items for systematic review and meta-analysis protocols (PRISMA-P) 2015 statement," *Systematic Reviews*, vol. 4, no. 1, 2015.

[10] B. C. Wallace, C. H. Schmid, J. Lau, and T. A. Trikalinos, "Meta-Analyst: software for meta-analysis of binary, continuous and diagnostic data," *BMC Medical Research Methodology*, vol. 9, no. 1, 2009.

[11] S. H. Downs and N. Black, "The feasibility of creating a checklist for the assessment of the methodological quality both of randomised and non-randomised studies of health care interventions," *Journal of Epidemiology and Community Health.*, vol. 52, no. 6, pp. 377–384, 1998.

[12] P. H. Ahn, J. C. Finlay, S. M. Gallagher-Colombo et al., "Lesion oxygenation associates with clinical outcomes in premalignant and early stage head and neck tumors treated on a phase 1 trial of photodynamic therapy," *Photodiagnosis and Photodynamic Therapy*, vol. 21, pp. 28–35, 2018.

[13] P. H. Ahn, H. Quon, B. W. O'Malley et al., "Toxicities and early outcomes in a phase 1 trial of photodynamic therapy for premalignant and early stage head and neck tumorsToxicities and early outcomes in a phase 1 trial of photodynamic therapy for premalignant and early stage head and neck tumors," *Oral Oncology*, vol. 55, pp. 37–42, 2016.

[14] M. P. Copper, M. Triesscheijn, I. B. Tan, M. C. Ruevekamp, and F. A. Stewart, "Photodynamic therapy in the treatment of multiple primary tumours in the head and neck, located to the oral cavity and oropharynxPhotodynamic therapy in the treatment of multiple primary tumours in the head and neck, located to the oral cavity and oropharynx," *Clinical Otolaryngology*, vol. 32, no. 3, pp. 185–189, 2007.

[15] M. P. Copper, I. B. Tan, H. Oppelaar, M. C. Ruevekamp, and F. A. Stewart, "Meta-tetra(hydroxyphenyl)chlorin Photodynamic Therapy in Early-Stage Squamous Cell Carcinoma of the Head and NeckMeta-tetra(hydroxyphenyl)chlorin photodynamic therapy in early-stage squamous cell carcinoma of the head and neck," *Archives of Otolaryngology – Head & Neck Surgery*, vol. 129, no. 7, pp. 709–711, 2003.

[16] H. Ikeda, S. Ohba, K. Egashira, and I. Asahina, "The effect of photodynamic therapy with talaporfin sodium, a second-generation photosensitizer, on oral squamous cell carcinoma: aA series of eight casesThe effect of photodynamic therapy with talaporfin sodium, a second-generation photosensitizer, on oral squamous cell carcinoma: A series of eight cases," *Photodiagnosis and Photodynamic Therapy*, vol. 21, pp. 176–180, 2018.

[17] S. Toratani, R. Tani, T. Kanda, K. Koizumi, Y. Yoshioka, and T. Okamoto, "Photodynamic therapy using Photofrin and excimer dye laser treatment for superficial oral squamous cell carcinomas with long-term follow up," *Photodiagnosis and Photodynamic Therapy.*, vol. 14, pp. 104–110, 2016.

[18] N. Rigual, G. Shafirstein, M. T. Cooper et al., "Photodynamic therapy with 3-(1'-hexyloxyethyl) pyropheophorbide a for cancer of the oral cavity," *Clinical Cancer Research*, vol. 19, no. 23, pp. 6605–6613, 2013.

[19] B. Karakullukcu, S. D. Stoker, A. P. E. Wildeman, M. P. Copper, M. A. Wildeman, and I. B. Tan, "A matched cohort comparison of mTHPC-mediated photodynamic therapy and trans-oral surgery of early stage oral cavity squamous cell cancerA matched cohort comparison of mTHPC-mediated photodynamic therapy and trans-oral surgery of early stage oral cavity squamous cell cancer," *European Archives of Oto-Rhino-Laryngology*, vol. 270, no. 3, pp. 1093–1097, 2013.

[20] H. Ikeda, T. Tobita, S. Ohba, M. Uehara, and I. Asahina, "Treatment outcome of Photofrin-based photodynamic therapy for T1 and T2 oral squamous cell carcinoma and dysplasia," *Photodiagnosis and Photodynamic Therapy*, vol. 10, no. 3, pp. 229–235, 2013.

[21] B. Karakullukcu, K. van Oudenaarde, M. P. Copper et al., "Photodynamic therapy of early stage oral cavity and

oropharynx neoplasms: an outcome analysis of 170 patients," *European Archives of Oto-Rhino-Laryngology*, vol. 268, no. 2, pp. 281–288, 2011.

[22] N. R. Rigual, K. Thankappan, M. Cooper et al., "Photodynamic therapy for head and neck dysplasia and cancer," *Archives of Otolaryngology – Head & Neck Surgery*, vol. 135, no. 8, pp. 784–788, 2009.

[23] C. Hopper, A. Kübler, H. Lewis, I. B. Tan, G. Putnam, and the Foscan 01 Study Group, "mTHPC-mediated photodynamic therapy for early oral squamous cell carcinomamTHPC-mediated photodynamic therapy for early oral squamous cell carcinoma," *International Journal of Cancer*, vol. 111, no. 1, pp. 138–146, 2004.

[24] A. C. Kubler, J. de Carpentier, C. Hopper, A. G. Leonard, and G. Putnam, "Treatment of squamous cell carcinoma of the lip using Foscan-mediated Photodynamic TherapyTreatment of squamous cell carcinoma of the lip using Foscan-mediated photodynamic therapy," *International Journal of Oral and Maxillofacial Surgery*, vol. 30, no. 6, pp. 504–509, 2001.

[25] T. Yoshida, H. Kato, T. Okunaka et al., "Photodynamic therapy for head and neck cancer," *Diagnostic and Therapeutic Endoscopy*, vol. 3, no. 1, pp. 41–51, 1996.

[26] W. E. Grant, C. Hopper, P. M. Speight, A. J. Macrobert, and S. G. Bown, "Photodynamic therapy of malignant and premalignant lesions in patients with 'field cancerization' of the oral cavityPhotodynamic therapy of malignant and premalignant lesions in patients with 'field cancerization' of the oral cavity," *Journal of Laryngology and Otology*, vol. 107, no. 12, pp. 1140–1145, 1993.

[27] W. Jerjes, T. Upile, Z. Hamdoon, C. Alexander Mosse, M. Morcos, and C. Hopper, "Photodynamic therapy outcome for T1/T2 N0 oral squamous cell carcinoma," *Lasers in Surgery and Medicine*, vol. 43, no. 6, pp. 463–469, 2011.

[28] S. A. H. J. de Visscher, L. J. Melchers, P. U. Dijkstra et al., "mTHPC-mediated photodynamic therapy of early stage oral squamous cell carcinoma: a comparison to surgical treatment," *Annals of Surgical Oncology*, vol. 20, no. 9, pp. 3076–3082, 2013.

[29] K. F. M. Fan, C. Hopper, P. M. Speight, G. A. Buonaccorsi, and S. G. Bown, "Photodynamic therapy using mTHPC for malignant disease in the oral cavity," *International journal of cancer*, vol. 73, no. 1, pp. 25–32, 1997.

[30] M. A. Biel, "Photodynamic therapy of head and neck cancers," *Methods in molecular biology*, vol. 635, pp. 281–293, 2010.

[31] V. G. Schweitzer and M. L. Somers, "PHOTOFRIN-mediated photodynamic therapy for treatment of early stage (Tis-T2N0M0) SqCCa of oral cavity and oropharynx," *Lasers in Surgery and Medicine*, vol. 42, no. 1, pp. 1–8, 2010.

[32] K. J. Lorenz and H. Maier, "Photodynamic therapy with meta-tetrahydroxyphenylchlorin (Foscan) in the management of squamous cell carcinoma of the head and neck: experience with 35 patients," *European Archives of Oto-Rhino-Laryngology*, vol. 266, no. 12, pp. 1937–1944, 2009.

[33] P. Tandon, A. Dadhich, H. Saluja, S. Bawane, and S. Sachdeva, "The prevalence of squamous cell carcinoma in different sites of oral cavity at our Rural Health Care Centre in Loni, Maharashtra - a retrospective 10-year study," *Contemporary oncology*, vol. 2, no. 2, pp. 178–183, 2017.

[34] A. J. Cowan, C. Allen, A. Barac et al., "Global bBurden of mMultiple mMyeloma: aA sSystematic aAnalysis for the gGlobal bBurden of dDisease sStudy 2016Global Burden of Multiple Myeloma," *JAMA oncology*, vol. 4, no. 9, pp. 1221–1227, 2018.

[35] F. Bray, J. Ferlay, I. Soerjomataram, R. L. Siegel, L. A. Torre, and A. Jemal, "Global cancer statistics 2018: GLOBOCAN estimates of incidence and mortality worldwide for 36 cancers in 185 countriesGlobal cancer statistics 2018: GLOBOCAN estimates of incidence and mortality worldwide for 36 cancers in 185 countries," *CA: a cancer journal for clinicians*, vol. 68, no. 6, pp. 394–424, 2018.

[36] A. Almangush, A. A. Mäkitie, A. Triantafyllou et al., "Staging and grading of oral squamous cell carcinoma: An update," *Oral oncology*, vol. 107, article 104799, 2020.

[37] W. Jerjes, T. Upile, Z. Hamdoon, C. A. Mosse, S. Akram, and C. Hopper, "Photodynamic therapy outcome for oral dysplasia," *Lasers in surgery and medicine*, vol. 43, no. 3, pp. 192–199, 2011.

[38] G. Taybos, "Oral changes associated with tobacco use," *The American journal of the medical sciences.*, vol. 326, no. 4, pp. 179–182, 2003.

[39] D. Kessel, "Photodynamic therapy: a brief history," *Journal of clinical medicine*, vol. 8, no. 10, p. 1581, 2019.

[40] A. Kübler, T. Haase, C. Staff, B. Kahle, M. Rheinwald, and J. Mühling, "Photodynamic therapy of primary nonmelanomatous skin tumours of the head and neck," *Lasers in surgery and medicine*, vol. 25, no. 1, pp. 60–68, 1999.

[41] J. Savary, P. Monnier, C. Fontolliet et al., "Photodynamic therapy for early squamous cell carcinomas of the esophagus, bronchi, and mouth with m-tetra (hydroxyphenyl) chlorin-Photodynamic Therapy for Early Squamous Cell Carcinomas of the Esophagus, Bronchi, and Mouth With m-Tetra(Hydroxyphenyl) Chlorin," *Archives of Otolaryngology - Head and Neck Surgery*, vol. 123, no. 2, pp. 162–168, 1997.

[42] T. J. Dougherty, G. Lawrence, J. H. Kaufman, D. Boyle, K. R. Weishaupt, and A. Goldfarb, "Photoradiation in the treatment of recurrent breast carcinoma," *Journal of the National Cancer Institute*, vol. 62, no. 2, pp. 231–237, 1979.

[43] G. Loewen, R. Pandey, D. Bellnier, B. Henderson, and T. Dougherty, "Endobronchial photodynamic therapy for lung cancerEndobronchial photodynamic therapy for lung cancer," *Lasers in surgery and medicine*, vol. 38, no. 5, pp. 364–370, 2006.

[44] J.-T. Lin, "Progress of medical lasers: fundamentals and applications," *Medical Devices and Diagnostic Engineering*, vol. 1, no. 2, pp. 36–41, 2016.

[45] X. Li, J. F. Lovell, J. Yoon, and X. Chen, "Clinical development and potential of photothermal and photodynamic therapies for cancer," *Nature Reviews Clinical Oncology*, vol. 17, no. 11, pp. 657–674, 2020.

[46] D. M. Ozog, A. M. Rkein, S. G. Fabi et al., "Photodynamic tTherapy: aA cClinical cConsensus gGuide," *Dermatologic Surgery*, vol. 42, no. 7, pp. 804–827, 2016.

[47] P. Babilas, S. Schreml, M. Landthaler, and R.-M. Szeimies, "Photodynamic therapy in dermatology: state-of-the-art," *Photodermatology Photoimmunology & Photomedicine*, vol. 26, no. 3, pp. 118–132, 2010.

[48] Y. Wang, H. Wang, L. Zhou et al., "Photodynamic therapy of pancreatic cancer: where have we come from and where are we going?," *Photodiagnosis and photodynamic therapy*, vol. 101876, 2020.